

NASA TECHNICAL NOTE



NASA TN D-5738

NASA TN D-5738



LOAN COPY: RETURN TO
AFWL (WL0L)
KIRTLAND AFB, N MEX

EXPERIMENTAL CAVITATION
AND FLASHING OF POTASSIUM
FLOWING ADIABATICALLY THROUGH
A VENTURI SIZED AS A BOILER INLET

by Orlando A. Gutierrez and David B. Fenn
Lewis Research Center
Cleveland, Ohio





0132328

| | | | |
|--|--|---|----------------------|
| 1. Report No. NASA TN D-5738 | 2. Government Accession No. | 3. Recipient's Catalog No. | |
| 4. Title and Subtitle EXPERIMENTAL CAVITATION AND FLASHING OF POTASSIUM FLOWING ADIABATICALLY THROUGH A VENTURI SIZED AS A BOILER INLET | | 5. Report Date April 1970 | |
| | | 6. Performing Organization Code | |
| 7. Author(s) Orlando A. Gutierrez and David B. Fenn | | 8. Performing Organization Report No. E-5346 | |
| 9. Performing Organization Name and Address Lewis Research Center National Aeronautics and Space Administration Cleveland, Ohio 44135 | | 10. Work Unit No. 120-27 | |
| | | 11. Contract or Grant No. | |
| 12. Sponsoring Agency Name and Address National Aeronautics and Space Administration Washington, D. C. 20546 | | 13. Type of Report and Period Covered Technical Note | |
| | | 14. Sponsoring Agency Code | |
| 15. Supplementary Notes | | | |
| 16. Abstract Subcooled liquid potassium was flashed adiabatically in a 0.1015-in. - (0.2578-cm-) throat-diameter venturi. Data were obtained before, during, and after flashing at flow rates from 300 to 660 lbm/hr (38 to 83 g/sec) and temperatures from 1140 ⁰ to 1460 ⁰ F (889 to 1066 K). Flow rate after flashing depended only on inlet pressure and temperature. Liquid tensions/superheats were obtained prior to incipient flashing, with some pressures falling below absolute zero. Maximum liquid tensions were correlated by a force-balance equation for vapor bubbles with radii between 1×10^{-4} and 0.5×10^{-4} in. (2.54×10^{-4} and 1.27×10^{-4} cm). Incipency data are compared with non-adiabatic data for potassium in the literature. | | | |
| 17. Key Words (Suggested by Author(s)) Potassium Flashing Venturi Liquid tension/superheat Cavitation Experimental | | 18. Distribution Statement Unclassified - unlimited | |
| 19. Security Classif. (of this report) Unclassified | 20. Security Classif. (of this page) Unclassified | 21. No. of Pages 72 | 22. Price* \$3.00 |

*For sale by the Clearinghouse for Federal Scientific and Technical Information
Springfield, Virginia 22151

CONTENTS

| | Page |
|--|------|
| SUMMARY | 1 |
| INTRODUCTION | 1 |
| BACKGROUND | 2 |
| APPARATUS | 4 |
| Test Facility | 4 |
| Test Section | 4 |
| Venturis | 5 |
| Control venturi | 5 |
| Test venturi without artificial throat cavity | 5 |
| Test venturi with artificial throat cavity | 6 |
| Research Instrumentation | 6 |
| Pressures | 6 |
| Temperatures | 6 |
| Flow | 7 |
| Noise | 8 |
| EXPERIMENTAL PROCEDURE | 8 |
| Preoperative Procedure | 8 |
| Data-Taking Procedure | 9 |
| Postoperative Procedure | 10 |
| RESULTS AND DISCUSSION | 10 |
| General Venturi Behavior | 11 |
| Liquid Performance | 15 |
| Flashed Performance | 16 |
| Incipency Characteristics | 18 |
| Cavitation incipency | 19 |
| Flashing incipency | 20 |
| Comparison of incipency results with heat-addition data in the literature | 21 |
| Metallographic Inspection | 23 |
| CONCLUDING REMARKS | 24 |
| SUMMARY OF RESULTS | 25 |

APPENDIXES

| | |
|--|----|
| A - SYMBOLS | 27 |
| B - ACCURACY OF TEMPERATURE AND FLOW MEASUREMENTS | 29 |
| C - CALCULATION OF TEST VENTURI THROAT PRESSURE, DYNAMIC HEAD, AND THERMODYNAMIC EXIT QUALITY | 32 |
| REFERENCES | 34 |

EXPERIMENTAL CAVITATION AND FLASHING OF POTASSIUM FLOWING ADIABATICALLY THROUGH A VENTURI SIZED AS A BOILER INLET

by Orlando A. Gutierrez and David B. Fenn

Lewis Research Center

SUMMARY

Tests were conducted on the adiabatic initiation of vapor in a venturi with a 0.1015-inch (0.2578-cm) throat diameter, with high-purity potassium used as the test fluid. A venturi of this size could be used as a boiler tube inlet device. The inside surface of the venturi was machined and polished to a 6 rms finish. Data were obtained at constant flow rates and inlet temperatures by changing the pressure level in a recirculating loop. Flow rates ranged from 300 to 660 pounds mass per hour (38 to 83 g/sec) at inlet temperatures from 1140^o to 1460^o F (889 to 1066 K).

The behavior of the venturi in the all-liquid and two-phase states is presented, as well as data for incipient cavitation and flashing. Flow rate in the flashed condition is dependent only on inlet pressure and temperature. Nonequilibrium conditions at incipency are correlated by a force-balance equation for vapor bubbles with critical radii between 1×10^{-4} and 0.5×10^{-4} inch (2.54×10^{-4} and 1.27×10^{-4} cm). These radii agree well with the maximum sizes of wall cavities detected by metallographic examination of the venturi inner surface. Some of the throat absolute pressures at incipency are calculated to be below zero. The addition of an artificial cavity of 0.008 inch (0.020 cm) diameter in the wall at the venturi throat did not have any effect on incipient conditions. It did affect the flashed venturi performance, apparently by inducing vapor into the throat.

The incipient flashing data obtained adiabatically herein are compared with data on incipient boiling obtained with heat addition that are available in the literature for potassium.

INTRODUCTION

This investigation was conducted to study experimentally the conditions at initiation of two-phase flow in liquid potassium flowing adiabatically through a venturi sized as a

boiler tube inlet, as well as the flow behavior in the venturi before and after such an initiation.

Two of the problems encountered with once-through boilers for use in low-specific-weight, Rankine-cycle systems are boiler instability and the tendency of alkali metals used as cycle fluids to support large amounts of liquid superheat. Research has shown that the introduction of large pressure drops at the boiler inlet decreases the feed-system coupling instabilities. As for the second problem, the alkali metals considered as cycle fluids (potassium, sodium, etc.) tend to remain in the liquid phase at temperatures well above saturation temperature. This is caused by their high purity and low gas solubility as well as their ability to wet the walls and flood cavities which otherwise might act as nucleating sites. This characteristic of the alkali metals makes it hard for designers to predict the location in a boiler where the vapor phase will develop, with the possibility that large boiler lengths may become adiabatic.

A cavitating venturi is a converging-diverging nozzle of such size that initially sub-cooled liquid flowing through it will reach a local static pressure well below its saturation vapor pressure, thus causing the formation of the vapor phase. Such a venturi will have a large pressure drop. It will also force the formation of vapor at a well-determined location. Therefore, a cavitating venturi at the entrance of a boiler tube should aid in the solution of both previously mentioned boiler problems.

This investigation was conducted at the Lewis Research Center. The venturi used had a throat diameter of 0.1015 inch (0.2578 cm) and was machined from type-316 stainless steel to very close tolerances. The inside surface was highly polished. The venturi was tested with and without an artificial cavity at the throat. Tests were conducted on a forced-circulation, well-insulated, closed loop.

Data were obtained over a flow range of 300 to 660 pounds mass per hour (38 to 83 g/sec) and at fluid temperatures from 1140° to 1460° F (889 to 1066 K). Results are presented and discussed for incipient cavitation, incipient flashing, liquid and two-phase performance of the venturi, and effects of the artificial throat cavity. Results obtained in this investigation are compared with the nonadiabatic liquid superheat data for potassium that are available in the literature.

BACKGROUND

Stone and Sekas (refs. 1 and 2) studied the performance of a cavitating venturi as a water-boiler inlet device. They concluded that its use would greatly reduce the feed-system coupling instabilities described by Dorsch (ref. 3). Hammitt and Robinson (ref. 4) examined the flows of water and mercury in a cavitating venturi. Both refer-

ences 2 and 4 state that their flows behaved as "choked" (i.e., flow rate was independent of outlet pressure).

Ruggeri, Gelder, and Moore studied cavitation of water (ref. 5) and Freon-114 (ref. 6) in a large-diameter, small-area-ratio venturi and reported liquid tensions supported by both fluids.

Many researchers have studied the superheating of alkali liquid metals, with most of the investigations done nonadiabatically. The results obtained vary greatly because of the large number of variables affecting this problem. Hsu (ref. 7) presents a theory that predicts bubble initiation in ether, water, and pentane based on the size range of active cavity sites in the wall. Holtz (ref. 8) notes the importance of pressure-temperature history on liquid superheats, and defines factors necessary to make a physical cavity become an active nucleation site. Edwards and Hoffman (ref. 9) present data on the superheating of liquid potassium and sodium obtained in a natural-convection boiling loop. They show how the addition of a series of 0.006-inch- (0.015-cm-) diameter drilled holes reduced the obtainable liquid superheat. Chen (ref. 10) points out the following factors which contribute to the ability of a liquid to maintain superheat without boiling: surface cavities, gas entrapment in the surface, pressure-temperature history of the surface and fluid, and the gas content and impurities present in the liquid. The present authors were unable to find reference to any previous experimental work on boiling initiation in potassium through adiabatic means.

The terms "liquid superheat" and "liquid tension" appear in the literature and should be clarified. Liquid superheat is the temperature increment of the liquid in excess of the saturation temperature at the local pressure. Liquid tension is the pressure decrement of the liquid below the saturation pressure at the local temperature. Both terms denote a nonequilibrium condition in the liquid. The use of one term over the other has been dictated mainly by the experimental process involved and the reporter's point of view. Those studying the change in fluid pressures at constant temperatures use the liquid-tension term. Those changing temperatures at constant pressures tend to use liquid superheat to denote the nonequilibrium state. However, at absolute pressures below zero, liquid superheat becomes infinite and meaningless.

The existence of liquids at pressures below absolute zero, that is, under negative absolute pressure, has long been known. Blake (ref. 11) in his introduction states that under suitable conditions liquids can withstand very considerable negative external pressures without rupturing. He attributes this phenomenon to the considerable magnitude of the intermolecular cohesive forces. Many experimental measurements of these negative absolute pressures in liquid water appear in the literature, among them those by Briggs (ref. 12) and Gavrilenko and Topchiyan (ref. 13). Briggs (ref. 14) also measured negative absolute pressures on such organic liquids as acetic acid, benzene, aniline, carbon tetrachloride, and chloroform.

Two other terms that appear in this report should be defined: "cavitation" and "flashing." In referring to the venturi, the term cavitation is applied when formation and collapse of vapor is indicated, without the venturi deviating noticeably from its liquid flow - pressure-drop characteristics. The term flashing is used when the cavitation causes the pressure-drop characteristics to change appreciably from the liquid behavior.

APPARATUS

Test Facility

A schematic diagram of the equipment used for these tests appears in figure 1. The closed loop had an electromagnetic (EM) pump which forced liquid potassium at rates up to 700 pounds per hour (88 g/sec) through two electric heaters. The heaters had a maximum capacity of 10 kilowatts each and were mounted in series. The potassium then passed through the horizontal test section and returned to the pump, flowing through an air-cooled section. This air-cooled section lowered the potassium temperature to prevent cavitation at the pump inlet. An expansion tank, located above the highest point in the loop, was connected to the system at the cooler inlet. Loop pressure level was controlled through argon and vacuum lines connected to the top of this tank. Flow rate was controlled through a combination of throttle and bypass valves and pump speed control. Type-316 stainless steel was used throughout the loop. Piping size was primarily 0.50 inch outside diameter by 0.060 inch wall thickness (1.27 by 0.152 cm). The loop was heavily insulated except at the air cooler.

In addition, the test equipment incorporated a titanium-filled hot trap for liquid-metal purification. The hot trap was mounted on the pump bypass line. A sample tube that allowed sampling of the potassium while running and a dump tank to hold the potassium prior to fill completed the test loop.

There was an EM flowmeter located on the return line from the test section. The loop was also equipped with pressure and temperature instrumentation to facilitate operation. This instrumentation is not shown.

Test Section

The test section (fig. 1) consisted of two venturis of equal dimensions, mounted in series and separated by a valve. This valve was used for pressure and flow control (PFC). The PFC valve created enough pressure drop to allow the control venturi, lo-

cated upstream of the valve, to operate always above saturation vapor pressure even when the test venturi downstream of the valve was cavitating.

The main purpose of the control venturi was to provide a means of determining the throat pressure in the test venturi without need of instrument penetrations into the throat of the test venturi. Such penetrations might have changed the behavior of the venturi. The schematic diagram of the test section (fig. 2) shows how the test venturi throat pressure was obtained from the measured pressure at the control venturi throat and from the similarity of the two venturis.

The test section also included two flow-straightening assemblies, one ahead of each venturi. These flow-straighteners eliminated any vorticity in the potassium flow approaching the venturis. Details of the flow straighteners are shown in figure 3.

Venturis

The control venturi (fig. 4) and the test venturi (fig. 5) were two of a series of three identical venturis machined to the dimensions shown in figure 4. The inlet nozzle contour followed the dimensions of a 2:1 ellipse. The conical diffuser had an included angle of 11.5° . These two sections blended together tangentially without an appreciable length of constant cross section in between. They were formed from a single rod of type-316 stainless steel by electric discharge machining (EDM). The inside surfaces were lapped to a mirror finish. Measurements of the surface after lapping showed between a 5 and 6 rms finish. The minimum diameter measured between 0.1010 and 0.1020 inch (0.2565 and 0.2591 cm). A value of 0.1015 inch (0.2578 cm) was used as the actual throat diameter for all venturis.

The third venturi in the series was made so that a venturi could be retained in the "as-received" condition. This as-received venturi was used for destructive metallographic comparisons after completion of tests. A water flow calibration was conducted on this venturi also.

The only differences between the control and test venturis were on the penetrations made into each to incorporate instrumentation and inserts.

Control venturi. - Three penetrations were made into the control venturi (fig. 4). These penetrations were 0.04 inch (0.10 cm) in diameter. The holes were drilled before the surface was lapped. As shown in figure 4, the holes were located at the venturi inlet, outlet, and throat. All three holes were connected to pressure-measuring devices. Thermocouples were spot welded to the venturi outside surface at the inlet T_{C1} and the outlet T_{C2} .

Test venturi without artificial throat cavity. - The test venturi was tested first without any artificial throat cavities, as shown in figure 5(a). Only two holes were

drilled through to the inside surface; at the venturi inlet and outlet. Both holes were 0.04 inch (0.10 cm) in diameter and were connected to pressure-measuring devices. The inside surface of the test venturi was unbroken by any penetrations in the zone of reduced area. Four holes 0.070 inch (0.178 cm) in diameter were drilled to within 0.06 inch (0.15 cm) of the inside surface at the locations shown in figure 5(a). Thermocouples T_1 , T_2 , T_3 , and T_4 were spot welded at the bottoms of these holes. In addition, two thermocouples, T_{in} and T_{out} , were spot welded to the outside surface of the venturi inlet and outlet, as was done on the control venturi. An accelerometer was mounted at the end of a 1/4-inch- (0.6-cm-) diameter, 10-inch- (25-cm-) long tube. This tube was attached to the test venturi near the throat area.

Test venturi with artificial throat cavity. - The test venturi was modified after the first series of experiments, as shown in figure 5(b). The hole located in the plane of the throat was drilled through and reamed to 0.076 inch (0.193 cm) diameter. A throat cavity insert was placed in this hole, replacing thermocouple T_1 . The end of the insert was seal welded to the outside surface of the venturi. This throat cavity insert is detailed in figure 6.

All the machining necessary to install the cavity insert was done with the venturi installed in the loop. In addition to the 0.008-inch- (0.020-cm-) diameter reentrant cavity in the insert, there also was a 0.0005-inch- (0.0013-cm-) wide annular gap between the cavity insert and the hole drilled in the venturi wall after installation. Examination after completion of tests showed that the insert had twisted during mounting. This resulted in a mismatch of the contoured surfaces of insert and venturi. Part of the insert edge protruded into the flow passage as much as 0.005 inch (0.013 cm), while part of it was below surface level.

Research Instrumentation

Pressures. - Pressures were measured at the control venturi inlet P_1 , throat P_2 , and outlet P_3 ; and also at the test venturi inlet P_4 and outlet P_5 .

The pressure-measuring devices were absolute pressure transducers of the unbonded strain-gage type. Their range was 0 to 50 psia (0 to 34.5 N/cm²) with a 0- to 10-millivolt output. All pressure transducers were mounted in a constant-temperature oven held at 190° F (361 K). Pressure transducers were connected by potassium-filled lines to the locations shown in figures 1, 2, 4, and 5. The signal from each transducer had two parallel readouts: a null-balance strip recorder and a multichannel oscillograph.

The pressure-recording system was calibrated after the loop was filled with potassium. Calibration was made by applying known gas pressures at the top of the expansion tank with no flow in the system. Gas pressure was measured with a 0- to 100-psia

(0- to 68.9-N/cm² abs) Bourdon-type gage accurate to 0.1 percent of full scale. Calibrations were performed before and after running the two series of tests. Straight-line, least-squares fit of all calibrations showed a deviation of ± 0.2 psi (0.14 N/cm²) maximum and ± 0.1 psi (0.07 N/cm²) average for the strip-recorder readings and double these figures for the oscillograph readings.

Temperatures. - Eight temperatures were measured, as shown in figures 4 and 5: outside wall temperatures at the control venturi inlet T_{C1} and outlet T_{C2} and at the test venturi inlet T_{in} and outlet T_{out} ; and four temperatures T_1 , T_2 , T_3 , and T_4 at the bottom of four holes drilled to within 0.060 inch (0.152 cm) of the inside surface of the test venturi. For the second series of tests, thermocouple T_1 was removed to make room for the cavity insert.

Chromel-Alumel thermocouples were used to measure all temperatures. The thermocouple wire had a diameter of 0.020 inch (0.051 cm) and was purchased to ISA type-K special limit of error ($\pm 3/8$ percent). Thermocouple bare junctions were spot welded to the points of measurement. Outputs were recorded in one null-balance multipoint strip recorder with a range of 0° to 1800° F (255 to 1255 K). The record span was 11 inches (27.9 cm), and the smallest division was 10° F (5.56 K).

Direct, in-place calibration of the thermocouples was not made because of the difficulty of introducing an accurate reference in the loop. However, the test venturi outlet thermocouple T_{out} was compared with the potassium saturation temperature corresponding to the test venturi outlet pressure P_5 on those runs where vapor phase was known to exist at that location. The measured temperature was 6.5° F (3.6 K) lower than the saturation temperature on the mean, with no allowances made for heat losses. In addition, a measure of the scatter between the six thermocouples around the test venturi was obtained by comparing their readings during liquid runs, when the venturi was isothermal. The mean deviations are all within the limit of error of the thermocouple wire. The results of these comparisons are discussed in more detail in appendix B. (Symbols are defined in appendix A.)

Flow. - Flow rate was measured by an electromagnetic (EM) flowmeter located downstream of the test venturi. The liquid-metal flow member of the flowmeter was a type-316 stainless-steel tube with a 0.500 inch (1.27 cm) outside diameter and 0.065 inch (0.165 cm) wall thickness. The maximum field strength was 3307 gauss (0.3307 T) with a variation of 1 percent of the maximum throughout the field. The output of the flowmeter varied between 149 and 153 pounds mass per hour per millivolt (18.8 and 19.3 g/(sec) (mV)) depending on the liquid-metal temperature. The electrical output was recorded on a null-balance strip recorder, as well as in one of the channels of the multichannel oscillograph which was also recording the pressure transducer signals.

The pressure drop across the control venturi, together with the water flow calibration of the as-received venturi, was used as a secondary flow reading for cases where

low-quality vapor flowing through the EM flowmeter distorted its output.

There was no direct calibration of the EM flowmeter. However, the flow rates measured by it and the flow rates obtained from the control venturi agree within 5 percent, as shown in appendix B.

Noise. - A high-sensitivity, general-purpose piezoelectric accelerometer was attached at the end of a 10-inch- (25-cm-) long tube. The accelerometer was capable of measuring vibrations to 1000 g's over the frequency range of 2 to 7000 hertz. The tube was welded to the body of the test venturi in the neighborhood of the throat area. The purpose of the accelerometer was to detect pressure pulses that might indicate the formation and/or collapse of bubbles.

The output of the accelerometer was routed through a charge amplifier to a channel of the multichannel oscillograph which was also recording pressures and flow signals. The signal was also paralleled to an oscilloscope for visual monitoring.

No calibration of this device was attempted, as its purpose was to give qualitative rather than quantitative data.

EXPERIMENTAL PROCEDURE

Two series of tests were made:

- (1) Test venturi without artificial throat cavity (series I)
- (2) Test venturi with artificial throat cavity (series II)

The same experimental procedure was followed for both series, unless otherwise specified. Considerable details are presented because of the possible effects of the pressure-temperature history of the surface and fluid on liquid superheats, as pointed out by Holtz (ref. 8) and Chen (ref. 10). However, only those steps in the procedure which may have bearing on the results are described.

The procedure can be divided into three parts: preoperative, data taking, and post-operative. It is worthwhile to note that operation of the loop was continuous for each series once liquid metal was introduced into the system.

Preoperative Procedure

The preoperative procedure was as follows:

- (1) The empty loop was pressurized with high-purity argon to 3 atmospheres, then evacuated to 0.030 torr. This step was repeated three times.
- (2) The empty loop was pumped down to 0.010 torr, heated to 400⁰ F (477 K), and held under these conditions for 48 hours.

(3) The potassium in the dump tank was melted and the liquid heated to 400° F (477 K) by trace heaters.

(4) Liquid potassium was forced into the loop until a predetermined level in the expansion tank was reached.

(5) The pressure level of liquid potassium was increased to 30 psia (20.7 N/cm²) by applying argon pressure above the potassium in the inventory tank.

(6) Liquid potassium was circulated at 700 pounds mass per hour (88 g/sec) and the temperature raised to 1300° F (978 K). Flow was maintained at these conditions for 60 hours for purification purposes. A potassium sample taken after this time showed an oxide concentration of less than 10 parts per million.

(7) The temperature of the circulating potassium was decreased to 800° F (700 K) and flow stopped. Pressure transducers were calibrated by varying the argon pressure at the inventory tank from 0 to 50 psia (0 to 34.5 N/cm² abs).

(8) Flow was reestablished. Temperature level and flow rate were brought to those values required for the acquisition of data.

Data-Taking Procedure

The data-taking procedure was as follows:

(1) All-liquid performance curves of the venturis were obtained. The pressure level was maintained higher than the vapor pressure throughout the loop. Flow rate varied from 120 to 700 pounds mass per hour (15 to 88 g/sec).

(2) Cavitation and flashing data on the test venturi were obtained. For each set of runs, a given flow rate and temperature were established. Starting with the minimum loop pressure (at the test venturi throat) above vapor pressure, the pressure level in the loop was decreased in small steps by reducing the gas pressure at the inventory tank. During time of change, an oscillograph recording was taken. After each change, a data point was recorded from the oscillograph as well as by readings from the strip recorders. This procedure was continued until cavitation and/or flashing developed. The change in system pressure affected the flow rate in some cases. If so, corrections were made to bring the flow rate and temperature back to the preestablished conditions before the steady-state data points were taken. Sometimes the set of data was ended as soon as flashing developed; at other times, the pressure level was decreased even further. In some series, the pressure level was raised again until all-liquid performance was clearly reestablished. Some "ramped" data sets were also taken. These data differ from the data just described in two respects: the decrease or increase in pressure level was continuous, and the loop was not readjusted when flow rate was affected. During these runs, a continuous oscillograph recording was taken.

(3) Another all-liquid performance curve of the venturis was obtained. After all the desired cavitation data were taken, the first step of the data-taking procedure was repeated. This step was not taken for the first series of tests, the one with the test venturi without artificial throat cavity.

Postoperative Procedure

The postoperative procedure was as follows:

(1) Liquid-potassium temperature was decreased to 800°F (700 K) and flow stopped. The pressure transducers were calibrated again.

(2) Liquid potassium was forced from the loop into the dump tank by argon pressure. Argon pressure was maintained at 20 psia ($13.8\text{ N/cm}^2\text{ abs}$) in the empty loop.

(3) The post-test procedure differed in test series I and II.

(a) After series I (test venturi without artificial throat cavity), the insulation around the test section was removed. Thermocouple T_1 was pulled out and its blind hole drilled through to the inside of the venturi at the throat, as shown in figure 5(b). This operation was performed while the loop was pressurized above atmospheric pressure with argon. Care was exercised to minimize disturbances to the inside surface. The hole was drilled undersized and then reamed to required size with a series of drills. The cavity insert shown in figure 6 was installed and seal welded to the outside surface of the venturi. The test section was reinsulated; then the preoperational procedure already described was repeated for series II.

(b) After series II (test venturi with artificial throat cavity), the test section was cut out of the loop as one piece and capped while still full of argon gas. The control and test venturis were separated in a moisture- and oxygen-free atmosphere. Each of the venturis was placed in a vacuum and heated to evaporate any potassium traces. They were then sectioned to allow examination of the inside surface.

RESULTS AND DISCUSSION

The conditions and nature of the experimental data acquired in this program are summarized in table I. Detailed data for all the runs appear in tables II and III. The runs are listed in the same sequence in which data were acquired. The tabulated data are measured values, with the exception of the dynamic head q , the test venturi throat pressure P_t , the exit thermodynamic quality X , the overall pressure-drop ratio $(P_4 - P_5)/(P_1 - P_3)$, and the saturation pressures P_{vin} and P_{vout} , which are calculated from the measured data. Details of the calculations of q , P_t , and X appear in appendix C.

The results are separated into different sections for discussion purposes as follows:

- (1) General venturi behavior
- (2) Liquid performance
- (3) Flashed performance
- (4) Incipient characteristics
 - (a) Cavitation incipency
 - (b) Flashing incipency
 - (c) Comparison with heat-addition-data in the literature
- (5) Metallographic inspection

The effect of the artificial cavity at the venturi throat is discussed under each of these sections.

General Venturi Behavior

Classification of data points is given in the remarks column in tables II and III. The accelerometer output signal and the overall pressure-drop ratio form the basis for this classification. Liquid runs are those where the accelerometer outputs show no noise and the overall pressure-drop ratio of test to control venturi is approximately 1 (± 0.15). Cavitated runs show appreciable noise but no increase in the overall pressure-drop ratio. Flashed runs have an increase in overall pressure-drop ratio (larger than 1.4). The two remaining categories cover the conditions existing immediately before the appearance of noise (incipient cavitation), and before the change in overall pressure-drop ratio (incipient flashing).

Incipency data were taken from oscillograms such as the one in figure 7. This particular oscillogram was taken during ramped change between runs 105 and 106. Two sections are shown: one covering the incipient cavitation point (run 105a), the other covering the incipient flashing condition (run 105b). The point where noise starts is obvious from the accelerometer trace, even though flow rate and pressure traces are undisturbed. With a further decrease in pressure, the high noise level becomes fully established until the point of incipient flashing is reached. At this point, the following events occur:

- (1) The high level of noise disappears.
- (2) Flow rate decreases.
- (3) Overall pressure drop in the control venturi $P_1 - P_3$ decreases, reflecting the flow rate decrease.
- (4) Overall pressure drop in the test venturi $P_4 - P_5$ increases.

The point of incipient flashing, run 105b in this case, consists of the operating conditions existing just prior to these changes.

The general behavior of the venturi without the artificial throat cavity is shown in figure 8 by two typical sets of data. The throat pressure, calculated as shown in appendix C, was plotted against the outlet pressure for constant values of flow rate and inlet temperature after any necessary readjustments were made. In figures 8(a) and (b), the outlet pressure started at a high level, was decreased to a minimum, and then was raised again. The circles represent points taken during the pressure decreases; the squares are points taken during pressure increases. As the outlet pressure decreased, the throat pressure decreased an equal amount. This relation remained unchanged even after the appearance of cavitation. The incipency of cavitation noise is shown by the first open circle encountered as the outlet pressure decreases. Figure 8 shows that cavitation did not appear until the throat pressure was appreciably below the vapor pressure corresponding to the inlet temperature P_{vin} . This indicated the liquid was under tension, at least in the throat area. Comparison of the outlet pressure P_5 with the value of P_{vin} (superimposed on both ordinates of fig. 8) shows that in one case (fig. 8(a)) cavitation occurred while the venturi outlet pressure was still above the vapor pressure. When the diffuser dimensions and the corresponding dynamic head recovery are taken into account, this means that part of the diffuser was also above vapor pressure. In the other case (fig. 8(b)), the venturi was all liquid even when the outlet pressure was below vapor pressure, which means that liquid tension existed throughout the diffuser. It is also worthy of note that three points in figure 8(b) show cavitation characteristics even though the whole diffuser is under tension.

Further decrease in outlet pressure resulted in a sudden and appreciable increase in throat pressure. After loop conditions were adjusted to restore the established values of flow rate and inlet temperature, any further decrease in outlet pressure did not affect the value of throat pressure, as shown in figure 8(a).

An appreciable hysteresis was encountered when the outlet pressure was increased. Increasing the outlet pressure from the flashed condition had no effect on the throat pressure, as shown by the square symbols in figure 8, until the outlet pressure reached a higher value than the value at which incipient flashing occurred during the pressure decrease. After deflashing, the venturi pressure-drop characteristics returned to original preflashed conditions, with the throat pressure again indicating liquid tension without cavitation when steady-state operating conditions were restored.

The limiting value of throat pressure achieved after flashing was slightly lower than the vapor pressure at inlet temperature P_{vin} . This difference could be the thermodynamic depression necessary to create vapor, as indicated in reference 6, and/or an indication of the vapor conglomeration (of whatever nature) occurring in the diffuser after a certain amount of pressure recovery had taken place.

Similar results for two sets of data for the test venturi with the artificial cavity at the throat are presented in figure 9. Each of these sets is composed of two different ex-

cursions in pressure. The cavitation characteristics for the venturi with the 0.008-inch (0.020-cm) artificial cavity were very similar to the ones obtained for the venturi without an artificial cavity: liquid tensions/superheats were observed, and the inception of cavitation did not change the pressure-drop characteristics. Again, a limiting calculated throat pressure was achieved after flashing. Flashing occurred sharply, as before. Hysteresis between flashing and unflashing points was again present. A major difference between the results in figure 9 and those described in figure 8 for the venturi without the artificial throat cavity was the level of the limiting throat pressure reached. For the venturi with the artificial throat cavity, the calculated throat pressure was higher than the vapor pressure at inlet temperature. This can be explained by the presence of vapor at the throat of the venturi, which would cause the effective minimum flow area to decrease. Therefore, equation (9) of appendix C is no longer applicable to the calculation of the throat pressure of the test venturi for flashed runs.

Another difference observed was that in some cases the venturi returned to a liquid-tension (but cavitating) condition after deflashing. This is probably nothing more than an indication of randomness in the behavior of cavitation inception.

In figure 9(a), the point of incipient cavitation for the first decrease in the set (highest open circle) occurs at higher pressures than the second incipency point (highest open triangle). However, the points of incipient flashing are very close for both excursions. Set 12 (fig. 9(a)) is the first set of cavitating runs obtained after the system was filled with potassium for the second series of tests. The appearance of early cavitation in this set can be the result of residual gas from the fill procedure. This gas, accumulating in large-size cavities, may induce early cavitation. However, these cavities will soon be deactivated, as the gas is transported away without being replenished.

Figures 8 and 9 are composed of data points taken after flow rate and inlet temperature were returned to the preestablished constant values. As such they do not reflect the actual uncorrected changes taking place in pressures, temperatures, and flow, especially during flashing. The best way to describe the behavior of the venturi during an imposed change in outlet pressure is to plot all the venturi variables as a function of time. Such a graph is shown in figure 10. This figure covers the data taken during the ramped change between runs 105 and 106. The pressure, flow rate, and noise traces were taken from a continuous oscillogram, the temperatures from the recorder output. The vapor pressures P_{vin} and P_{vout} are the values corresponding to inlet temperature T_{in} and diffuser outlet temperature T_{out} , respectively. The pressure ramp was started at 0 seconds and continued until the venturi flashed (420 sec). At this time, the venturi outlet pressure was not reduced any further.

Figure 10 shows that from 0 seconds (at which time pressure level reduction started) to 330 seconds, all pressures were reduced equally, without any change in flow rate or temperature. The accelerometer trace gave no indication of pressure pulses associated

with the presence of bubbles. At 330 seconds, the throat pressure P_t indicated a large amount of tension. Actually, the indicated value of the throat pressure was below zero absolute pressure. At this time, the accelerometer trace increased in width, indicating bubble formation and/or collapse. This noise level was maintained until 420 seconds. During this interval, the pressures decreased in the same manner as before the appearance of bubbles; the temperatures were not affected, and the flow rate was not altered. Until this time, all the temperatures throughout the test venturi were equal. Flashing occurred at 420 seconds. The test venturi outlet pressure P_5 was the only variable that did not change during flashing as it was directly controlled by the bias gas pressure in the expansion tank. The rest of the pressures at both venturis increased with a jump, the flow rate decreased sharply, the noise level decreased, and the temperatures along the venturi wall took different values.

The decrease in flow rate is caused by the adjustment of the system to the higher pressure loss introduced by the flashed venturi. The reduced flow rate results in lower pressure drops in the all-liquid control venturi (P_1 , P_2 , and P_3). The test venturi pressure loss $P_4 - P_5$ has increased almost twofold. The calculated throat pressure P_t , which as indicated during the discussion of figure 9 is no longer a true estimate, appears higher than the vapor pressure at inlet temperature. The outlet pressure P_5 corresponds closely to the vapor pressure at the venturi outlet P_{vout} , indicating the presence of vapor at equilibrium conditions at the venturi outlet.

The increase in the temperature of the liquid potassium entering the control venturi T_{C1} is caused by the decrease in flow rate through the constant-heat-input electric heaters. The increase in temperature drop from control to test venturi is also a reflection of the reduced flow rate. The sudden drop occurring between the test venturi inlet temperature T_{in} and the venturi outlet temperature T_{out} is a measure of the thermodynamic depression necessary to produce the amount of vapor resulting from flashing (~1 percent quality at end of transient). The slow decay in the flow rate after flashing appears to be associated with the slow rise in inlet temperature T_{in} .

The nature of the change in the noise level can be explained by assuming that most of the pressure pulses are produced by bubble collapse, rather than formation. Before the appearance of vapor conglomerates, the bubbles are collapsing individually in essentially all liquid surroundings. After flashing, the compressible volume present dampens the pressure pulses.

All the data points obtained for the venturi with and without the artificial cavity at the throat are shown in figure 11. The overall pressure drop $P_4 - P_5$ is plotted as a function of superficial dynamic head at the throat q .

The nonflashed data, whether all-liquid or cavitated, fall along the solid lines in figures 11(a) and (b). Flashing runs fall to the right of the dashed lines. It was not possible to obtain any data in the region between the solid and dashed lines, because the

system jumped from the liquid line to the flashed area and the reverse. This jump, during the onset of flashing as well as during deflashing, was very sharp and it was not accompanied by oscillations between the two states, even though figure 7 shows small local fluctuations in the pressure traces. Stone and Sekas (ref. 2), performing similar tests in water, did not consistently experience the jump between liquid-cavitated and flashed conditions. Whenever they observed a jump, its magnitude was small. Also, their data at the inception of flashing were highly oscillatory, as a rule. The difference in behavior between potassium and water (as to the irreversibility of the jump during flashing and deflashing) seems to depend on the properties of potassium, which allow large liquid superheats/liquid tensions, with the consequent storage of energy in a metastable condition. Among these properties of potassium are the purity of the liquid phase and the low solubility of gases, which eliminates potential nucleating sites within the liquid bulk; its high surface tension and ability to destroy oxide films from the containing walls, which drowns out most of the potential nucleating sites at the wall; and its high thermal conductivity, which allows the transfer of the stored energy to the vapor phase (once it is formed) with a minimum of temperature drop across the liquid bulk.

Liquid Performance

The solid lines in figures 11(a) and (b) represent the pressure-flow performance of the venturi when it is operating with potassium in the liquid phase. These liquid lines, over the Reynolds number range covered, indicate a constant loss coefficient

$$\frac{P_4 - P_5}{q} = C \quad (1)$$

Equation (1) neglects the difference in dynamic head between the venturi inlet and outlet, even though the two diameters are not equal (see fig. 4). The maximum value of this difference over the flow range studied was about 0.15 psi (0.1 N/cm²), which is smaller than the scatter in the pressure readings.

The liquid data for the venturi without the artificial throat cavity (sets 1 to 10, fig. 11(a)) are correlated by

$$\frac{P_4 - P_5}{q} = 0.44 \quad (2)$$

while the liquid data for the venturi with the artificial throat cavity (sets 11 to 20, fig. 11(b)) fit the relation

$$\frac{P_4 - P_5}{q} = 0.50 \quad (3)$$

which represents about a 13 percent increase in pressure losses over the venturi without the throat cavity (eq. (2)). This increase in losses is attributed to the small protrusion of the cavity insert into the flow channel, as described under Test Section.

It should be noted that the loss coefficient for the control venturi had a constant value of 0.48. This value of 0.48 for the control venturi with the very-sharp-edged pressure tap at the throat fell between the 0.44 obtained for the test venturi without a throat cavity and the 0.50 for the test venturi with the somewhat irregular throat cavity insert.

Flashed Performance

The pressure-flow characteristics of the venturi after flashing were quite different from those during liquid flow conditions. After flashing, the superficial dynamic head at the throat q is no longer a function of the venturi overall pressure drop (fig. 11). The overall pressure drop is now much larger than during the all-liquid operation. Different values of overall pressure drop were obtained for a given value of q .

The difference in behavior shown in figure 11 between the flashed and the liquid data indicates that the relation between venturi upstream and downstream pressures is no longer controlled by liquid loss mechanisms, but by some other independent factor. This independent factor could be the presence of a vapor continuum somewhere in the small flow area of the venturi. This being the case, the flow rate after flashing should become a function of some value of the potassium saturation vapor pressure and the inlet pressure P_4 . Figure 12 shows that the flow rate after flashing is a function of the difference between the inlet pressure P_4 and the potassium vapor pressure corresponding to the inlet liquid temperature P_{vin} . Plots similar to figure 12, but using vapor pressures corresponding to diffuser wall temperature P_{v2} , and outlet temperature P_{vout} , showed that the flow rate did not correlate with these vapor pressures when these were different from P_{vin} . This leads to the possible conclusion that during flashed operation the liquid potassium reaches saturated liquid conditions before vaporizing and the flow rate is determined by the difference between venturi inlet pressure and the vapor pressure at the inlet liquid temperature.

Figure 12 also shows that during flashed operation the relation between flow and inlet overpressure $P_4 - P_{vin}$ is greatly affected by the presence of the artificial cavity

at the throat. This is evidenced by the difference in slope between the two correlating lines.

Figure 13 compares, against superficial dynamic head at the throat, the difference between inlet and throat pressure $P_4 - P_t$ for the liquid data, and the difference between inlet pressure and inlet temperature vapor pressure $P_4 - P_{vin}$ for the flashed data.

For the venturi without the artificial throat cavity, the liquid pressure drop to the throat $P_4 - P_t$ is higher than the inlet overpressure during the flashed runs $P_4 - P_{vin}$, as shown in figure 13(a). Assuming that the liquid potassium is at equilibrium at the flashing location, the slight tension at the throat means that the equilibrium condition occurs downstream of the throat, after some pressure recovery has taken place. From the slope of the two curves in figure 13(a) and the geometric characteristics of the diffuser, and with the additional assumption that the nozzle performance did not change from the liquid condition, a distance of about 0.1 inch (0.25 cm) minimum between the throat and an effective interface location was estimated. This means, of course, that during flashed operation the liquid potassium remained under slight tension (equal to $P_{vin} - P_t$) while going through the venturi throat. Furthermore, the temperature readings at T_2 , located 0.4 inch (1.0 cm) downstream of the throat, show the presence of vapor continuum at this location already, when there is net vapor quality at the venturi outlet. Therefore, the location of the equivalent interface should be between a minimum of 0.1 inch (0.25 cm) downstream of the throat, as indicated by the pressure curves, and a maximum of 0.4 inch (1.0 cm) as indicated by the diffuser wall temperatures.

For the venturi with the artificial throat cavity, the results are reversed, as shown in figure 13(b). The inlet overpressure $P_4 - P_{vin}$ during flashing is higher than the liquid nozzle pressure drop $P_4 - P_t$ for a given value of superficial velocity head. This change can be explained by assuming that the artificial cavity induces vapor into the throat, thereby changing the minimum liquid flow area. Consequently, the superficial dynamic head at the throat q is no longer the maximum velocity head. If it is assumed that (1) the liquid at the throat is at equilibrium and (2) the difference in slope of the curves in figure 13(b) is the measure of the change in throat dynamic head, a throat area reduction of 7.3 percent would explain the results. To indicate the absolute magnitude of this change, it could be expressed as an annular vapor ring thickness of only 0.0019 inch (0.0048 cm) at the throat.

The behavior of the diffuser portion of the venturi during flashing is shown in figure 14. The difference between inlet pressure and inlet temperature vapor pressure $P_4 - P_{vin}$ is plotted as a function of overall pressure drop $P_4 - P_5$ in figure 14(a). The difference between inlet pressure and diffuser outlet vapor pressure $P_4 - P_{vout}$ is plotted in figure 14(b), also as a function of overall pressure drop. The solid symbols in both figures indicate those runs with a measurable temperature depression; that is, where temperature T_2 in the diffuser was lower than the inlet liquid temperature.

Figure 14(a) shows that the diffuser had a net pressure drop $[(P_4 - P_5) > (P_4 - P_{vin})]$ for those data where a temperature drop was measured. This diffuser net pressure drop, occurring with or without the artificial cavity at the throat, is to be expected for the higher fluid velocities associated with an exit vapor phase. As shown in tables II and III, vapor qualities as high as 1.3 percent were obtained at the diffuser exit. The diffuser net pressure drop changed with the values of quality calculated from the temperature depression. For the flashed data in which no temperature depression was observed, the diffuser had a pressure recovery $[(P_4 - P_5) < (P_4 - P_{vin})]$ meaning that very little vapor phase is being generated, and that the flow is returning to the all-liquid condition before leaving the diffuser. The change in magnitude of the pressure recovery indicates that the return to the all-liquid state occurs at variable positions within the diffuser.

The plot of pressure difference between inlet pressure and vapor pressure at outlet temperature $P_4 - P_{vout}$ as a function of overall pressure drop (fig. 14(b)) shows that for the flashed runs where a temperature depression existed, the outlet venturi pressure was at equilibrium with its vapor pressure $P_4 - P_{vout} = P_4 - P_5$. For those cases where no temperature depression existed, the outlet pressure P_5 was higher than the vapor pressure at outlet temperature.

The behavior of the flashed venturi can be summarized as follows:

- (1) The overall flow rate is determined by the difference between the inlet pressure and the vapor pressure corresponding to the inlet liquid temperature.
- (2) The overall pressure drop in the venturi determines the conditions of the mixture leaving the venturi. If the back pressure is higher than the vapor pressure at inlet temperature, the vapor phase will collapse someplace in the venturi; if it is lower, it will generate an equilibrium two-phase mixture, with the quality being dependent on the difference between outlet pressure and inlet vapor pressure. During these tests, exit qualities as high as 1.3 percent were measured.
- (3) The location where flashing starts appears to be slightly downstream of the throat in the smooth venturi and at the throat when the artificial cavity is installed at the throat. For the smooth venturi, pressure recovery characteristics locate the interface at least 0.1 inch (0.25 cm) downstream of the throat; the temperature data indicate that it is no more than 0.4 inch (1.0 cm) from the throat.

Incipency Characteristics

An important aspect of the cavitating venturi as a potassium boiler inlet device is its behavior at the initial appearance of the vapor phase. The maximum amount of liquid tension/superheat supported before incipency of vapor is of prime importance in deter-

mining how far a cavitating venturi backpressure must be lowered, or its flow rate increased, before two-phase flow is developed.

Two different types of incipency points were detected during this experimental program:

(1) Cavitation incipency: Determined by the output of the accelerometer attached to the venturi body. The sudden increase in amplitude of the "noise" signal was taken as an indication of bubble collapse.

(2) Flashing incipency: Determined by the sudden change in pressure-drop characteristics of the venturi. In some instances, as shown in the remarks column in table II, the cavitation and flashing incipency points coincided; in other cases, cavitation was detected prior to flashing.

The two-phase incipency results obtained are presented in figures 15 to 17 in plots of pressure at the throat P_t as a function of inlet liquid temperature. This type of presentation permits direct comparison of the data obtained in this project for potassium flowing adiabatically through a variable pressure field with the incipient data obtained by Chen (ref. 10), Edwards and Hoffman (ref. 9), and others, in a constant-pressure field with heat addition.

Cavitation incipency. - The minimum values of throat pressure P_t obtained before cavitation noise was detected by the accelerometer are plotted in figure 15 as a function of inlet temperature T_{in} . The throat pressures were determined from the venturi liquid characteristics, using equation (9) of appendix C. The results appearing in figure 15 cover both series of runs: with and without the artificial throat cavity. Also individually identified in this figure are the first and second chronological cavitation incipency points obtained for each series. Superimposed on the data appear two types of reference curves:

- (1) The potassium vapor pressure curve (solid)
- (2) A family of pressure-temperature curves (dashed) representing the liquid pressures necessary to maintain a force balance around vapor bubbles of different radii at thermal equilibrium with the liquid. The liquid pressures for this family of curves were obtained from

$$P = P_v - \left(\frac{2\sigma}{r} \right)_{T_v} \quad (5)$$

for values of r ranging from 1.0×10^{-3} to 1.0×10^{-5} inch (2.54×10^{-3} to 2.54×10^{-5} cm). The potassium vapor pressure curve, of course, agrees with equation (5) for a value of $r = \infty$.

The following conclusions can be drawn from figure 15:

(1) Fluid conditions at the throat of the venturi were not at equilibrium at cavitation incipency. This nonequilibrium condition, for most of the data, fell between the curves obtained from equation (5), with the critical radii between 1.0×10^{-4} and 0.5×10^{-4} inch (2.54×10^{-4} and 1.27×10^{-4} cm). A few data points did not show this trend. These exceptions are discussed in conclusions 2 and 3.

(2) The first cavitation incipency points in each series, with and without the artificial throat cavity, occurred very close to the potassium vapor pressure curve (see runs 4 and 77 in table II). These two points definitely did not follow the depression pattern of the rest of the cavitation incipency data. This difference in behavior appeared to be caused by the residual argon gas trapped in the surface cavities during fill (see section EXPERIMENTAL PROCEDURE). The residual argon must have accumulated in surface cavities of large size, preventing them from flooding and thus making them active cavitating sites, as indicated by Chen (ref. 10). During the first pressure decrease, the larger-size cavities probably caused cavitation at near-equilibrium conditions. After the first flashing and deflashing cycle, most of the large-size cavities were depleted of gas and were flooded, becoming inactive sites. Therefore, in successive pressure decreases the remaining smaller cavities caused larger decreases in pressure to be necessary in order to trigger cavitation.

(3) The artificial cavity at the throat of the venturi did not have any effect on the mean value of the liquid tension obtained. This means that in an adiabatic field, where the walls were not hotter than the fluid bulk, neither the 0.008-inch- (0.020-cm-) diameter reentrant hole, nor the 0.0005-inch (0.0015-cm) annular gap between the cavity insert and the drilled hole, were dependable active cavitation sites. However, a few of the incipency points obtained with the insert (other than the first of the series) approached the $r = 0.5 \times 10^{-3}$ inch (1.27×10^{-3} cm) line, indicating that the artificial cavity did act occasionally as a nucleating site.

(4) It can be seen that some points fall at a liquid pressure below absolute zero. These points can be described as having a finite liquid tension, but the corresponding liquid superheat would be infinite and meaningless.

Flashing incipency. - The results obtained on flashing incipency are presented in figure 16. The reference curves in this figure are the same as those already described for figure 15. The incipient flashing data consist of the pressure calculated at the venturi throat P_t immediately before the sudden change in venturi pressure-drop characteristics, as a function of inlet liquid temperature. As before, throat pressure was calculated by using equation (9) of appendix C. If the cavitating venturi is to be used as a boiler inlet, its flashing incipency characteristics are more important than the point where cavitation noise first develops, but without vapor agglomeration.

The following conclusions can be drawn about the flashing incipency:

(1) Fluid conditions at the throat of the venturi were not at equilibrium at flashing

incipiency. Throat pressures P_t as much as 16.1 psi (11.1 N/cm^2) below vapor pressure were measured. This occurred at a 1460° F (1066 K) liquid temperature.

(2) The point conditions at flashing incipency also follow the surface-tension curves obtained from equation (5) for a critical radius between 1.0×10^{-4} and 0.5×10^{-4} inch (2.54×10^{-4} and 1.27×10^{-4} cm). No appreciable difference in the mean value of correlating critical radius between the flashing incipency data and the cavitation incipency data can be noted.

(3) There is no effect at all of the artificial throat cavity on the values obtained for pressure and temperature at flashing incipency.

(4) Some of the throat pressures reached at flashing incipency show large values of negative absolute pressure, as much as -6.5 psia ($-4.5 \text{ N/cm}^2 \text{ abs}$).

(5) The incipient flashing points (fig. 16), without exception, follow the trend indicated by the constant critical radius lines. Some of the incipient cavitation points (fig. 15), as discussed previously, deviate appreciably from the mean critical radius values. This appears to be the biggest difference between the incipient flashing and the incipient cavitation results.

Comparison of incipency results with heat-addition data in the literature. - The incipient flashing results obtained in this project are replotted in figure 17, together with other potassium boiling incipency data available in the literature. The reference curves shown are the same as those used in figures 15 and 16.

A search of the literature for potassium flashing initiation data did not yield any data obtained adiabatically through pressure decreases. A few investigators, however, have published data on the boiling incipency of potassium with heat addition. Shown in figure 17 are data published by Edwards and Hoffman (ref. 9); Chen (ref. 10); Spiller, et al. (ref. 15); and Grass, et al. (ref. 16). The methods used by these investigators to promote boiling and to determine the point of incipency are quite varied. Great variation also exists in the type of surfaces used, the range of heat fluxes, the potassium purity, gas content, and fluid velocity, among other factors, as pointed out by Fauske in reference 17. Some of these conditions for the data shown in figure 17 are summarized in the following table:

| | Edwards and Hoffman (ref. 9) | Chen (ref. 10) | Spiller, et al. (ref. 15) | Grass, et al. (ref. 16) | This report |
|---|--|---|--|--|--|
| Test method | Heat addition | Heat addition | Heat addition | Heat addition | Adiabatic pressure decrease |
| Potassium flow | Natural circulation | Forced circulation | Stagnant | Natural and forced circulation | Forced circulation |
| Heating method | Electric clam-shell heaters around wall | Electric clam-shell heaters around wall | Electric current flowing through wall and liquid; heat generated mostly within fluid | Same as ref. 15 | None |
| Heat-flux range, Btu/(hr)(ft ²) (W/m ²) | 16 000 to 37 000; (50 400 to 116 600) | 2 000 to 50 000 (6 300 to 157 500) | Not applicable | Not applicable | None |
| Surface | Drawn tubing; type-347 stainless steel; 0.622-in. (1.58-cm) i.d.; (a) As received (b) With a series of eight 0.006-in. - (0.015-cm-) diam holes (drilled) | Gun drilling; Haynes alloy 25; 0.622-in. (1.58-cm) i.d.; as received | Not important according to author as it is colder than fluid | Tube; 0.276-in. (0.7-cm) i.d.; 78.7 in. (200 cm) long | Machined venturi, 5 to 6 rms surface finish; 0.1015-in. (0.2578-cm) throat diam; type-316 stain- less steel; (a) As received (b) With 0.008-in. - (0.020-cm-) diam reentrant throat cavity (EDM) |
| Determination of superheat | Maximum temperature at heated surface; minimum temperature at condenser | Pressure and tempera- ture measurements | Change in electric potential distribution along test section | Same as ref. 15 | Pressure and tempera- ture measurements |
| Pressure-temperature history | Not given | Detailed | Not given | Not given | Given |

The data of Spiller, et al. (ref. 15) on stagnant potassium, show a large scatter, and the results appear to have no relation to the surface-tension curves. The rest of the data appear to follow the surface-tension trends. However, the values of critical bubble radius vary largely from investigator to investigator. The adiabatic flashing data obtained herein seem to agree best with the data obtained by Chen (ref. 10). This result should be expected, because in his tests the fill and testing procedure and the nature of the test surface more closely approximated the conditions of the adiabatic tests in the venturi.

Comparison of our adiabatic results with those of Edwards and Hoffman (ref. 9) shows the difference in effect of relatively large-size cavities at the wall between the heat-addition case and the adiabatic case. With heat addition, the presence of eight 0.006-inch- (0.015-cm-) diameter holes in the wall decreased the superheat at incipency very markedly. Our adiabatic data, on the other hand, showed no effect whatsoever on incipency from a reentrant cavity of 0.008 inch (0.020 cm) diameter or the annular gap 0.0005 inch (0.0012 cm) wide around the cavity insert. This indicates that potassium floods cavities of this size. These cavities may become active cavitation sites if heated, but will not do so adiabatically.

It should be noted that Chen's data (ref. 10) indicate a critical radius of 10^{-4} inch (2.54×10^{-4} cm), similar to our data; Edwards (ref. 9) suggests a critical radius smaller than 10^{-5} inch (2.54×10^{-5} cm) for the as-received surface, while the stagnant potassium data of reference 15 show no critical radius value whatsoever, but indicate very high superheats.

Metallographic Inspection

After completion of the tests, the inside surfaces of the test and control venturis were inspected. Also inspected was the venturi not used in the potassium tests (the as-received venturi). The results of these inspections appear in figures 18 and 19. The venturis were sectioned longitudinally. Figure 18(a) shows views normal to the diffuser surfaces of the three venturis. This figure shows what was apparent to the unaided eye: the surface finish had changed after approximately 250 hours of operation with potassium. The as-received surface had a high shine, whereas surfaces on test and control venturis had a dull finish.

Larger magnifications ($\sim 35\times$) of the same inside surface of the diffusers are shown in figure 18(b). The as-received venturi diffuser shows circumferential scratches caused by the polishing process. It also shows large-size pits, greater than 4×10^{-4} inch (1.02×10^{-3} cm). Both the polishing scratches and large-size pits are absent from the surfaces of the control and test venturis. This must be attributed to the effect of liquid

potassium flow rather than cavitation or flashing, as the control venturi was not cavitated during operation.

The test and as-received venturis were cross sectioned at the beginning of the diffuser (near the throat). Photomicrographs (fig. 19) were taken of the inside surfaces of the venturis. The inside surfaces shown are perpendicular to the direction of flow. The surface of each venturi was observed under the microscope, and typical cross sections are shown. The inside surface of the test venturi appeared rougher than that of the as-received venturi at this magnification. It shows many cavities in the 10^{-4} - to 10^{-5} -inch (2.54×10^{-4} - to 2.54×10^{-5} -cm) size range, which coincides with the critical radii curves correlating the data in figures 15 and 16. Very few cavities of this type can be seen on the as-received surface. The cavities appearing on the test venturi surface cover a gamut of shapes: conical, spherical, reentrant. However, they did not penetrate deeply into the wall.

Of secondary importance is the change in structure noted in the type-316 stainless steel. The as-received venturi had a large grain structure with no carbide precipitation. After 250 hours of operation, mostly between 1300° and 1500° F (978 and 1089 K), there was a large amount of intergranular and matrix carbide precipitation. The grain size seemed to have decreased considerably. All venturis were made from the same bar of material and exposed to the same metalworking processes. There is no reason to believe that the structure of the test venturi was different at the start from that shown in figure 14(a).

CONCLUDING REMARKS

The behavior of an adiabatic venturi with subcooled-liquid-potassium feed was studied experimentally before, during, and after the development of two-phase flow. The results indicate that a venturi inlet that will cause flashing of the subcooled liquid into two-phase flow, without oscillations and with large pressure drops, can be designed for a potassium boiler tube. Prior to the start of flashing, a metastable condition with large liquid tensions/superheats may be encountered. After flashing, only a small amount of tension/superheat, if any, will be found, and the total liquid flow rate will be independent of downstream conditions and influenced only by the liquid temperature and inlet pressure.

The large pressure drop at the boiler tube inlet tends to improve boiler stability, as indicated by other investigators. The total flow rate independence from downstream pressure, also noted in water flow by others, should be most advantageous in establishing good flow distribution in multitube boilers, where differences in downstream condi-

tions between the parallel tubes are caused by such factors as mechanical tolerances, poor distribution of heating fluids, and wall deposits.

The lack of oscillations during flashing noted with the potassium venturi is a further advantage, not typically found in water tests by others. The sharpness of the potassium flashing initiation is attributed to the hysteresis encountered between flashing and unflashing conditions. This hysteresis, in turn, is probably a result of the thermophysical properties of potassium, which allow the high local liquid superheats observed prior to flashing. However, this same superheating presents some startup difficulties which must be taken into consideration when establishing operating procedures.

Not evaluated in this study were the nature of the flow patterns obtained with two-phase flow or the behavior of the venturi with heat addition.

SUMMARY OF RESULTS

Experimental data were obtained on the flow of subcooled potassium through an adiabatic, smooth-wall venturi with a throat diameter of 0.1015 inch (0.2578 cm). This venturi is in the size range suitable for use as a liquid-metal-boiler inlet device. Data were taken at flow rates ranging between 300 and 660 pounds mass per hour (38 to 83 g/sec) and fluid temperatures from 1140° to 1460° F (889 to 1060 K). Behavior of the venturi in the all-liquid and flashed states, as well as at incipient cavitation and flashing conditions was observed with the following major results:

1. Nonequilibrium conditions were measured in the venturi at flashing incipency. This nonequilibrium consisted of liquid in tension at pressures below the vapor pressure corresponding to the liquid saturation temperature, as much as 16.1 psi (11.1 N/cm²) at a 1460° F (1066 K) liquid temperature.

2. Incipient cavitation and flashing pressures below saturation vapor pressure followed the trends predicted by a force-balance equation across bubbles of critical radii between 1×10^{-4} and 0.5×10^{-4} inch (2.54×10^{-4} and 1.27×10^{-4} cm). Metallographic inspection of the inside surface of the venturi showed the largest cavities to be in the 10^{-4} - to 10^{-5} -inch (2.54×10^{-4} - to 2.54×10^{-5} -cm) range.

3. Pressures lower than absolute zero existed at the venturi throat at some flashing incipency conditions. The largest negative absolute pressure calculated was -6.5 psia (-4.5 N/cm² abs).

4. Total potassium flow rate through a flashed venturi with subcooled inlet conditions and a particular geometry is determined exclusively by the inlet pressure and the inlet temperature, which determine the vapor pressure at the interface. The effect of the backpressure on the flashed venturi behavior is limited to controlling either the quality

of the two-phase mixture leaving the venturi, or the location in the diffuser where the vapor phase will collapse. Exit vapor qualities as high as 1.3 percent were calculated.

5. Neither the unheated reentrant 0.008-inch- (0.020-cm-) diameter artificial throat cavity nor the 0.0005-inch- (0.0013-cm-) wide annular gap had any effect on incipency conditions. The artificial cavity did appear to induce vapor into the throat area after flashing, thereby producing a larger pressure drop for a given flow rate.

6. The data obtained adiabatically in this investigation were compared with data available in the literature for potassium boiling initiation through heat addition. Both types of data show similar trends, except for some data on boiling stagnant potassium of high purity.

7. The flow of hot liquid potassium through the venturi for a period of 250 hours changed the surface finish on the type-316 stainless-steel venturi. Large-size pits and polishing marks disappeared, and small cavities of the 10^{-4} - to 10^{-5} -inch (2.54×10^{-4} - to 2.54×10^{-5} -cm) diameter range were formed or exposed at the surface.

Lewis Research Center,

National Aeronautics and Space Administration,

Cleveland, Ohio, November 10, 1969,

120-27.

APPENDIX A

SYMBOLS

| | | | |
|---------------|---|------------|--|
| C | constant | P_{v2} | potassium vapor pressure corresponding to temperature T_2 |
| C_1 | dimensional factor in eq. (10) of appendix C, $144 \text{ in.}^2/\text{ft}^2$; $10^4 \text{ cm}^2/\text{m}^2$ | P_{vin} | potassium vapor pressure corresponding to temperature T_{in} |
| d | diameter at venturi throat, in. ; cm | P_{vout} | potassium vapor pressure corresponding to temperature T_{out} |
| g_c | gravitational conversion factor, $4.173 \times 10^8 \text{ (lbm-ft)(hr}^2\text{)/lbf}$; $1 \text{ (kg-m)(sec}^2\text{)/N}$ | P_1 | measured pressure at control venturi inlet (fig. 4) |
| h_{fin} | saturated liquid enthalpy of potassium at venturi inlet temperature T_{in} , Btu/lbm; J/kg | P_2 | measured pressure at control venturi throat (fig. 4) |
| h_{fout} | saturated liquid enthalpy of potassium at venturi outlet temperature T_{out} , Btu/lbm; J/kg | P_3 | measured pressure at control venturi outlet (fig. 4) |
| $h_{fg, out}$ | heat of vaporization of potassium at venturi outlet temperature T_{out} , Btu/lbm; J/kg | P_4 | measured pressure at test venturi inlet (fig. 5) |
| N | number of runs | P_5 | measured pressure at test venturi outlet (fig. 5) |
| P | pressure, psia; N/cm^2 abs | q | superficial dynamic head at venturi throat, psi; N/cm^2 |
| P_t | pressure at test venturi throat, calculated from the five measured pressures (eq. (9) of appendix C) | r | bubble radius, in. ; cm |
| P_v | potassium vapor pressure at saturation temperature T_v | T | temperature, $^{\circ}\text{F}$; K |
| | | T_{C1} | measured wall temperature at control venturi inlet |
| | | T_{C2} | measured wall temperature at test venturi inlet |
| | | T_{in} | measured wall temperature at control venturi outlet |
| | | T_{out} | measured wall temperature at test venturi outlet |

| | | | |
|-------|--|----------|--|
| T_v | potassium saturation temperature | W | potassium liquid flow rate, lbm/hr; g/sec |
| T_1 | measured wall temperature at test venturi, 0.50 in. (1.27 cm) from inlet | W_v | potassium flow rate calculated from venturi characteristics, lbm/hr; g/sec |
| T_2 | measured wall temperature at test venturi, 0.90 in. (2.29 cm) from inlet | X | thermodynamic quality at ven- turi outlet, percent |
| T_3 | measured wall temperature at test venturi, 1.30 in. (3.30 cm) from inlet | γ | standard deviation as defined by eq. (7), $^{\circ}\text{F}$; K |
| T_4 | measured wall temperature at test venturi, 1.70 in. (4.32 cm) from inlet | ρ | potassium liquid density, lbm/ft ³ ; g/m ³ |
| | | σ | potassium surface tension, lbf/in.; N/cm |

APPENDIX B

ACCURACY OF TEMPERATURE AND FLOW MEASUREMENTS

As indicated in the Research Instrumentation section of the main text, no direct calibration of the temperature- or flow-measuring devices was attempted. However, indirect observations of the readings obtained give indications of their own validity.

Temperatures

The thermocouple readings of interest are the six around the test venturi (T_{in} , T_1 to T_4 , and T_{out}). The data presented in tables II and III allow two comparisons to be made to show the validity of these temperature readings:

(1) Comparison of T_{out} with the saturation temperature of potassium corresponding to the measured outlet pressure P_5 in those runs which show a net vapor quality leaving the venturi. This comparison measures the accuracy of the thermocouple T_{out} .

(2) Comparison of the other five thermocouples with T_{out} on the all-liquid runs. These runs are very near isothermal, as the potassium flow rates are large enough to prevent heat losses from creating a large temperature drop along the venturi length. This type of comparison shows the scatter in readings among the six thermocouples.

Comparison of T_{out} with saturation temperature of potassium. - The readings obtained from thermocouple T_{out} are plotted in figure 20 against the values of potassium saturation temperature at the outlet pressure P_5 , for all the runs where net quality at the outlet was observed. Saturation temperatures were obtained from the potassium vapor curve reported in reference 14. The values of the measured temperature T_{out} were 6.5°F (3.6 K) lower on the mean than the saturation temperature. The standard deviation of the mean difference was 3.5°F (1.9 K).

About 3°F (1.7 K) of the mean difference in temperature can be accounted for by heat losses. At the operating temperature level there should be about a 1.5°F (0.8 K) temperature drop across the stainless-steel wall. This would be the result of the heat leakage by conduction through 7 inches of ceramic fiber insulation. An additional 1.5°F (0.8 K) error should be expected from the thermocouple as a result of heat leakage by conduction along the leads. The additional error encountered is well within the combined limit of error of the thermocouple wire and the calibration error of the pressure-measuring device.

As shown in figure 20, the readings with the larger discrepancies are those where the estimated exit quality is smaller than 0.4 percent. It is possible that in these runs

the venturi exit is no longer at saturation, making the comparison not applicable.

Comparison of other thermocouples with T_{out} - Comparison of the other five thermocouples, T_{in} and T_1 to T_4 , with T_{out} for those runs where the test venturi should be nearly isothermal gives an indication of the relative accuracy of the six thermocouples involved. Thermocouple T_{out} is singled out as the basis for comparison because its absolute accuracy was established from the potassium vapor pressure curve, as already described.

The test venturi should be isothermal during the all-liquid runs, when no change in phase occurs. The only deviation from constant temperature is that created by the heat losses through the insulated walls of the venturi. This small deviation from isothermal conditions along the length of the venturi was estimated for each of the five thermocouple stations. This estimate was obtained by a balance between the heat losses across the venturi wall and the 7 inch (18 cm) thickness of insulation and the temperature drop of the potassium flowing along the venturi. The correction, a function of potassium flow rate and temperature, was applied to each thermocouple reading before it was compared with T_{out} .

The results of the comparisons are summarized in figure 21. The mean difference $\bar{\Delta}$ between each temperature and T_{out} is the arithmetic mean of the differences for all the liquid runs

$$\bar{\Delta}_i = \frac{\sum (T_i - T_{out})}{N} \quad (6)$$

where i denotes one of the subscripts in , 1, 2, 3, or 4. The number of all-liquid runs N was 158 for all the thermocouples, except T_1 which was removed early in order to install the throat cavity insert. Only 56 runs were used to evaluate the mean difference between T_1 and T_{out} . As shown in figure 21, the mean differences between T_{out} and the other thermocouples were less than $1.5^{\circ} F$ (0.8 K), except for T_3 which had a larger error.

The standard deviation from the mean difference γ was estimated from

$$\gamma_i = \left[\frac{\sum (\Delta_i - \bar{\Delta}_i)^2}{N} \right]^{1/2} \quad (7)$$

where $\Delta_i = T_i - T_{out}$ and i denotes one of the subscripts in , 1, 2, 3, or 4. As shown in figure 21, the standard deviations range from $1.1^{\circ} F$ (0.6 K) for T_4 to $2.2^{\circ} F$ (1.2 K)

for T_3 . The distribution of runs for all five deviations is equal, with 73 percent of all readings being within 1γ of the mean difference.

These differences between the six thermocouples are well within the limits of error of the thermocouple wire. The temperature readings reported on all data tables are uncorrected values obtained from the thermocouples.

Flow

No direct calibration of the electromagnetic (EM) flowmeter was attempted. An indication of the reliability of flow rate results is given by comparison of the EM flowmeter readings with the flow rates obtained from the inlet-to-throat pressure drop in the control venturi.

The control venturi was not calibrated directly. However, a flow calibration was run on the as-received venturi using water and a weight tank. Flow coefficients obtained from the water calibration of the as-received venturi, when used with the pressure drops $P_1 - P_2$, obtained in the control venturi during operation, provided a second source of flow measurement. The data shown in figure 22 for the all-liquid potassium runs show that the flow rates from both sources agree within 5 percent throughout the entire operating range.

The flow rates reported in the data tables are the values obtained from the EM flowmeter. For the runs where the EM flowmeter output was distorted, the pressure drop on the control venturi was used to determine the flow rate. In these cases, however, the flow rate was corrected by using the ratio of 0.95 from figure 22.

APPENDIX C

CALCULATION OF TEST VENTURI THROAT PRESSURE, DYNAMIC HEAD, AND THERMODYNAMIC EXIT QUALITY

Test Venturi Throat Pressure

The test venturi throat pressure P_t was obtained from the measured pressures in the control and test venturis. It was not measured directly as no instrument penetrations into the reduced-area section of the test venturi were allowed. In figure 2, pressures P_1 to P_5 are the measured values. The control and test venturis are dimensionally equal. If there were absolutely no difference at all, P_t could be obtained from

$$P_t = P_4 - (P_1 - P_2) \quad (8)$$

However, a small difference between the two venturis existed. Because of the small diameter at the throat of the venturis, even the close specified tolerances allowed a difference in overall performance between the two venturis. This is indicated by the overall pressure-drop ratio $(P_4 - P_5)/(P_1 - P_3)$. If it is assumed that the overall pressure losses are a function of the dynamic head at the minimum throat diameter and that the pressure-drop distribution of the two venturis is similar, the test venturi throat pressure can be calculated from

$$P_t = P_4 - (P_1 - P_2) \frac{P_4 - P_5}{P_1 - P_3} \quad (9)$$

Equation (9) is applicable to runs where flow is in the liquid phase through both venturis, and to those cavitating runs where the overall pressure-drop ratio does not deviate from the all-liquid value. For the runs where the overall pressure-drop ratio does vary from the all-liquid value, equation (9) was still used to calculate the throat pressure. For these cases, however, the value of the overall pressure-drop ratio from the preceding all-liquid run was used.

Dynamic Head at Venturi Throat

The dynamic head q was calculated as a superficial value at the test venturi throat:

$$q = C_1 \frac{8}{\pi^2} \frac{W^2}{g_c \rho d^4} \quad (10)$$

The diameter d used for calculating the superficial dynamic head was the nominal room-temperature value of 0.1015 inch (0.2578 cm). The potassium liquid density was evaluated at the test venturi inlet temperature T_{in} . The potassium density, as well as all other thermodynamic and transport properties, was obtained from reference 14.

Thermodynamic Quality at Venturi Exit

The thermodynamic quality of potassium at the venturi exit X was calculated from

$$X = \frac{(h_{fin} - h_{fout}) \times 100}{h_{fg, out}}, \text{ percent} \quad (11)$$

The values of enthalpy were all evaluated from the corresponding temperature readings. It was decided, after the results of appendix B were studied, that discrepancies obtained in this way would be smaller than if some enthalpies obtained from pressure readings were compared with others obtained from temperature sources. However, the results obtained at quality values below 0.4 percent border on the value of possible error.

The effect of axial heat conduction along the thick venturi wall on T_{out} was neglected as the flashed data showed very small differences between the readings of thermocouples T_4 and T_{out} . The inlet temperature T_{in} was measured too far upstream of the area where temperature changes occurred to be affected by the gradient.

REFERENCES

1. Stone, James R.; and Sekas, Nick J.: Tests of a Single Tube-in-Shell Water-Boiling Heat Exchanger with a Helical-Wire Insert and Several Inlet Flow-Stabilizing Devices. NASA TN D-4767, 1968.
2. Stone, James R.; and Sekas, Nick J.: Water Flow and Cavitation in Converging-Diverging Boiler-Inlet Nozzle. NASA TM X-1689, 1968.
3. Dorsch, Robert G.: Frequency Response of a Forced-Flow Single-Tube Boiler. Presented at Symposium on Two-Phase Flow Dynamics, Technological University of Eindhoven and Euratom, Eindhoven, The Netherlands, Sept. 4-9, 1967.
4. Hammitt, Frederick G.; and Robinson, M. John: Choked Flow Analogy for Very Low Quality Two-Phase Flows. Rep. 03424-18-T, Univ. Michigan (NASA CR-75127), Mar. 1966.
5. Ruggeri, Robert S.; and Gelder, Thomas F.: Effects of Air Content and Water Purity on Liquid Tension at Incipient Cavitation In Venturi Flow. NASA TN D-1459, 1963.
6. Gelder, Thomas F.; Ruggeri, Robert S.; and Moore, Royce D.: Cavitation Similarity Considerations Based on Measured Pressure and Temperature Depressions in Cavitated Regions of Freon-114. NASA TN D-3509, 1966.
7. Hsu, Y. Y.: On the Size Range of Active Nucleation Cavities on a Heating Surface. J. Heat Transfer, vol. 84, no. 3, Aug. 1962, pp. 207-216.
8. Holtz, Robert E.: The Effect of the Pressure-Temperature History Upon Incipient-Boiling Superheats in Liquid Metals. Rep. ANL-7184, Argonne National Lab., June 1966.
9. Edwards, J. A.; and Hoffmann, H. W.: Superheats with Boiling Alkali Metals. Proceedings of the Conference on Application of High Temperature Instrumentation to Liquid-Metal Experiments. Rep. ANL-7100, Argonne National Lab. (NASA CR-76450), 1965, pp. 515-534.
10. Chen, J. C.: Incipient Boiling Superheats in Liquid Metals. J. Heat Transfer, vol. 90, no. 3, Aug. 1968, pp. 303-312.
11. Blake, F. G., Jr.: The Tensile Strength of Liquids: A Review of the Literature. Tech. Memo 9, Harvard Univ., Acoustic Res. Lab., June 11, 1949.
12. Briggs, Lyman J.: Limiting Negative Pressure of Water. J. Appl. Phys., vol. 21, no. 7, July 1950, pp. 721-722.

13. Gavrilenko, T. P.; and Topchiyan, M. E.: Dynamic Tensile Strength of Water. J. Appl. Mech. Tech. Phys., vol. 7, no. 4, July-Aug. 1966, pp. 128-129.
14. Briggs, Lyman J.: The Limiting Negative Pressure of Acetic Acid, Benzene, Aniline, Carbon Tetrachloride, and Chloroform. J. Chem. Phys., vol. 19, no. 7, July 1951, pp. 970-972.
15. Spiller, K. H.; Grass, G.; and Perschke, D.: Superheating and Single Bubble Ejection in the Vaporization of Stagnating Liquid Metals. Rep. AERE-Trans-1078, United Kingdom Atomic Energy Authority, June 1967.
16. Grass, G.; Kottowski, H.; and Warnsing, R.: Boiling of Liquid Alkali Metals. Rep. ANL-Trans-390, Argonne National Lab., Sept. 1966.
17. Fauske, Hans K.: Liquid Metal Boiling in Relation to Liquid Metal Fast Breeder Reactor Safety Design. Chem. Eng. Progr. Symp. Ser., vol. 65, no. 92, 1969, pp. 138-149.
18. Weatherford, W. D., Jr.; Tyler, John C.; and Ku, P. M.: Properties of Inorganic Energy-Conversion and Heat-Transfer Fluids for Space Applications. Southwest Research Inst. (WADD-TR-61-96), Nov. 1961.

TABLE I. - SUMMARY OF EXPERIMENTAL DATA

| (a) U. S. customary units | | | | | | | (b) SI units | | | | | | |
|--|------------|-----------------|-----------|---------------|-----------------------|---------|--|------------|-----------------|-----------|--------------|----------------------|---------|
| Set | Runs | Pressure change | Flow rate | | Inlet temperature, °F | | Set | Runs | Pressure change | Flow rate | | Inlet temperature, K | |
| | | | Mode | Range, lbm/hr | Minimum | Maximum | | | | Mode | Range, g/sec | Minimum | Maximum |
| Series I: Test venturi <u>without</u> artificial throat cavity | | | | | | | Series I: Test venturi <u>without</u> artificial throat cavity | | | | | | |
| 1 | a to g | (a) | Variable | 125 to 700 | 1128 | 1330 | 1 | a to g | (a) | Variable | 15.8 to 88.2 | 882 | 994 |
| 2 | 1 to 8 | Steps | Constant | 635 to 662 | 1174 | 1199 | 2 | 1 to 8 | Steps | Constant | 80.0 to 83.4 | 908 | 921 |
| 3 | 9 to 19 | ↓ | ↓ | 522 to 533 | 1142 | 1193 | 3 | 9 to 19 | ↓ | ↓ | 65.8 to 67.2 | 890 | 918 |
| 4 | 20 to 29 | ↓ | ↓ | 406 to 410 | 1210 | 1230 | 4 | 20 to 29 | ↓ | ↓ | 51.2 to 51.7 | 928 | 939 |
| 5 | 30 to 36 | ↓ | ↓ | 515 to 527 | 1458 | 1462 | 5 | 30 to 36 | ↓ | ↓ | 64.9 to 66.4 | 1065 | 1068 |
| 6 | 37 to 40 | ↓ | ↓ | 443 to 447 | 1430 | 1460 | 6 | 37 to 40 | ↓ | ↓ | 55.8 to 56.3 | 1050 | 1066 |
| 7 | 41 to 55 | ↓ | ↓ | 493 to 498 | 1312 | 1325 | 7 | 41 to 55 | ↓ | ↓ | 62.1 to 62.7 | 984 | 991 |
| 8 | 56 to 68 | ↓ | ↓ | 370 to 375 | 1311 | 1330 | 8 | 56 to 68 | ↓ | ↓ | 46.6 to 47.3 | 984 | 994 |
| 9 | 69 to 70 | Ramp | ----- | 493 to 445 | 1221 | 1261 | 9 | 69 to 70 | Ramp | ----- | 62.1 to 56.1 | 934 | 956 |
| 10 | 71 to 72 | Ramp | ----- | 498 to 398 | 1349 | 1375 | 10 | 71 to 72 | Ramp | ----- | 62.7 to 50.1 | 1005 | 1019 |
| Series II: Test venturi <u>with</u> artificial throat cavity | | | | | | | Series II: Test venturi <u>with</u> artificial throat cavity | | | | | | |
| 11 | h to r | (a) | Variable | 119 to 600 | 1346 | 1388 | 11 | h to r | (a) | Variable | 15.0 to 75.6 | 1003 | 1026 |
| 12 | 73 to 104 | Steps | Constant | 483 to 489 | 1289 | 1321 | 12 | 73 to 104 | Steps | Constant | 60.9 to 61.6 | 971 | 989 |
| 13 | 105 to 107 | Ramp | ----- | 490 to 368 | 1308 | 1345 | 13 | 105 to 107 | Ramp | ----- | 61.7 to 46.4 | 982 | 1003 |
| 14 | 108 to 123 | Steps | Constant | 355 to 363 | 1240 | 1271 | 14 | 108 to 123 | Steps | Constant | 44.7 to 45.7 | 944 | 961 |
| 15 | 124 to 144 | ↓ | ↓ | 355 to 363 | 1301 | 1318 | 15 | 124 to 144 | ↓ | ↓ | 44.7 to 45.7 | 978 | 988 |
| 16 | 145 to 176 | ↓ | ↓ | 352 to 362 | 1408 | 1445 | 16 | 145 to 176 | ↓ | ↓ | 44.4 to 45.6 | 1038 | 1058 |
| 17 | 177 to 204 | ↓ | ↓ | 478 to 485 | 1391 | 1418 | 17 | 177 to 204 | ↓ | ↓ | 60.2 to 61.1 | 1028 | 1043 |
| 18 | 205 to 214 | ↓ | ↓ | 421 to 429 | 1398 | 1411 | 18 | 205 to 214 | ↓ | ↓ | 53.0 to 54.1 | 1032 | 1039 |
| 19 | 215 to 219 | Ramp | ----- | 424 to 427 | 1390 | 1410 | 19 | 215 to 219 | Ramp | ----- | 53.4 to 53.8 | 1028 | 1039 |
| 20 | s to x | (a) | Variable | 129 to 660 | 820 | 949 | 20 | s to x | (a) | Variable | 16.3 to 83.2 | 711 | 783 |

^aNot applicable, all-liquid run.

TABLE II. - DETAILED DATA FOR VENTURI WITHOUT ARTIFICIAL THROAT CAVITY (SERIES I)

(a) U. S. customary units

| Set | Run | Flow rate, W, lbm/hr | Dynamic head, q, psi | Control venturi | | | | | Test venturi | | | | | | | | | | Noise indication | Pressure-drop ratio, $\frac{P_4 - P_5}{P_1 - P_3}$ | Vapor pressure at T_{in} , P_{vin} , psia | Vapor pressure at T_{out} , P_{vout} , psia | Exit quality, X, percent | Remarks |
|-----|-----|----------------------|----------------------|-----------------|---------------|---------------|-----------------|------------------|----------------|---------------|---------------|-----------------|---------------------|----------------|----------------|------|-------------------|--------|------------------|--|---|---|--------------------------|---------|
| | | | | Pressure, psia | | | Temperature, °F | | Pressure, psia | | | Temperature, °F | | | | | | | | | | | | |
| | | | | Inlet, P_1 | Throat, P_2 | Outlet, P_3 | Inlet, T_{C1} | Outlet, T_{C2} | Inlet, P_4 | Outlet, P_5 | Throat, P_t | Inlet, T_{in} | Distance from inlet | | | | Outlet, T_{out} | | | | | | | |
| | | | | | | | | | | | | 0.5 in., T_1 | 0.9 in., T_2 | 1.3 in., T_3 | 1.7 in., T_4 | | | | | | | | | |
| 1 | a | 580 | 21.1 | 48.5 | 24.6 | 38.4 | 1342 | 1342 | 36.6 | 27.9 | 16.0 | 1330 | 1330 | 1330 | 1330 | 1330 | 1330 | None | 0.87 | 10.3 | ---- | ---- | All-liquid flow | |
| | b | 125 | .9 | 26.9 | 25.8 | 26.3 | ---- | ---- | 26.3 | 25.9 | 25.3 | 1202 | 1202 | 1202 | 1202 | 1202 | 1201 | None | .54 | 4.9 | ---- | ---- | calibration | |
| | c | 255 | 3.9 | 30.1 | 25.8 | 28.2 | 1140 | 1140 | 27.9 | 26.2 | 24.2 | 1128 | 1128 | 1128 | 1128 | 1128 | 1128 | None | .86 | 3.0 | ---- | ---- | | |
| | d | 375 | 8.5 | 35.4 | 25.6 | 31.0 | 1170 | 1170 | 30.3 | 26.6 | 22.0 | 1159 | 1159 | 1159 | 1159 | 1159 | 1157 | None | .85 | 3.7 | ---- | ---- | | |
| | e | 494 | 14.8 | 42.8 | 25.9 | 35.5 | 1180 | 1176 | 34.4 | 28.0 | 19.6 | 1168 | 1168 | 1168 | 1168 | 1170 | 1168 | None | .87 | 3.9 | ---- | ---- | | |
| | f | 610 | 22.6 | 50.9 | 25.0 | 39.9 | 1195 | 1194 | 38.0 | 28.5 | 15.7 | 1188 | 1188 | 1188 | 1188 | 1189 | 1187 | None | .86 | 4.4 | ---- | ---- | | |
| | g | 700 | 30.2 | 58.2 | 23.8 | 43.7 | 1248 | 1248 | 41.3 | 28.9 | 11.8 | 1240 | 1240 | 1240 | 1240 | 1241 | 1240 | None | .86 | 6.1 | ---- | ---- | | |
| 2 | 1 | 662 | 26.8 | 56.2 | 25.8 | 43.3 | 1209 | 1206 | 39.1 | 28.1 | 13.1 | 1199 | 1199 | 1200 | 1200 | 1200 | 1198 | None | 0.86 | 4.8 | ---- | ---- | Liquid | |
| | 2 | 662 | 26.8 | 53.6 | 22.9 | 40.7 | 1205 | 1203 | 36.4 | 25.3 | 10.0 | 1196 | 1196 | 1198 | 1198 | 1199 | 1197 | None | .86 | 4.7 | ---- | ---- | Liquid | |
| | 3 | 659 | 26.6 | 50.6 | 20.1 | 37.8 | 1200 | 1200 | 33.6 | 22.5 | 7.2 | 1190 | 1190 | 1191 | 1191 | 1192 | 1190 | None | .86 | 4.5 | ---- | ---- | Liquid | |
| | 4 | 655 | 26.2 | 47.5 | 17.4 | 35.0 | 1195 | 1194 | 30.7 | 19.7 | 4.4 | 1187 | 1187 | 1188 | 1188 | 1189 | 1188 | High | .87 | 4.5 | ---- | ---- | Incipient cavitation | |
| | 5 | 655 | 26.2 | 45.3 | 15.1 | 32.9 | 1193 | 1191 | 28.7 | 17.6 | 1.7 | 1184 | 1184 | 1185 | 1185 | 1185 | 1184 | None | .89 | 4.4 | ---- | ---- | Cavitated | |
| | 6 | 659 | 26.5 | 43.3 | 13.1 | 30.9 | 1191 | 1190 | 26.7 | 15.7 | 0.0 | 1183 | 1183 | 1184 | 1184 | 1185 | 1186 | None | .88 | 4.4 | ---- | ---- | Cavitated | |
| | 7 | 654 | 26.0 | 40.0 | 9.8 | 27.4 | 1188 | 1187 | 23.2 | 12.4 | -2.9 | 1176 | 1176 | 1178 | 1178 | 1179 | 1177 | None | .87 | 4.1 | ---- | ---- | Cavitated | |
| | 7a | 654 | 26.0 | 36.6 | 6.4 | 24.1 | ---- | ---- | 19.7 | 8.9 | -6.5 | 1174 | ---- | ---- | ---- | ---- | ---- | Medium | .86 | 4.1 | ---- | ---- | Incipient flashing | |
| 8 | 635 | 24.5 | 41.8 | 13.5 | 29.8 | 1183 | 1181 | 26.0 | 9.2 | 1.8 | 1174 | 1174 | 1173 | 1174 | 1175 | 1173 | Medium | 1.40 | 4.1 | 4.1 | ---- | Flashed | | |
| 3 | 9 | 527 | 16.9 | 41.1 | 21.5 | 32.8 | 1200 | 1200 | 30.0 | 23.0 | 13.5 | 1190 | 1190 | 1190 | 1190 | 1191 | 1190 | None | 0.84 | 4.5 | ---- | ---- | Liquid | |
| | 10 | | | 37.3 | 17.7 | 29.0 | 1202 | | 26.2 | 19.2 | 9.5 | | | | | | 1189 | None | .85 | | ---- | ---- | | |
| | 11 | | | 35.1 | 15.5 | 26.8 | 1201 | | 24.1 | 17.0 | 7.3 | | | | | | 1190 | None | .86 | | ---- | ---- | | |
| | 12 | | | 34.0 | 14.3 | 25.6 | 1201 | | 22.9 | 15.8 | 6.4 | | | | | | 1191 | None | .84 | | ---- | ---- | | |
| | 13 | | | 32.2 | 12.6 | 23.9 | 1202 | 1201 | 21.2 | 14.0 | 4.2 | 1191 | 1191 | 1191 | 1191 | 1192 | 1190 | None | .86 | 4.6 | ---- | ---- | | |
| | 14 | | | 30.2 | 10.5 | 21.8 | 1202 | 1201 | 19.1 | 12.0 | 2.4 | 1191 | 1191 | 1191 | 1191 | 1192 | 1189 | Low | .85 | | ---- | ---- | Incipient cavitation | |
| | 15 | 525 | 16.8 | 28.8 | 9.5 | 20.7 | 1203 | 1202 | 18.0 | 10.8 | 1.0 | 1192 | 1192 | 1192 | 1192 | 1194 | 1191 | High | .88 | | ---- | ---- | Cavitated | |
| | 16 | 524 | 16.8 | 27.6 | 8.3 | 19.4 | 1203 | 1202 | 16.7 | 9.7 | .4 | 1193 | 1192 | 1192 | 1192 | 1194 | 1192 | High | .84 | | ---- | ---- | | |
| | 17 | 522 | 16.7 | 26.0 | 6.6 | 17.6 | 1203 | 1202 | 14.9 | 7.9 | -1.9 | 1192 | 1192 | 1192 | 1192 | 1194 | 1192 | High | .84 | | ---- | ---- | | |
| | 18 | 530 | 17.1 | 25.5 | 5.5 | 17.1 | 1200 | 1200 | 14.3 | 7.0 | -3.2 | 1191 | 1191 | 1191 | 1191 | 1191 | 1190 | Medium | .87 | | ---- | ---- | | |
| | 18a | 530 | 17.1 | 23.6 | 3.8 | 15.3 | ---- | ---- | 12.4 | 5.2 | -4.7 | 1185 | ---- | ---- | ---- | ---- | ---- | Medium | .87 | 4.4 | ---- | ---- | Incipient flashing | |
| 19 | 533 | 17.2 | 29.5 | 9.7 | 21.1 | 1150 | 1150 | 18.2 | 4.8 | .6 | 1142 | 1141 | 1141 | 1141 | 1141 | 1139 | Medium | 1.59 | 3.2 | 3.2 | ---- | Flashed | | |
| 4 | 20 | 407 | 10.2 | 36.9 | 25.8 | 32.1 | 1224 | 1222 | 28.2 | 23.8 | 18.1 | 1210 | 1210 | 1210 | 1210 | 1211 | 1212 | None | 0.90 | 5.1 | ---- | ---- | Liquid | |
| | 21 | 409 | 10.3 | 24.9 | 13.6 | 20.0 | 1229 | 1226 | 16.1 | 11.6 | 5.7 | 1211 | 1212 | 1212 | 1212 | 1215 | 1214 | None | .91 | 5.2 | ---- | ---- | | |
| | 22 | 407 | 10.2 | 21.0 | 9.9 | 16.2 | 1229 | 1226 | 12.3 | 7.9 | 2.0 | 1214 | 1215 | 1215 | 1215 | 1217 | 1217 | None | .93 | 5.3 | ---- | ---- | | |
| | 23 | 406 | 10.1 | 19.5 | 8.3 | 14.7 | 1229 | 1226 | 10.8 | 6.4 | .7 | 1215 | 1215 | 1215 | 1215 | 1219 | 1219 | None | .90 | 5.3 | ---- | ---- | | |
| | 24 | | | 17.9 | 6.8 | 13.1 | 1230 | 1227 | 9.3 | 4.8 | -.9 | 1214 | 1215 | 1216 | 1216 | 1219 | 1219 | None | .92 | 5.3 | ---- | ---- | | |
| | 25 | | | 17.5 | 6.4 | 12.7 | 1235 | 1232 | 8.8 | 4.4 | -1.3 | 1220 | 1220 | 1220 | 1220 | 1220 | 1220 | High | .92 | 5.4 | ---- | ---- | Incipient cavitation | |
| | 26 | | | 17.2 | 6.0 | 12.2 | 1245 | 1245 | 8.3 | 4.0 | -1.3 | 1230 | 1231 | 1231 | 1231 | 1231 | 1230 | High | .86 | 5.8 | ---- | ---- | Cavitated | |
| | 26a | | | 17.0 | 6.1 | 12.5 | ---- | ---- | 8.3 | 4.0 | -2.0 | 1225 | ---- | ---- | ---- | ---- | ---- | Medium | .96 | 5.6 | ---- | ---- | Incipient flashing | |
| | 27 | 410 | 10.3 | 22.7 | 11.6 | 17.9 | 1235 | 1235 | 14.0 | 5.2 | 4.3 | 1220 | 1221 | 1219 | 1219 | 1219 | 1219 | Medium | 1.84 | 5.5 | 5.5 | ---- | Flashed | |
| | 28 | 406 | 10.1 | 22.7 | 11.6 | 17.9 | 1232 | 1230 | 14.0 | 6.4 | 4.2 | 1219 | 1219 | 1219 | 1219 | 1219 | 1219 | Medium | 1.56 | 5.4 | 5.4 | ---- | Flashed | |
| | 29 | 409 | 10.3 | 23.0 | 11.6 | 18.0 | 1230 | 1230 | 14.0 | 9.6 | 3.9 | 1218 | 1219 | 1219 | 1219 | 1219 | 1220 | None | .89 | 5.4 | ---- | ---- | Liquid | |

| | | | | | | | | | | | | | | | | | | | | | | | | |
|----|-----|-----|------|------|------|------|------|------|------|------|------|------|------|------|------|------|------|-----------|------|------|------|------|-----------------------------------|--------|
| 5 | 30 | 527 | 17.9 | 49.7 | 30.3 | 41.4 | 1473 | 1472 | 35.0 | 27.6 | 17.8 | 1456 | 1455 | 1456 | 1455 | 1456 | 1455 | None | 0.89 | 19.7 | ---- | ---- | Liquid | |
| | 31 | 526 | 17.8 | 45.3 | 26.0 | 37.1 | 1477 | 1475 | 30.7 | 23.2 | 13.1 | 1461 | 1460 | 1460 | 1460 | 1462 | 1460 | None | .92 | 20.1 | ---- | ---- | Liquid | |
| | 32 | 526 | 17.8 | 42.4 | 23.0 | 34.2 | 1476 | 1475 | 27.8 | 20.3 | 10.1 | 1458 | 1459 | 1460 | 1460 | 1462 | 1461 | None | .91 | 20.1 | ---- | ---- | Incipient cavitation | |
| | 33 | 521 | 17.5 | 39.0 | 20.1 | 31.0 | 1478 | 1478 | 24.7 | 17.4 | 7.5 | 1461 | 1462 | 1462 | 1463 | 1464 | 1462 | High | .91 | 20.3 | ---- | ---- | Cavitated | |
| | 34 | 520 | 17.4 | 38.2 | 19.2 | 30.1 | 1478 | 1478 | 23.8 | 16.5 | 6.8 | 1462 | 1462 | 1463 | 1465 | 1466 | 1463 | High | .89 | 20.3 | ---- | ---- | Cavitated | |
| | 35 | 520 | 17.4 | 36.7 | 18.0 | 28.7 | 1481 | 1480 | 22.5 | 15.2 | 5.6 | 1464 | 1464 | 1466 | 1466 | 1468 | 1467 | Medium | .90 | 20.5 | ---- | ---- | Cavitated | |
| | 36 | 515 | 17.1 | 34.9 | 16.3 | 26.9 | 1478 | 1477 | 20.8 | 13.6 | 4.0 | 1460 | 1460 | 1461 | 1463 | 1464 | 1463 | Medium | .90 | 20.1 | ---- | ---- | Incipient flashing | |
| 6 | 37 | 447 | 12.8 | 42.1 | 28.1 | 36.0 | 1489 | 1488 | 31.4 | 18.9 | 18.6 | 1461 | 1462 | 1448 | 1439 | 1439 | 1438 | Medium | 2.00 | 20.3 | 18.2 | 0.51 | Flashed | |
| | 38 | 446 | 12.7 | 40.2 | 26.4 | 34.3 | 1450 | 1449 | 29.7 | 18.4 | 17.1 | 1431 | 1431 | 1431 | 1431 | 1432 | 1431 | Medium | 1.93 | 17.6 | 17.6 | ---- | Flashed | |
| | 39 | 443 | 12.5 | 39.9 | 26.3 | 34.1 | 1452 | 1450 | 29.6 | 20.9 | 17.1 | 1431 | 1432 | 1432 | 1434 | 1435 | 1435 | High | 1.48 | 17.7 | 17.9 | ---- | Flashed | |
| | 40 | 446 | 12.7 | 37.5 | 23.7 | 31.6 | 1448 | 1446 | 27.0 | 21.6 | 14.3 | 1430 | 1429 | 1430 | 1430 | 1432 | 1431 | None | .92 | 17.4 | ---- | ---- | Liquid | |
| 7 | 41 | 498 | 15.5 | 51.3 | 33.9 | 43.8 | 1339 | 1338 | 36.6 | 29.5 | 20.2 | 1324 | 1322 | 1322 | 1321 | 1325 | 1323 | None | 0.94 | 9.9 | ---- | ---- | Liquid | |
| | 42 | 495 | 15.3 | 42.0 | 24.5 | 34.3 | 1338 | 1338 | 27.1 | 20.0 | 11.1 | 1321 | 1320 | 1320 | 1320 | 1321 | 1321 | ↓ | .92 | 9.8 | ---- | ---- | ↓ | |
| | 43 | ↓ | ↓ | 37.7 | 20.3 | 30.1 | 1332 | 1332 | 22.8 | 15.7 | 6.6 | 1312 | 1312 | 1312 | 1310 | 1315 | 1316 | ↓ | .93 | 9.3 | ---- | ---- | ↓ | |
| | 44 | ↓ | ↓ | 35.7 | 18.3 | 28.1 | 1334 | 1335 | 20.8 | 13.6 | 4.3 | 1319 | 1319 | 1319 | 1319 | 1319 | 1320 | 1319 | ↓ | .94 | 9.7 | ---- | ---- | ↓ |
| | 44a | ↓ | ↓ | 33.6 | 16.2 | 26.0 | ---- | ---- | 18.6 | 11.6 | 2.4 | 1319 | ---- | ---- | ---- | ---- | ---- | Medium | .92 | 9.7 | ---- | ---- | Incipient flashing and cavitation | |
| | 45 | ↓ | ↓ | 39.4 | 21.7 | 31.5 | 1335 | 1335 | 24.6 | 10.3 | 8.1 | 1317 | 1316 | 1316 | 1314 | 1318 | 1316 | ↓ | 1.82 | 9.5 | 9.5 | ---- | Flashed | |
| | 46 | 494 | 15.2 | 38.9 | 21.6 | 31.3 | 1335 | 1335 | 24.1 | 10.1 | 8.0 | 1316 | 1316 | 1315 | 1312 | 1315 | 1315 | ↓ | 1.85 | 9.5 | 9.5 | ---- | ↓ | |
| | 47 | 495 | 15.3 | 38.9 | 21.4 | 31.3 | 1335 | 1335 | 24.0 | 9.1 | 7.6 | 1311 | 1311 | 1302 | 1299 | 1300 | 1299 | Low | 1.96 | 9.3 | 8.6 | 0.27 | ↓ | |
| | 48 | 495 | 15.3 | 38.4 | 20.9 | 30.6 | 1342 | 1340 | 24.3 | 8.6 | 7.9 | 1319 | 1319 | 1309 | 1290 | 1290 | 1290 | ↓ | 2.02 | 9.7 | 8.2 | .64 | ↓ | |
| | 49 | 497 | 15.5 | 37.9 | 20.6 | 30.3 | 1343 | 1342 | 24.4 | 8.6 | 8.2 | 1321 | 1320 | 1310 | 1290 | 1290 | 1289 | ↓ | 2.07 | 9.8 | 8.1 | .69 | ↓ | |
| | 50 | 496 | 15.4 | 36.3 | 18.9 | 28.8 | 1345 | 1342 | 24.6 | 8.6 | 8.3 | 1321 | 1320 | 1310 | 1290 | 1289 | 1288 | ↓ | 2.14 | 9.8 | 8.1 | .71 | ↓ | |
| | 51 | 493 | 15.2 | 38.5 | 21.1 | 30.9 | 1345 | 1345 | 24.4 | 8.8 | 8.1 | 1320 | 1320 | 1310 | 1291 | 1289 | 1289 | ↓ | 2.05 | 9.8 | 8.1 | .66 | ↓ | |
| | 52 | ↓ | 15.3 | 39.0 | 21.5 | 31.3 | 1342 | 1342 | 24.8 | 10.4 | 8.5 | 1322 | 1321 | 1321 | 1319 | 1322 | 1320 | Medium | 1.86 | ↓ | 9.8 | ---- | ↓ | |
| | 53 | ↓ | ↓ | 38.9 | 21.5 | 31.3 | 1345 | 1345 | 25.0 | 13.2 | 8.7 | 1325 | 1325 | 1325 | 1325 | 1329 | 1328 | High | 1.54 | 10.0 | 10.2 | ---- | ↓ | |
| | 54 | ↓ | ↓ | 35.0 | 17.9 | 27.4 | 1342 | 1340 | 21.0 | 14.0 | 5.2 | 1324 | 1322 | 1322 | 1321 | 1329 | 1327 | None | .93 | 9.9 | ---- | ---- | Liquid | |
| | 55 | 495 | ↓ | 45.5 | 28.1 | 37.8 | 1340 | 1338 | 31.6 | 24.6 | 15.8 | 1321 | 1320 | 1320 | 1320 | 1321 | 1320 | None | .91 | 9.8 | ---- | ---- | Liquid | |
| | 8 | 56 | 373 | 8.7 | 36.0 | 25.8 | 31.5 | 1351 | 1350 | 28.1 | 23.9 | 18.4 | 1330 | 1329 | 1329 | 1329 | 1330 | 1329 | None | 0.96 | 10.3 | ---- | ---- | Liquid |
| 57 | | 370 | 8.6 | 27.8 | 18.1 | 23.5 | 1352 | 1350 | 20.2 | 16.1 | 11.1 | 1330 | 1330 | 1330 | 1329 | 1330 | 1330 | ↓ | .94 | 10.3 | ---- | ---- | ↓ | |
| 58 | | 370 | 8.6 | 23.2 | 13.4 | 18.9 | 1347 | 1345 | 15.7 | 11.6 | 6.3 | 1326 | 1325 | 1325 | 1322 | 1325 | 1323 | ↓ | .96 | 10.0 | ---- | ---- | ↓ | |
| 59 | | 373 | 8.7 | 21.5 | 11.7 | 17.2 | 1350 | 1350 | 13.9 | 9.8 | 4.6 | 1326 | 1325 | 1325 | 1324 | 1329 | 1326 | ↓ | .94 | 10.0 | ---- | ---- | ↓ | |
| 60 | | 373 | ↓ | 19.7 | 9.9 | 15.3 | 1342 | 1342 | 12.1 | 8.0 | 3.0 | 1321 | 1320 | 1320 | 1320 | 1321 | 1320 | ↓ | .93 | 9.8 | ---- | ---- | ↓ | |
| 61 | | 372 | ↓ | 17.9 | 8.0 | 13.5 | 1347 | 1345 | 10.1 | 6.0 | .9 | 1323 | 1322 | 1322 | 1321 | 1325 | 1323 | None/High | .93 | 9.9 | ---- | ---- | Incipient cavitation | |
| 62 | | ↓ | ↓ | 17.7 | 7.9 | 13.4 | 1342 | 1340 | 10.2 | 6.0 | .8 | 1320 | 1320 | 1320 | 1319 | 1321 | 1320 | High | .96 | 9.8 | ---- | ---- | Cavitated | |
| 63 | | ↓ | ↓ | 17.3 | 7.3 | 13.1 | 1342 | 1340 | 9.5 | 5.4 | -.3 | 1320 | 1320 | 1320 | 1320 | 1321 | 1320 | Low | .98 | 9.8 | ---- | ---- | Incipient flashing | |
| 64 | | ↓ | 8.6 | 24.6 | 14.9 | 20.3 | 1342 | 1340 | 17.0 | 7.3 | 7.7 | 1311 | 1310 | 1292 | 1270 | 1266 | 1264 | ↓ | 2.23 | 9.2 | 7.1 | 1.03 | Flashed | |
| 65 | | ↓ | 8.6 | 24.1 | 14.3 | 19.8 | 1343 | 1343 | 16.9 | 7.5 | 7.9 | 1312 | 1312 | 1293 | 1272 | 1268 | 1266 | ↓ | 2.33 | 9.3 | 7.1 | 1.00 | ↓ | |
| 66 | | ↓ | 8.6 | 25.7 | 15.7 | 21.3 | 1345 | 1345 | 17.3 | 7.5 | 7.8 | 1312 | 1313 | 1298 | 1273 | 1272 | 1271 | ↓ | 2.25 | 9.3 | 7.3 | .89 | ↓ | |
| 67 | | 375 | 8.8 | 27.7 | 17.7 | 23.2 | 1342 | 1340 | 17.4 | 9.0 | 7.7 | 1315 | 1315 | 1303 | 1295 | 1298 | 1297 | Medium | 1.86 | 9.4 | 8.5 | .39 | ↓ | |
| 68 | | 375 | 8.8 | 27.3 | 17.2 | 22.9 | 1341 | 1340 | 17.3 | 12.7 | 7.3 | 1321 | 1320 | 1319 | 1318 | 1320 | 1320 | None | .96 | 9.8 | ---- | ---- | Liquid | |
| 9 | 69 | 493 | 14.9 | 42.8 | 25.4 | 35.2 | 1243 | 1240 | 26.9 | 20.0 | 11.2 | 1221 | 1222 | 1223 | 1222 | 1225 | 1223 | None | 0.90 | 5.6 | ---- | ---- | Liquid | |
| | 69a | 493 | 14.9 | 31.9 | 14.5 | 24.5 | ---- | ---- | 16.1 | 8.9 | -.8 | 1239 | ---- | ---- | ---- | ---- | ---- | High | .97 | 6.2 | ---- | ---- | Incipient cavitation | |
| | 69b | 493 | 14.9 | 31.1 | 13.9 | 23.8 | ---- | ---- | 15.4 | 8.5 | -.9 | 1248 | ---- | ---- | ---- | ---- | ---- | Low | .95 | 6.4 | ---- | ---- | Incipient flashing | |
| | 70 | 445 | 12.3 | 31.9 | 17.6 | 25.6 | 1281 | 1279 | 18.7 | 7.4 | 5.7 | 1261 | 1260 | 1260 | 1258 | 1261 | 1260 | Low | 1.80 | 6.9 | 6.9 | ---- | Flashed | |
| 10 | 71 | 490 | 15.1 | 46.8 | 29.5 | 39.3 | 1373 | 1373 | 31.2 | 24.2 | 15.2 | 1356 | 1355 | 1358 | 1353 | 1358 | 1356 | None | 0.92 | 11.9 | ---- | ---- | Liquid | |
| | 71a | 490 | 15.1 | 34.6 | 17.4 | 27.3 | ---- | ---- | 19.2 | 12.2 | 2.7 | 1349 | ---- | ---- | ---- | ---- | ---- | High | .96 | 11.4 | ---- | ---- | Incipient cavitation | |
| | 71b | 490 | 15.1 | 32.0 | 14.8 | 24.7 | ---- | ---- | 16.5 | 9.5 | .0 | 1351 | ---- | ---- | ---- | ---- | ---- | Medium | .96 | 11.6 | ---- | ---- | Incipient flashing | |
| | 72 | 398 | 10.0 | 33.0 | 21.5 | 28.0 | 1410 | 1408 | 22.6 | 10.4 | 11.9 | 1375 | 1375 | 1355 | 1328 | 1324 | 1322 | Low | 2.44 | 13.3 | 9.9 | 1.15 | Flashed | |

^aShown only for flashed runs.

TABLE II. - Concluded. DETAILED DATA FOR VENTURI WITHOUT ARTIFICIAL THROAT CAVITY (SERIES I)

(b) SI units^a

| Set | Run | Flow rate, W, g/sec | Dynamic head, q, N/cm ² | Control venturi | | | | | | Test venturi | | | | | | | | | | Noise indication | Pressure-drop ratio, $\frac{P_4 - P_5}{P_1 - P_3}$ | Vapor pressure at T _{in} , P _{vin} , N/cm ² abs | Vapor pressure at T _{out} , P _{vout} , N/cm ² abs | |
|-----|------|---------------------|------------------------------------|---------------------------------|------------------------|------------------------|------------------------|-------------------------|---------------------------------|------------------------|------------------------|------------------------|------------------------|------------------------|------------------------|------------------------|--------------------------|-----------|------|------------------|--|--|--|------|
| | | | | Pressure, N/cm ² abs | | | Temperature, K | | Pressure, N/cm ² abs | | | Temperature, K | | | | | | | | | | | | |
| | | | | Inlet, P ₁ | Throat, P ₂ | Outlet, P ₃ | Inlet, T _{C1} | Outlet, T _{C2} | Inlet, P ₄ | Outlet, P ₅ | Throat, P _t | Inlet, T _{in} | Distance from inlet | | | | Outlet, T _{out} | | | | | | | |
| | | | | | | | | | | | | | 1.3 cm, T ₁ | 2.3 cm, T ₂ | 3.3 cm, T ₃ | 4.3 cm, T ₄ | | | | | | | | |
| 1 | a | 73.1 | 14.5 | 33.4 | 17.0 | 26.5 | 1001 | 1001 | 25.2 | 19.2 | 11.0 | 994 | 994 | 994 | 994 | 994 | 994 | None ↓ | 0.87 | 7.1 | ---- | | | |
| | b | 15.8 | .6 | 18.5 | 17.8 | 18.1 | ---- | ---- | 18.1 | 17.9 | 17.4 | 923 | 923 | 923 | 923 | 923 | 923 | | | | | .54 | 3.4 | ---- |
| | c | 32.1 | 2.7 | 20.8 | 17.8 | 19.4 | 889 | 889 | 19.2 | 18.1 | 16.7 | 882 | 882 | 882 | 882 | 882 | 882 | | | | | .86 | 2.1 | ---- |
| | d | 47.3 | 5.9 | 24.4 | 17.7 | 21.4 | 905 | 905 | 20.9 | 18.3 | 15.2 | 899 | 899 | 899 | 899 | 899 | 898 | | | | | .85 | 2.6 | ---- |
| | e | 62.2 | 10.2 | 29.5 | 17.9 | 24.5 | 911 | 909 | 23.7 | 19.3 | 13.5 | 904 | 904 | 904 | 904 | 905 | 904 | | | | | .87 | 2.7 | ---- |
| | f | 76.8 | 15.6 | 35.1 | 17.2 | 27.5 | 919 | 919 | 26.2 | 19.7 | 10.8 | 915 | 915 | 915 | 915 | 916 | 915 | | | | | .86 | 3.0 | ---- |
| | g | 88.2 | 20.8 | 40.1 | 16.4 | 30.1 | 949 | 949 | 28.5 | 19.9 | 8.1 | 944 | 944 | 944 | 944 | 945 | 944 | | | | | .86 | 4.2 | ---- |
| 2 | 1 | 83.4 | 18.5 | 38.7 | 17.8 | 29.9 | 927 | 925 | 27.0 | 19.4 | 9.0 | 921 | 921 | 922 | 922 | 922 | 921 | None | 0.86 | 3.3 | ---- | | | |
| | 2 | 83.4 | 18.5 | 37.0 | 15.8 | 28.1 | 925 | 924 | 25.1 | 17.4 | 6.9 | 920 | 920 | 921 | 921 | 921 | 920 | None | .86 | 3.2 | ---- | | | |
| | 3 | 83.0 | 18.3 | 34.9 | 13.9 | 26.1 | 922 | 922 | 23.2 | 15.5 | 5.0 | 916 | 916 | 917 | 917 | 918 | 916 | None | .86 | 3.1 | ---- | | | |
| | 4 | 82.5 | 18.1 | 32.8 | 12.0 | 24.1 | 919 | 919 | 21.2 | 13.6 | 3.0 | 915 | 915 | 915 | 915 | 916 | 915 | High | .87 | 3.1 | ---- | | | |
| | 5 | 82.5 | 18.1 | 31.2 | 10.4 | 22.7 | 918 | 917 | 19.8 | 12.1 | 1.2 | 913 | 913 | 914 | 914 | 914 | 913 | ↓ | .89 | 3.0 | ---- | | | |
| | 6 | 83.0 | 18.3 | 29.9 | 9.0 | 21.3 | 917 | 916 | 18.4 | 10.8 | 0 | 913 | 913 | 913 | 913 | 914 | 914 | ↓ | .88 | 3.0 | ---- | | | |
| | 7 | 82.4 | 17.9 | 27.6 | 6.8 | 18.9 | 915 | 915 | 16.0 | 8.5 | -2.0 | 909 | 909 | 910 | 910 | 910 | 909 | ↓ | .87 | 2.8 | ---- | | | |
| | 7a | 82.4 | 17.9 | 25.2 | 4.4 | 16.6 | ---- | ---- | 13.6 | 6.1 | -4.5 | 908 | ---- | ---- | ---- | ---- | ---- | Medium | .86 | 2.8 | ---- | | | |
| 8 | 80.0 | 16.9 | 28.8 | 9.3 | 20.5 | 913 | 911 | 17.9 | 6.3 | 1.2 | 908 | 908 | 907 | 908 | 908 | 907 | Medium | 1.40 | 2.8 | 2.8 | | | | |
| 3 | 9 | 66.4 | 11.7 | 28.3 | 14.8 | 22.6 | 922 | 922 | 20.7 | 15.9 | 9.3 | 916 | 916 | 916 | 916 | 917 | 916 | None | 0.84 | 3.1 | ---- | | | |
| | 10 | ↓ | ↓ | 25.7 | 12.2 | 20.0 | 923 | ↓ | 18.1 | 13.2 | 6.6 | ↓ | ↓ | ↓ | ↓ | ↓ | 916 | ↓ | .85 | ↓ | ---- | | | |
| | 11 | ↓ | ↓ | 24.2 | 10.7 | 18.5 | ↓ | ↓ | 16.6 | 11.7 | 5.0 | ↓ | ↓ | ↓ | ↓ | ↓ | 916 | ↓ | .86 | ↓ | ---- | | | |
| | 12 | ↓ | ↓ | 23.4 | 9.9 | 17.7 | ↓ | ↓ | 15.8 | 10.9 | 4.4 | ↓ | ↓ | ↓ | ↓ | ↓ | 917 | ↓ | .84 | ↓ | ---- | | | |
| | 13 | ↓ | ↓ | 22.2 | 8.7 | 16.5 | ↓ | 923 | 14.6 | 9.7 | 2.9 | 917 | 917 | 917 | 917 | 918 | 916 | ↓ | .86 | 3.2 | ---- | | | |
| | 14 | ↓ | ↓ | 20.8 | 7.2 | 15.0 | ↓ | ↓ | 13.2 | 8.3 | 1.7 | 917 | 917 | 917 | 917 | 918 | 916 | Low | .85 | ↓ | ---- | | | |
| | 15 | 66.2 | 11.6 | 19.9 | 6.6 | 14.3 | 924 | ↓ | 12.4 | 7.4 | .7 | 918 | 918 | 918 | 918 | 919 | 917 | High | .88 | ↓ | ---- | | | |
| | 16 | 66.0 | 11.6 | 19.0 | 5.7 | 13.4 | 924 | ↓ | 11.5 | 6.7 | .3 | 918 | 918 | 918 | 918 | 919 | 918 | High | .84 | ↓ | ---- | | | |
| | 17 | 65.8 | 11.5 | 17.9 | 4.6 | 12.1 | 924 | ↓ | 10.3 | 5.4 | -1.3 | 918 | 918 | 918 | 918 | 919 | 918 | High | .84 | ↓ | ---- | | | |
| | 18 | 66.8 | 11.8 | 17.6 | 3.8 | 11.8 | 922 | 922 | 9.9 | 4.8 | -2.2 | 917 | 917 | 917 | 917 | 917 | 916 | Medium | .87 | ↓ | ---- | | | |
| | 18a | 66.8 | 11.8 | 16.3 | 2.6 | 10.5 | ---- | ---- | 8.5 | 3.6 | -3.2 | 914 | ---- | ---- | ---- | ---- | ---- | Medium | .87 | 3.0 | ---- | | | |
| 19 | 67.2 | 11.9 | 20.3 | 6.7 | 14.5 | 894 | 894 | 12.5 | 3.3 | .4 | 890 | 889 | 889 | 889 | 889 | 888 | Medium | 1.59 | 2.2 | 2.2 | | | | |
| 4 | 20 | 51.3 | 7.0 | 25.4 | 17.8 | 22.1 | 935 | 934 | 19.4 | 16.4 | 12.5 | 928 | 928 | 928 | 928 | 928 | 929 | None | 0.90 | 3.5 | ---- | | | |
| | 21 | 51.5 | 7.1 | 17.2 | 9.4 | 13.8 | 938 | 936 | 11.1 | 8.0 | 3.9 | 928 | 929 | 929 | 929 | 930 | 930 | ↓ | .91 | 3.6 | ---- | | | |
| | 22 | 51.3 | 7.0 | 14.5 | 6.8 | 11.2 | 938 | 936 | 8.5 | 5.4 | 1.4 | 930 | 930 | 930 | 930 | 931 | 931 | ↓ | .93 | 3.7 | ---- | | | |
| | 23 | 51.2 | ↓ | 13.4 | 5.7 | 10.1 | 938 | 936 | 7.4 | 4.4 | .5 | 930 | 930 | 930 | 930 | 933 | 933 | ↓ | .90 | ↓ | ---- | | | |
| | 24 | ↓ | ↓ | 12.3 | 4.7 | 9.0 | 939 | 937 | 6.4 | 3.3 | -.6 | 930 | 930 | 931 | 931 | 933 | 933 | ↓ | .92 | ↓ | ---- | | | |
| | 25 | ↓ | ↓ | 12.1 | 4.4 | 8.8 | 941 | 940 | 6.1 | 3.0 | -.9 | 933 | 933 | 933 | 933 | 933 | 933 | High | .92 | ↓ | ---- | | | |
| | 26 | ↓ | ↓ | 11.9 | 4.1 | 8.4 | 947 | 947 | 5.7 | 2.8 | -.9 | 939 | 939 | 939 | 939 | 939 | 939 | High | .86 | 4.0 | ---- | | | |
| | 26a | ↓ | ↓ | 11.7 | 4.2 | 8.6 | ---- | ---- | 5.7 | 2.8 | -1.4 | 936 | ---- | ---- | ---- | ---- | ---- | Medium | .96 | 3.9 | ---- | | | |
| | 27 | 51.7 | 7.1 | 15.7 | 8.0 | 12.3 | 942 | 942 | 9.7 | 3.6 | 3.0 | 933 | 934 | 933 | 933 | 933 | 933 | Medium | 1.84 | 3.8 | 3.8 | | | |
| | 28 | 51.2 | 7.0 | 15.7 | 8.0 | 12.3 | 940 | 939 | 9.7 | 4.4 | 2.9 | 933 | 933 | 933 | 933 | 933 | 933 | Medium | 1.56 | 3.7 | 3.7 | | | |
| 29 | 51.5 | 7.1 | 15.9 | 8.0 | 12.4 | 939 | 939 | 9.7 | 6.6 | 2.7 | 932 | 933 | 933 | 933 | 933 | 933 | None | .89 | 3.7 | ---- | | | | |

| | | | | | | | | | | | | | | | | | | | | | |
|----|-----|------|------|------|------|------|------|------|------|------|------|------|------|------|------|------|------|--------|------|------|------|
| 5 | 30 | 66.4 | 12.3 | 34.3 | 20.9 | 28.5 | 1074 | 1073 | 24.1 | 19.0 | 12.3 | 1064 | 1064 | 1064 | 1064 | 1064 | 1064 | None | 0.89 | 13.6 | ---- |
| | 31 | 66.3 | 12.3 | 31.2 | 17.9 | 25.6 | 1076 | 1075 | 21.2 | 16.0 | 9.0 | 1067 | 1066 | 1066 | 1066 | 1068 | 1066 | None | .92 | 13.9 | ---- |
| | 32 | 66.3 | 12.3 | 29.2 | 15.9 | 23.6 | 1075 | 1075 | 19.2 | 14.0 | 7.0 | 1065 | 1066 | 1066 | 1066 | 1068 | 1067 | None | .91 | 13.9 | ---- |
| | 33 | 65.6 | 12.1 | 26.9 | 13.9 | 21.4 | 1076 | 1076 | 17.0 | 12.0 | 5.2 | 1067 | 1068 | 1068 | 1068 | 1069 | 1068 | High | .91 | 14.0 | ---- |
| | 34 | 65.5 | 12.0 | 26.3 | 13.2 | 20.8 | 1078 | 1076 | 16.4 | 11.4 | 4.7 | 1068 | 1068 | 1068 | 1069 | 1070 | 1068 | High | .89 | 14.0 | ---- |
| | 35 | 65.5 | 12.0 | 25.3 | 12.4 | 19.8 | 1078 | 1078 | 15.5 | 10.5 | 3.9 | 1069 | 1069 | 1070 | 1070 | 1071 | 1070 | Medium | .90 | 14.1 | ---- |
| | 36 | 64.9 | 11.8 | 24.1 | 11.2 | 18.5 | 1076 | 1076 | 14.3 | 9.4 | 2.8 | 1066 | 1066 | 1067 | 1068 | 1069 | 1068 | Medium | .90 | 13.9 | ---- |
| 6 | 37 | 56.3 | 8.8 | 29.0 | 19.4 | 24.8 | 1083 | 1082 | 21.7 | 13.0 | 12.8 | 1067 | 1068 | 1060 | 1055 | 1055 | 1054 | Medium | 2.00 | 14.0 | 12.5 |
| | 38 | 56.2 | 8.8 | 27.7 | 18.2 | 23.6 | 1061 | 1060 | 20.5 | 12.7 | 11.8 | 1050 | 1050 | 1050 | 1050 | 1051 | 1050 | Medium | 1.93 | 12.1 | 12.1 |
| | 39 | 55.8 | 8.6 | 27.5 | 18.1 | 23.5 | 1062 | 1061 | 20.4 | 14.4 | 11.8 | 1050 | 1051 | 1051 | 1052 | 1053 | 1053 | High | 1.48 | 12.2 | 12.3 |
| | 40 | 56.2 | 8.8 | 25.9 | 16.3 | 21.8 | 1060 | 1059 | 18.6 | 14.9 | 9.9 | 1050 | 1049 | 1050 | 1050 | 1051 | 1050 | None | .92 | 12.0 | ---- |
| 7 | 41 | 62.7 | 10.7 | 35.4 | 23.4 | 30.2 | 999 | 999 | 25.2 | 20.3 | 13.9 | 991 | 990 | 990 | 989 | 991 | 990 | None | 0.94 | 6.8 | ---- |
| | 42 | 62.4 | 10.5 | 29.0 | 16.9 | 23.6 | 999 | 999 | 18.7 | 13.8 | 7.7 | 989 | 989 | 989 | 989 | 989 | 989 | ↓ | .92 | 6.8 | ---- |
| | 43 | | | 26.0 | 14.0 | 20.8 | 995 | 995 | 15.7 | 10.8 | 4.6 | 984 | 984 | 984 | 983 | 986 | 986 | | .93 | 6.4 | ---- |
| | 44 | | | 24.6 | 12.6 | 19.4 | 996 | 997 | 14.3 | 9.4 | 3.0 | 988 | 988 | 988 | 988 | 989 | 988 | | .94 | 6.7 | ---- |
| | 44a | | | 23.2 | 11.2 | 17.9 | ---- | ---- | 12.8 | 8.0 | 1.7 | 988 | ---- | ---- | ---- | ---- | ---- | Medium | .92 | 6.7 | ---- |
| | 45 | | | 27.2 | 15.0 | 21.7 | 997 | 997 | 17.0 | 7.1 | 5.6 | 987 | 986 | 986 | 985 | 988 | 986 | ↓ | 1.82 | 6.6 | 6.6 |
| | 46 | 62.2 | | 26.8 | 14.9 | 21.6 | 997 | 997 | 16.6 | 7.0 | 5.5 | 986 | 986 | 986 | 984 | 986 | 986 | | 1.85 | 6.6 | 6.6 |
| | 47 | 62.4 | | 26.8 | 14.8 | 21.6 | 997 | 997 | 16.5 | 6.3 | 5.2 | 984 | 984 | 979 | 977 | 978 | 977 | | 1.96 | 6.4 | 5.9 |
| | 48 | 62.4 | | 26.5 | 14.4 | 21.1 | 1001 | 1000 | 16.8 | 5.9 | 5.4 | 988 | 988 | 983 | 972 | 972 | 972 | Low | 2.02 | 6.7 | 5.7 |
| | 49 | 62.6 | 10.7 | 26.1 | 14.2 | 20.9 | 1001 | 1001 | 16.8 | 5.9 | 5.7 | 989 | 989 | | 972 | 972 | 971 | ↓ | 2.07 | 6.8 | 5.6 |
| | 50 | 62.5 | 10.6 | 25.0 | 13.0 | 19.9 | 1003 | 1001 | 17.0 | 5.9 | 5.7 | 989 | | | 972 | 971 | 971 | | 2.14 | | 5.6 |
| | 51 | 62.1 | 10.5 | 26.5 | 14.5 | 21.3 | 1003 | 1003 | 16.8 | 6.1 | 5.6 | 989 | | | 973 | 971 | 971 | | 2.05 | | 5.6 |
| | 52 | | | 26.9 | 14.8 | 21.6 | 1001 | 1001 | 17.1 | 7.2 | 5.9 | 980 | | 988 | 988 | 990 | 989 | Medium | 1.86 | | 6.8 |
| | 53 | | | 26.8 | 14.8 | 21.6 | 1003 | 1003 | 17.2 | 9.1 | 6.0 | 991 | 991 | 991 | 991 | 994 | 993 | High | 1.54 | 6.9 | 7.0 |
| | 54 | | | 24.1 | 12.3 | 18.9 | 1001 | 1000 | 14.5 | 9.7 | 3.6 | 991 | 990 | 990 | 989 | 994 | 993 | None | .93 | 6.8 | ---- |
| | 55 | 62.4 | | 31.4 | 19.4 | 26.1 | 1000 | 999 | 21.8 | 17.0 | 10.9 | 989 | 989 | 989 | 989 | 989 | 989 | None | .91 | 6.8 | ---- |
| 8 | 56 | 47.0 | 6.0 | 24.8 | 17.8 | 21.7 | 1006 | 1005 | 19.4 | 16.5 | 12.7 | 994 | 994 | 994 | 994 | 994 | 994 | None | 0.96 | 7.1 | ---- |
| | 57 | 46.6 | 5.9 | 19.2 | 12.5 | 16.2 | 1006 | 1005 | 13.9 | 11.1 | 7.7 | 994 | 994 | 994 | 994 | 994 | 994 | ↓ | .94 | 7.1 | ---- |
| | 58 | 46.6 | 5.9 | 16.0 | 9.2 | 13.0 | 1004 | 1003 | .8 | 8.0 | 4.3 | 992 | 991 | 991 | 990 | 991 | 990 | | .96 | 6.9 | ---- |
| | 59 | 47.0 | 6.0 | 14.8 | 8.1 | 11.9 | 1005 | 1005 | 9.6 | 6.8 | 3.2 | 992 | 991 | 991 | 991 | 994 | 992 | | .94 | 6.9 | ---- |
| | 60 | 47.0 | | 13.6 | 6.8 | 10.5 | 1001 | 1001 | 8.3 | 5.5 | 2.1 | 989 | 989 | 989 | 989 | 989 | 989 | ↓ | .93 | 6.8 | ---- |
| | 61 | 46.9 | | 12.3 | 5.5 | 9.3 | 1004 | 1003 | 7.0 | 4.1 | .6 | 990 | 990 | 990 | 989 | 991 | 990 | | .93 | | ---- |
| | 62 | | | 12.2 | 5.4 | 9.2 | 1001 | 1000 | 7.0 | 4.1 | .6 | 989 | 989 | 989 | 988 | 989 | 989 | | .96 | | ---- |
| | 63 | | | 11.9 | 5.0 | 9.0 | | 1000 | 6.6 | 3.7 | -.2 | 989 | 989 | 989 | 989 | 989 | 989 | High | .98 | | ---- |
| | 64 | | 5.9 | 17.0 | 10.3 | 14.0 | | 1000 | 11.7 | 5.0 | 5.3 | 984 | 983 | 973 | 961 | 959 | 958 | Low | 2.23 | 6.3 | 4.9 |
| | 65 | | 5.9 | 16.6 | 9.9 | 13.7 | | 1001 | 11.7 | 5.2 | 5.4 | 984 | 984 | 974 | 962 | 960 | 959 | ↓ | 2.33 | 6.4 | 5.0 |
| | 66 | | 5.9 | 17.7 | 10.8 | 14.7 | 1003 | 1003 | 11.9 | 5.2 | 5.4 | 984 | 985 | 976 | 963 | 962 | 961 | | 2.25 | 6.4 | 5.0 |
| | 67 | 47.3 | 6.1 | 19.1 | 12.2 | 16.0 | 1001 | 1000 | 12.0 | 6.2 | 5.3 | 986 | 986 | 979 | 974 | 976 | 976 | | 1.86 | 6.5 | 5.9 |
| | 68 | 47.3 | 6.1 | 18.8 | 11.9 | 15.8 | 1000 | 1000 | 11.9 | 8.8 | 5.0 | 989 | 989 | 988 | 988 | 989 | 989 | None | .96 | 6.8 | ---- |
| 9 | 69 | 62.1 | 10.3 | 29.5 | 17.5 | 24.3 | 946 | 944 | 18.5 | 13.8 | 7.7 | 934 | 934 | 935 | 934 | 936 | 935 | None | 0.90 | 3.9 | ---- |
| | 69a | 62.1 | 10.3 | 22.0 | 10.0 | 16.9 | ---- | ---- | 11.1 | 6.1 | -.6 | 944 | ---- | ---- | ---- | ---- | ---- | High | .97 | 4.3 | ---- |
| | 69b | 62.1 | 10.3 | 21.4 | 9.6 | 16.4 | ---- | ---- | 10.6 | 5.9 | -.6 | 949 | ---- | ---- | ---- | ---- | ---- | Low | .95 | 4.4 | ---- |
| | 70 | 56.1 | 8.5 | 22.0 | 12.1 | 17.7 | 967 | 966 | 12.9 | 5.1 | 3.9 | 956 | 955 | 955 | 954 | 955 | 955 | Low | 1.80 | 4.8 | 4.8 |
| 10 | 71 | 61.7 | 10.4 | 32.3 | 20.3 | 27.1 | 1018 | 1018 | 21.5 | 16.7 | 10.5 | 1009 | 1008 | 1010 | 1007 | 1010 | 1009 | Low | 0.92 | 8.2 | ---- |
| | 71a | 61.7 | 10.4 | 23.9 | 12.0 | 18.8 | ---- | ---- | 13.2 | 8.4 | 1.9 | 1005 | ---- | ---- | ---- | ---- | ---- | High | .96 | 7.9 | ---- |
| | 71b | 61.7 | 10.4 | 22.1 | 10.2 | 17.0 | ---- | ---- | 11.4 | 6.6 | 0 | 1006 | ---- | ---- | ---- | ---- | ---- | Medium | .96 | 8.0 | ---- |
| | 72 | 50.1 | 6.9 | 22.7 | 14.8 | 19.3 | 1039 | 1038 | 15.6 | 7.2 | 8.2 | 1019 | 1019 | 1008 | 991 | 991 | 990 | Low | 2.44 | 9.2 | 6.8 |

^aFor quality values and remarks see table II(a).

^bShown only for flashed runs.

TABLE III. - DETAILED DATA FOR VENTURI WITH ARTIFICIAL THROAT CAVITY (SERIES II)

(a) U. S. customary units

| Set | Run | Flow rate, W, lbm/hr | Dynamic head, q, psi | Control venturi | | | | | | Test venturi | | | | | | | | Noise indication | Pressure drop ratio, $\frac{P_4 - P_5}{P_1 - P_3}$ | Vapor pressure at T_{in} , P_{vin} , psia | Vapor pressure at T_{out} , P_{vout} , psia | Exit quality, X, percent | Remarks |
|-----|-----|----------------------|----------------------|-----------------|---------------|---------------|--------------------------|------------------|--------------|----------------|---------------|-----------------|--------------------------|----------------|-------|-------------------|------------|------------------|--|---|---|-----------------------------|---------|
| | | | | Pressure, psia | | | Temperature, $^{\circ}F$ | | | Pressure, psia | | | Temperature, $^{\circ}F$ | | | | | | | | | | |
| | | | | Inlet, P_1 | Throat, P_2 | Outlet, P_3 | Inlet, T_{C1} | Outlet, T_{C2} | Inlet, P_4 | Outlet, P_5 | Throat, P_t | Inlet, T_{in} | Distance from inlet | | | Outlet, T_{out} | | | | | | | |
| | | | | | | | | | | | | 0.9 in., T_2 | 1.3 in., T_3 | 1.7 in., T_4 | | | | | | | | | |
| 11 | h | 545 | 18.8 | 52.0 | 31.3 | 43.3 | 1388 | 1382 | 42.0 | 32.9 | 20.5 | 1372 | 1372 | 1371 | 1377 | 1375 | None | 1.04 | 13.0 | --- | ---- | All-liquid flow calibration | |
| | j | 600 | 22.8 | 56.1 | 31.2 | 45.8 | 1380 | 1374 | 44.4 | 33.2 | 17.5 | 1368 | 1368 | 1366 | 1370 | 1369 | 1.08 | 12.8 | --- | ---- | | | |
| | k | 481 | 14.6 | 47.3 | 31.5 | 40.7 | 1388 | 1381 | 39.7 | 32.5 | 22.3 | 1371 | 1371 | 1370 | 1373 | 1371 | 1.10 | 13.0 | --- | ---- | | | |
| | m | 419 | 11.1 | 43.7 | 31.5 | 38.5 | 1368 | 1362 | 37.8 | 32.3 | 24.8 | 1350 | 1350 | 1349 | 1352 | 1351 | 1.07 | 11.6 | --- | ---- | | | |
| | n | 360 | 8.2 | 40.5 | 31.5 | 36.7 | 1364 | 1358 | 36.1 | 32.0 | 26.4 | 1346 | 1346 | 1344 | 1348 | 1347 | 1.07 | 11.3 | --- | ---- | | | |
| | p | 297 | 5.6 | 37.6 | 31.4 | 34.9 | 1383 | 1386 | 34.6 | 31.7 | 28.0 | 1360 | 1359 | 1358 | 1362 | 1361 | 1.06 | 12.8 | --- | ---- | | | |
| | q | 240 | 3.6 | 35.3 | 31.3 | 33.5 | 1384 | 1378 | 33.3 | 31.5 | 29.2 | 1360 | 1358 | 1356 | 1359 | 1359 | 1.03 | 12.1 | --- | ---- | | | |
| | r | 119 | .9 | 41.6 | 40.5 | 41.1 | 1417 | 1414 | 41.0 | 40.6 | 40.0 | 1388 | 1387 | 1384 | 1388 | 1386 | .87 | 14.2 | --- | ---- | | | |
| 12 | 73 | 486 | 14.7 | 54.5 | 38.4 | 48.0 | 1322 | 1316 | 38.8 | 31.4 | 20.4 | 1303 | 1303 | 1300 | 1306 | 1306 | None | 1.14 | 8.9 | --- | ---- | Liquid | |
| | 74 | 489 | 14.9 | 51.4 | 35.0 | 44.6 | 1327 | 1322 | 35.3 | 27.9 | 17.6 | 1309 | 1309 | 1305 | 1310 | 1309 | 1.08 | 9.2 | --- | ---- | | | |
| | 75 | 487 | 14.8 | 45.1 | 28.7 | 38.1 | 1327 | 1322 | 28.9 | 21.5 | 11.6 | 1309 | 1309 | 1304 | 1310 | 1309 | 1.05 | 9.2 | --- | ---- | | | |
| | 76 | 484 | 14.7 | 41.7 | 25.5 | 34.8 | 1325 | 1320 | 25.5 | 18.2 | 8.1 | 1307 | 1307 | 1302 | 1309 | 1308 | 1.07 | 9.1 | --- | ---- | | | |
| | 77 | 486 | 14.7 | 40.1 | 23.7 | 33.1 | 1320 | 1315 | 23.8 | 16.4 | 6.4 | 1302 | 1302 | 1299 | 1303 | 1303 | None/High | 1.06 | 8.8 | --- | ---- | | |
| | 78 | 487 | 14.8 | 38.6 | 22.1 | 31.6 | 1322 | 1318 | 22.1 | 14.6 | 4.4 | 1305 | 1305 | 1302 | 1308 | 1307 | High | 1.07 | 9.0 | --- | ---- | | |
| | 79 | 487 | 14.8 | 37.0 | 20.5 | 30.0 | 1323 | 1318 | 20.4 | 13.0 | 3.0 | 1306 | 1306 | 1302 | 1308 | 1307 | High | 1.05 | 9.0 | --- | ---- | | |
| | 80 | 487 | 14.8 | 34.7 | 18.1 | 27.7 | 1323 | 1317 | 18.1 | 10.6 | .5 | 1307 | 1306 | 1302 | 1309 | 1308 | Medium | 1.06 | 9.1 | --- | ---- | | |
| | 81 | 483 | 14.6 | 45.1 | 29.1 | 38.5 | 1340 | 1335 | 29.7 | 10.7 | 12.7 | 1320 | 1319 | 1315 | 1319 | 1317 | Low | 2.89 | 9.8 | 9.6 | ---- | | |
| | 82 | 484 | | 43.5 | 27.1 | 36.6 | 1335 | 1330 | 29.1 | 8.8 | 11.7 | 1310 | 1299 | 1290 | 1295 | 1293 | | 2.92 | 9.2 | 8.3 | 0.37 | | |
| | 83 | 484 | | 42.2 | 25.9 | 35.2 | 1332 | 1327 | 28.9 | 8.1 | 11.6 | 1308 | 1290 | 1280 | 1281 | 1279 | | 2.99 | 9.1 | 7.6 | .63 | | |
| | 84 | 484 | | 41.5 | 25.1 | 34.7 | 1331 | 1325 | 29.0 | 7.9 | 11.6 | 1303 | 1288 | 1275 | 1279 | 1278 | | 3.09 | 8.9 | 7.6 | .54 | | |
| | 85 | 489 | 14.9 | 41.8 | 25.3 | 34.9 | 1331 | 1325 | 29.3 | 8.3 | 11.8 | 1305 | 1290 | 1281 | 1288 | 1288 | | 3.04 | 9.0 | 8.1 | .36 | | |
| | 86 | 486 | 14.8 | 43.0 | 26.6 | 36.0 | 1328 | 1325 | 29.0 | 10.0 | 11.6 | 1310 | 1308 | 1302 | 1310 | 1309 | | 2.74 | 9.2 | 9.2 | ---- | | |
| | 87 | 483 | 14.6 | 42.8 | 26.3 | 35.7 | 1322 | 1318 | 28.9 | 11.1 | 11.4 | 1308 | 1305 | 1301 | 1309 | 1307 | Medium | 2.54 | 9.1 | 9.1 | ---- | | |
| | 88 | 486 | 14.7 | 37.2 | 20.7 | 30.3 | 1301 | 1295 | 21.2 | 13.7 | 3.3 | 1289 | 1287 | 1281 | 1289 | 1288 | High | 1.09 | 8.1 | --- | ---- | | |
| | 89 | 489 | 14.9 | 38.5 | 22.0 | 31.6 | 1308 | 1303 | 22.6 | 15.1 | 4.7 | 1290 | 1290 | 1289 | 1290 | 1289 | High | 1.08 | 8.2 | --- | ---- | | |
| | 90 | 488 | 14.8 | 40.5 | 23.9 | 33.5 | 1309 | 1305 | 24.4 | 16.9 | 6.7 | 1290 | 1290 | 1289 | 1291 | 1290 | High | 1.07 | 8.2 | --- | ---- | | |
| | 91 | 488 | 14.8 | 40.4 | 23.8 | 33.4 | 1310 | 1306 | 24.4 | 16.9 | 6.5 | 1291 | 1290 | 1289 | 1292 | 1290 | None | 1.08 | 8.2 | --- | ---- | | |
| | 92 | 486 | 14.7 | 42.3 | 25.7 | 35.3 | 1305 | 1302 | 26.3 | 18.8 | 8.5 | 1289 | 1289 | 1285 | 1290 | 1288 | None | 1.07 | 8.1 | --- | ---- | | |
| | 93 | 486 | 14.7 | 39.8 | 23.2 | 32.9 | 1315 | 1310 | 23.8 | 16.3 | 5.7 | 1299 | 1299 | 1294 | 1300 | 1299 | None | 1.09 | 8.7 | --- | ---- | | |
| | 94 | 486 | 14.7 | 37.7 | 21.3 | 30.9 | 1317 | 1310 | 21.8 | 14.3 | 3.8 | 1299 | 1299 | 1294 | 1300 | 1299 | | 1.10 | 8.7 | --- | ---- | | |
| | 95 | 483 | 14.6 | 36.5 | 20.2 | 29.6 | 1325 | 1320 | 20.7 | 13.2 | 3.1 | 1306 | 1306 | 1301 | 1309 | 1308 | | 1.08 | 9.0 | --- | ---- | | |
| | 96 | 483 | 14.6 | 35.4 | 19.1 | 28.5 | 1327 | 1320 | 19.5 | 12.1 | 2.1 | 1309 | 1309 | 1306 | 1310 | 1309 | | 1.07 | 9.2 | --- | ---- | | |
| | 97 | 489 | 14.9 | 35.1 | 18.4 | 28.0 | 1326 | 1320 | 18.8 | 11.3 | 1.1 | 1309 | 1309 | 1304 | 1310 | 1310 | | 1.06 | | --- | ---- | | |
| | 98 | 484 | 14.7 | 33.6 | 17.0 | 26.6 | 1328 | 1323 | 17.5 | 10.0 | -.2 | 1310 | 1310 | 1308 | 1311 | 1310 | High | 1.07 | | --- | ---- | | |
| | 98a | 485 | 14.7 | 33.3 | 16.7 | 26.2 | ----- | ----- | 16.9 | 9.5 | -.4 | 1310 | ----- | ----- | ----- | ----- | Medium/Low | 1.04 | | --- | ---- | | |
| | 99 | 483 | 14.6 | 42.4 | 26.2 | 35.7 | 1333 | 1328 | 29.4 | 9.0 | 12.1 | 1310 | 1301 | 1299 | 1301 | 1301 | Low | 3.06 | | 8.7 | 0.20 | | |
| 100 | 484 | 14.7 | 43.2 | 26.8 | 36.3 | 1338 | 1333 | 29.9 | 10.6 | 12.4 | 1319 | 1318 | 1313 | 1318 | 1318 | Medium | 2.80 | 9.7 | 9.6 | ----- | | | |
| 101 | 484 | 14.7 | 43.3 | 26.8 | 36.4 | 1340 | 1335 | 30.1 | 12.4 | 12.4 | 1321 | 1320 | 1319 | 1321 | 1321 | High | 2.57 | 9.8 | 9.8 | ----- | | | |
| 102 | 484 | 14.7 | 35.8 | 19.2 | 28.8 | 1335 | 1330 | 22.4 | 14.7 | 4.1 | 1319 | 1316 | 1311 | 1319 | 1318 | High | 1.10 | 9.7 | --- | ---- | | | |
| 103 | 483 | 14.6 | 37.1 | 20.7 | 30.3 | 1328 | 1322 | 23.8 | 16.2 | 5.6 | 1310 | 1308 | 1305 | 1312 | 1311 | None | 1.11 | 9.2 | --- | ---- | | | |
| 104 | 483 | 14.6 | 40.2 | 23.6 | 33.1 | 1323 | 1318 | 26.8 | 19.2 | 9.0 | 1305 | 1305 | 1302 | 1307 | 1307 | None | 1.07 | 9.0 | --- | ---- | | | |

| | | | | | | | | | | | | | | | | | | | | | | | |
|----|------|-----|------|------|------|------|------|------|------|------|------|------|------|------|------|------|-----------|------|------|-----|------|----------------------|------------------|
| 13 | 105 | 490 | 15.0 | 40.5 | 23.7 | 33.5 | 1325 | 1320 | 27.0 | 19.3 | 8.4 | 1308 | 1308 | 1305 | 1310 | 1309 | None | 1.11 | 9.1 | --- | --- | Liquid | Pressure ramp |
| | 105a | 490 | 15.0 | 31.3 | 14.6 | 24.3 | --- | --- | 17.5 | 10.0 | -5 | 1310 | --- | --- | --- | --- | High | 1.07 | 9.2 | --- | --- | Incipient cavitation | |
| | 105b | 490 | 15.0 | 29.7 | 13.0 | 22.9 | --- | --- | 16.2 | 8.7 | -2.2 | 1311 | --- | --- | --- | --- | High Low | 1.10 | 9.2 | --- | --- | Incipient flashing | |
| | 106 | 368 | 8.5 | 31.1 | 21.4 | 26.9 | 1385 | 1380 | 23.2 | 8.9 | 12.6 | 1345 | 1319 | 1302 | 1300 | 1299 | Low | 3.45 | 11.2 | 8.6 | 1.00 | Flashed | |
| | 107 | 483 | 14.6 | 39.9 | 23.5 | 33.1 | 1324 | 1320 | 26.8 | 19.2 | 8.8 | 1308 | 1306 | 1304 | 1308 | 1307 | None | 1.10 | 9.1 | --- | --- | Liquid | |
| 14 | 108 | 361 | 8.1 | 44.3 | 35.1 | 40.3 | 1290 | 1285 | 22.6 | 18.6 | 13.3 | 1268 | 1268 | 1267 | 1272 | 1270 | None | 1.02 | 7.2 | --- | --- | Liquid | |
| | 109 | 362 | 8.1 | 40.4 | 31.4 | 36.7 | 1290 | 1286 | 18.9 | 14.7 | 8.8 | 1271 | 1268 | 1266 | 1272 | 1269 | None | 1.12 | 7.4 | --- | --- | Liquid | |
| | 109a | 358 | 7.9 | 37.3 | 28.1 | 33.2 | --- | --- | 15.6 | 11.6 | 6.8 | 1270 | --- | --- | --- | --- | None High | .97 | 7.4 | --- | --- | Incipient cavitation | |
| | 110 | 358 | 7.9 | 36.9 | 28.1 | 33.1 | 1290 | 1286 | 15.5 | 11.6 | 6.4 | 1270 | 1268 | 1266 | 1272 | 1269 | High | 1.03 | 7.3 | --- | --- | Cavitated | |
| | 111 | 355 | 7.8 | 34.8 | 26.2 | 31.1 | 1288 | 1284 | 13.6 | 9.6 | 4.4 | 1268 | 1265 | 1263 | 1267 | 1265 | ↓ | 1.07 | 7.2 | --- | --- | ↓ | |
| | 112 | 360 | 8.0 | 32.9 | 24.1 | 29.1 | 1277 | 1273 | 12.1 | 8.0 | 2.7 | 1258 | 1256 | 1253 | 1258 | 1256 | ↓ | 1.06 | 6.8 | --- | --- | ↓ | |
| | 113 | 355 | 7.8 | 31.1 | 22.5 | 27.3 | 1275 | 1270 | 10.6 | 6.7 | 1.6 | 1254 | 1253 | 1250 | 1255 | 1254 | ↓ | 1.06 | 6.7 | --- | --- | ↓ | |
| | 114 | 355 | 7.8 | 30.2 | 21.6 | 26.5 | 1272 | 1268 | 9.7 | 5.7 | .4 | 1252 | 1250 | 1248 | 1252 | 1251 | Medium | 1.08 | 6.6 | --- | --- | ↓ | |
| | 115 | 358 | 7.9 | 29.6 | 20.9 | 25.8 | 1270 | 1265 | 8.9 | 4.9 | -2 | 1250 | 1248 | 1246 | 1250 | 1250 | Low | 1.04 | 6.5 | --- | --- | ↓ | |
| | 116 | 353 | 7.7 | 28.9 | 20.4 | 25.2 | 1270 | 1265 | 8.7 | 4.8 | -3 | 1248 | 1248 | 1245 | 1250 | 1248 | ↓ | 1.06 | 6.4 | --- | --- | ↓ | |
| | 117 | 363 | 8.1 | 20.9 | 11.8 | 16.9 | 1265 | 1261 | 8.9 | 4.8 | -6 | 1248 | 1245 | 1243 | 1247 | 1245 | ↓ | 1.04 | 6.4 | --- | --- | ↓ | |
| | 118 | ↓ | ↓ | 26.8 | 18.1 | 23.1 | 1261 | 1255 | 8.7 | 4.6 | -9 | 1240 | 1238 | 1236 | 1240 | 1238 | ↓ | 1.10 | 6.2 | --- | --- | ↓ | |
| | 118a | ↓ | ↓ | 20.0 | ↓ | 25.1 | --- | --- | 10.0 | 6.0 | .5 | 1240 | --- | --- | --- | --- | ↓ | 1.05 | --- | --- | --- | Incipient flashing | |
| | 119 | ↓ | ↓ | 28.9 | 20.1 | 25.1 | 1261 | 1257 | 16.3 | 6.0 | 6.9 | 1240 | 1229 | 1225 | 1228 | 1226 | ↓ | 2.75 | --- | 5.6 | 0.30 | Flashed | |
| | 120 | ↓ | ↓ | 31.2 | 22.5 | 27.6 | 1261 | 1258 | 16.4 | 7.8 | 7.1 | 1241 | 1238 | 1237 | 1241 | 1240 | ↓ | 2.37 | --- | 6.1 | --- | Flashed | |
| | 121 | 360 | 8.0 | 33.2 | 24.4 | 29.4 | 1263 | 1260 | 13.6 | 9.7 | 4.3 | 1242 | 1242 | 1238 | 1242 | 1240 | High | 1.06 | --- | --- | --- | Cavitated | |
| | 122 | 360 | 8.0 | 35.3 | 26.5 | 31.5 | 1265 | 1262 | 15.8 | 11.8 | 6.6 | 1244 | 1245 | 1242 | 1247 | 1246 | High | 1.04 | 6.3 | --- | --- | Cavitated | |
| | 123 | 361 | 8.1 | 37.0 | 28.0 | 33.1 | 1267 | 1263 | 17.2 | 13.1 | 7.6 | 1249 | 1246 | 1244 | 1248 | 1247 | None | 1.07 | 6.4 | --- | --- | Liquid | |
| 15 | 124 | 361 | 8.2 | 36.9 | 28.0 | 33.2 | 1335 | 1330 | 17.2 | 13.1 | 7.6 | 1312 | 1311 | 1310 | 1313 | 1310 | None | 1.08 | 9.3 | --- | --- | Liquid | |
| | 125 | 360 | 8.1 | 35.0 | 26.0 | 31.1 | 1339 | 1332 | 15.0 | 11.0 | 5.7 | 1315 | 1315 | 1311 | 1319 | 1317 | High | 1.04 | 9.5 | --- | --- | Incipient cavitation | |
| | 125a | ↓ | ↓ | 33.4 | 24.5 | 30.0 | --- | --- | 13.4 | 9.5 | 3.5 | 1315 | --- | --- | --- | --- | High Low | 1.15 | 9.5 | --- | --- | Incipient flashing | |
| | 126 | ↓ | ↓ | 39.7 | 30.9 | 35.9 | 1340 | 1335 | 20.0 | 9.2 | 10.8 | 1315 | 1301 | 1299 | 1301 | 1300 | Low | 2.81 | 9.5 | 8.7 | 0.33 | Flashed | |
| | 127 | ↓ | ↓ | 40.1 | 31.1 | 36.2 | 1345 | 1340 | 20.3 | 8.0 | 11.0 | 1311 | 1290 | 1280 | 1281 | 1279 | ↓ | 3.17 | 9.3 | 7.7 | .70 | ↓ | |
| | 128 | 361 | 8.2 | 30.4 | 21.6 | 26.6 | 1340 | 1335 | 20.2 | 7.4 | 11.1 | 1309 | 1281 | 1270 | 1270 | 1269 | ↓ | 3.38 | 9.2 | 7.2 | .87 | ↓ | |
| | 129 | 360 | 8.1 | 29.5 | 20.6 | 25.6 | 1335 | 1330 | 20.0 | 7.0 | 10.3 | 1301 | 1278 | 1261 | 1261 | 1260 | ↓ | 3.32 | 8.8 | 6.9 | .89 | ↓ | |
| | 130 | 360 | ↓ | 29.5 | ↓ | 25.5 | 1335 | 1330 | 20.0 | 8.0 | 10.8 | 1304 | 1285 | 1276 | 1280 | 1278 | ↓ | 3.08 | 8.9 | 7.6 | .57 | ↓ | |
| | 131 | 360 | ↓ | 29.5 | ↓ | 25.6 | 1332 | 1328 | 20.1 | 9.7 | 10.8 | 1310 | 1305 | 1301 | 1309 | 1302 | ↓ | 2.05 | 9.2 | 8.8 | --- | ↓ | |
| | 132 | 363 | ↓ | 29.6 | ↓ | 25.7 | 1329 | 1322 | 20.0 | 10.6 | 10.5 | 1309 | 1305 | 1301 | 1309 | 1302 | ↓ | 2.39 | 9.2 | 8.8 | --- | ↓ | |
| | 133 | 360 | ↓ | 27.6 | 18.7 | 23.7 | 1328 | 1321 | 16.9 | 12.8 | 7.6 | 1305 | 1304 | 1301 | 1308 | 1306 | None | 1.05 | 9.0 | --- | --- | Liquid | |
| | 134 | 355 | 7.9 | 28.8 | 20.0 | 25.0 | 1330 | 1325 | 18.3 | 14.3 | 9.0 | 1310 | 1309 | 1305 | 1310 | 1308 | None | 1.06 | 9.2 | --- | --- | Liquid | |
| | 135 | 360 | 8.1 | 27.4 | 18.4 | 23.5 | 1331 | 1325 | 16.6 | 12.5 | 7.3 | 1310 | 1309 | 1305 | 1310 | 1308 | ↓ | 1.03 | 9.2 | --- | --- | Liquid | |
| | 136 | ↓ | ↓ | 25.8 | 16.7 | 21.8 | 1335 | 1330 | 15.0 | 10.9 | 5.5 | 1318 | 1318 | 1314 | 1318 | 1316 | ↓ | 1.05 | 9.7 | --- | --- | Liquid | |
| | 136a | ↓ | ↓ | 24.5 | 15.4 | 20.7 | --- | --- | 13.5 | 9.5 | 3.9 | 1318 | --- | --- | --- | --- | ↓ | 1.05 | 9.7 | --- | --- | Incipient flashing | |
| | 137 | ↓ | ↓ | 31.3 | 22.3 | 27.5 | 1340 | 1335 | 20.6 | 9.7 | 11.1 | 1318 | 1306 | 1300 | 1303 | 1300 | ↓ | 2.88 | 9.7 | 8.7 | 0.40 | Flashed | |
| | 138 | ↓ | ↓ | 31.2 | 22.2 | 27.4 | 1341 | 1335 | 20.5 | 8.0 | 11.0 | 1310 | 1290 | 1279 | 1281 | 1280 | ↓ | 3.24 | 9.2 | 7.7 | .65 | ↓ | |
| | 139 | ↓ | ↓ | 32.0 | 23.0 | 28.2 | 1341 | 1336 | 20.5 | 7.5 | 11.1 | 1310 | 1281 | 1270 | 1269 | 1265 | ↓ | 3.44 | 9.2 | 7.2 | .89 | ↓ | |
| | 140 | ↓ | ↓ | 32.0 | 22.9 | 28.3 | 1340 | 1335 | 20.4 | 7.3 | 10.9 | 1309 | 1281 | 1268 | 1265 | 1265 | ↓ | 3.49 | 9.2 | 7.1 | .83 | ↓ | |
| | 141 | 357 | 8.0 | 31.8 | 22.9 | 28.0 | 1343 | 1340 | 20.4 | 9.5 | 11.1 | 1318 | 1309 | 1301 | 1305 | 1302 | ↓ | 2.89 | 9.7 | 8.8 | .35 | ↓ | |
| | 142 | 358 | 8.1 | 32.0 | 23.0 | 28.2 | 1338 | 1332 | 20.6 | 10.3 | 11.1 | ↓ | 1311 | 1310 | 1312 | 1310 | Low | 2.71 | --- | 9.2 | .17 | ↓ | |
| | 143 | 358 | 8.1 | 31.9 | 22.9 | 28.1 | 1339 | 1334 | 20.4 | 11.7 | 11.0 | 1314 | 1311 | 1318 | 1316 | 1316 | Medium | 2.28 | --- | 9.5 | --- | ↓ | |
| | 144 | 360 | 8.1 | 28.8 | 19.8 | 24.9 | 1339 | 1334 | 17.3 | 13.1 | 7.4 | ↓ | 1316 | 1312 | 1319 | 1317 | None | 1.11 | --- | --- | --- | Liquid | |

^aShown only for flashed runs.

TABLE III. - Continued. DETAILED DATA FOR VENTURI WITH ARTIFICIAL THROAT CAVITY (SERIES II)

(a) Concluded. U.S. customary units

| Set | Run | Flow rate, W, lbm/hr | Dynamic head, q, psi | Control venturi | | | | | | Test venturi | | | | | | | | Noise indication | Pressure-drop ratio, $\frac{P_4 - P_5}{P_1 - P_3}$ | Vapor pressure at T_{in} , P_{vin} , psia | Vapor pressure at T_{out} , P_{vout} , psia | Exit quality, X, percent | Remarks |
|-----|------|----------------------|----------------------|-----------------|---------------|---------------|-----------------|------------------|--------------|----------------|---------------|-----------------|---------------------|----------------|----------------|-------------------|---------------|------------------|--|---|---|--------------------------|-----------------------------------|
| | | | | Pressure, psia | | | Temperature, °F | | | Pressure, psia | | | Temperature, °F | | | | | | | | | | |
| | | | | Inlet, P_1 | Throat, P_2 | Outlet, P_3 | Inlet, T_{C1} | Outlet, T_{C2} | Inlet, P_4 | Outlet, P_5 | Throat, P_t | Inlet, T_{in} | Distance from inlet | | | Outlet, T_{out} | | | | | | | |
| | | | | | | | | | | | | | 0.9 in., T_2 | 1.3 in., T_3 | 1.7 in., T_4 | | | | | | | | |
| 16 | 145 | 352 | 7.9 | 36.5 | 27.7 | 32.8 | 1445 | 1440 | 25.4 | 21.3 | 15.7 | 1419 | 1419 | 1416 | 1420 | 1419 | None | 1.10 | 16.7 | ---- | ---- | ---- | Liquid |
| | 146 | 352 | 7.9 | 34.7 | 25.9 | 31.0 | 1445 | 1440 | 23.5 | 19.4 | 13.8 | 1421 | 1420 | 1419 | 1421 | 1420 | None | 1.11 | 16.8 | ---- | ---- | ---- | Liquid |
| | 147 | 354 | 8.0 | 29.0 | 20.2 | 25.2 | 1447 | 1440 | 17.7 | 13.6 | 8.2 | 1422 | 1421 | 1419 | 1421 | 1420 | None | 1.06 | 16.9 | ---- | ---- | ---- | Liquid |
| | 147a | 357 | 8.1 | 27.5 | 18.7 | 23.9 | ---- | ---- | 16.0 | 12.0 | 6.2 | 1422 | ---- | ---- | ---- | ---- | Medium | 1.11 | 16.9 | ---- | ---- | ---- | Incipient cavitation |
| | 147b | ↓ | ↓ | 27.2 | 18.4 | 23.6 | ---- | ---- | 15.7 | 11.9 | 6.4 | 1422 | ---- | ---- | ---- | ---- | Low | 1.06 | 16.9 | ---- | ---- | ---- | Incipient flashing |
| | 148 | ↓ | ↓ | 37.6 | 28.7 | 33.8 | 1455 | 1446 | 26.3 | 12.3 | 16.8 | 1408 | 1372 | 1353 | 1352 | 1352 | ↓ | 3.65 | 15.7 | 11.7 | 1.23 | 1.23 | Flashed |
| | 149 | ↓ | ↓ | 37.5 | 28.6 | 33.7 | 1455 | 1450 | 26.2 | 11.9 | 16.8 | 1409 | 1372 | 1351 | 1349 | 1348 | ↓ | 3.81 | 15.8 | 11.4 | 1.33 | 1.33 | ↓ |
| | 150 | 354 | 8.0 | 37.3 | 28.5 | 33.6 | 1455 | 1448 | 26.1 | 12.4 | 16.8 | 1409 | 1376 | 1358 | 1355 | 1353 | ↓ | 3.71 | 15.8 | 11.7 | 1.23 | 1.23 | ↓ |
| | 151 | 352 | 7.9 | 37.7 | 28.9 | 34.1 | 1459 | 1452 | 26.4 | 13.1 | 17.1 | 1411 | 1381 | 1367 | 1365 | 1365 | ↓ | 3.67 | 16.0 | 12.5 | 1.01 | 1.01 | ↓ |
| | 152 | 354 | 8.0 | 37.7 | 28.8 | 34.0 | 1455 | 1445 | 26.4 | 13.9 | 17.0 | 1411 | 1384 | 1376 | 1379 | 1378 | ↓ | 3.35 | 16.0 | 13.5 | .72 | .72 | ↓ |
| | 153 | 354 | 8.0 | 37.7 | 28.8 | 34.0 | 1450 | 1445 | 26.5 | 14.9 | 17.1 | 1415 | 1391 | 1389 | 1389 | 1389 | ↓ | 3.14 | 16.3 | 14.3 | .58 | .58 | ↓ |
| | 154 | 352 | 7.9 | 37.8 | 29.1 | 34.2 | 1449 | 1440 | 26.8 | 16.0 | 17.5 | 1419 | 1401 | 1399 | 1400 | 1399 | ↓ | 2.98 | 16.7 | 15.1 | .44 | .44 | ↓ |
| | 155 | 354 | 8.0 | 39.0 | 30.2 | 35.3 | 1445 | 1440 | 27.8 | 17.4 | 18.4 | 1420 | 1415 | 1412 | 1415 | 1413 | ↓ | 2.77 | 16.7 | 10.1 | .15 | .15 | ↓ |
| | 156 | 352 | 7.9 | 38.8 | 30.1 | 35.1 | 1453 | 1447 | 28.5 | 18.3 | 19.2 | 1429 | 1421 | 1420 | 1422 | 1420 | ↓ | 2.76 | 17.5 | 16.7 | .20 | .20 | ↓ |
| | 157 | 355 | 8.1 | 39.0 | 30.1 | 35.3 | 1452 | 1447 | 28.5 | 19.3 | 19.1 | 1430 | 1426 | 1422 | 1430 | 1428 | Medium | 2.45 | 17.5 | 17.3 | ---- | ---- | ↓ |
| | 158 | 355 | 8.1 | 45.2 | 36.3 | 41.5 | 1450 | 1445 | 25.1 | 21.0 | 15.2 | 1426 | 1422 | 1421 | 1426 | 1423 | None | 1.11 | 17.2 | ---- | ---- | ---- | Liquid |
| | 159 | 360 | 8.3 | 36.1 | 26.8 | 32.5 | 1448 | 1442 | 24.7 | 20.7 | 14.6 | 1424 | 1422 | 1420 | 1424 | 1422 | None | 1.08 | 12.0 | ---- | ---- | ---- | Liquid |
| | 160 | 358 | 8.2 | 32.9 | 24.0 | 29.0 | 1446 | 1442 | 22.0 | 17.9 | 12.6 | 1422 | 1418 | 1418 | 1423 | 1420 | None | 1.06 | 16.9 | ---- | ---- | ---- | Liquid |
| | 161 | ↓ | ↓ | 30.0 | 21.2 | 26.1 | 1450 | 1445 | 19.1 | 15.0 | 9.9 | 1425 | 1425 | 1423 | 1424 | 1425 | None | 1.04 | 17.1 | ---- | ---- | ---- | Liquid |
| | 161a | ↓ | ↓ | 28.1 | 19.3 | 24.3 | ---- | ---- | 17.1 | 13.2 | 8.1 | 1425 | ---- | ---- | ---- | ---- | None/Medium | 1.03 | 17.1 | ---- | ---- | ---- | Incipient cavitation |
| | 161b | ↓ | ↓ | 27.6 | 18.9 | 23.9 | ---- | ---- | 16.6 | 12.8 | 7.6 | 1425 | ---- | ---- | ---- | ---- | Medium/Low | 1.03 | 17.1 | ---- | ---- | ---- | Incipient flashing |
| | 162 | 357 | 8.1 | 37.5 | 28.5 | 33.6 | 1461 | 1455 | 26.6 | 12.9 | 17.1 | 1414 | 1382 | 1365 | 1364 | 1364 | Low | 3.54 | 16.2 | 12.5 | 1.01 | 1.01 | Flashed |
| | 163 | 360 | 8.3 | 38.5 | 29.6 | 34.8 | 1470 | 1464 | 27.7 | 14.6 | 18.2 | 1428 | 1398 | 1386 | 1385 | 1386 | Low | 3.50 | 17.3 | 14.0 | .92 | .92 | Flashed |
| | 164 | 358 | 8.2 | 33.4 | 24.5 | 29.5 | 1458 | 1451 | 22.6 | 18.5 | 13.2 | 1432 | 1430 | 1428 | 1432 | 1431 | None | 1.06 | 17.7 | ---- | ---- | ---- | Liquid |
| | 165 | ↓ | ↓ | 31.7 | 22.8 | 27.8 | 1468 | 1461 | 20.7 | 16.6 | 11.3 | 1442 | 1439 | 1438 | 1442 | 1440 | ↓ | 1.06 | 18.5 | ---- | ---- | ---- | Liquid |
| | 166 | ↓ | ↓ | 29.5 | 20.5 | 25.6 | 1470 | 1464 | 18.5 | 14.4 | 9.0 | 1445 | 1443 | 1440 | 1442 | 1441 | ↓ | 1.06 | 18.8 | ---- | ---- | ---- | Liquid |
| | 166a | ↓ | ↓ | 28.2 | 19.4 | 24.3 | ---- | ---- | 17.1 | 13.2 | 8.4 | 1445 | ---- | ---- | ---- | ---- | ↓ | 1.00 | 18.8 | ---- | ---- | ---- | Incipient flashing |
| | 167 | 354 | 8.0 | 37.5 | 28.8 | 33.9 | 1470 | 1462 | 27.0 | 13.3 | 17.8 | 1420 | 1386 | 1369 | 1369 | 1369 | ↓ | 3.81 | 16.7 | 13.5 | 1.06 | 1.06 | Flashed |
| | 168 | 357 | 8.2 | 44.6 | 35.8 | 40.8 | 1468 | 1464 | 29.3 | 19.1 | 20.0 | 1441 | 1433 | 1430 | 1433 | 1432 | ↓ | 2.69 | 18.5 | 17.7 | .31 | .31 | Flashed |
| | 169 | 360 | 8.3 | 44.6 | 35.6 | 40.8 | 1468 | 1461 | 29.0 | 24.9 | 19.5 | 1442 | 1442 | 1440 | 1447 | 1442 | ↓ | 1.06 | 18.6 | ---- | ---- | ---- | Liquid |
| | 170 | 357 | 8.2 | 39.3 | 30.4 | 35.4 | 1465 | 1460 | 23.7 | 19.7 | 14.6 | 1441 | 1440 | 1438 | 1441 | 1440 | None | 1.02 | 18.4 | ---- | ---- | ---- | Liquid |
| | 171 | 352 | 8.0 | 36.1 | 27.4 | 32.4 | 1458 | 1458 | 20.6 | 16.6 | 11.4 | 1435 | 1432 | 1432 | 1435 | 1434 | ↓ | 1.06 | 18.0 | ---- | ---- | ---- | ↓ |
| | 172 | 357 | 8.1 | 34.3 | 25.5 | 30.4 | 1448 | 1445 | 18.5 | 14.5 | 9.4 | 1426 | 1425 | 1424 | 1427 | 1426 | ↓ | 1.03 | 17.2 | ---- | ---- | ---- | ↓ |
| | 173 | 358 | 8.2 | 32.6 | 23.7 | 28.7 | 1450 | 1443 | 16.7 | 12.6 | 7.5 | 1425 | 1423 | 1422 | 1426 | 1424 | ↓ | 1.03 | 17.1 | ---- | ---- | ---- | ↓ |
| | 173a | 357 | 8.1 | 30.7 | 22.2 | 27.2 | ---- | ---- | 15.1 | 11.2 | 5.4 | 1425 | ---- | ---- | ---- | ---- | None/High/Low | 1.11 | 17.1 | ---- | ---- | ---- | Incipient cavitation and flashing |
| | 174 | 355 | 8.1 | 35.5 | 26.8 | 31.7 | 1446 | 1440 | 20.0 | 16.0 | 10.7 | 1422 | 1420 | 1418 | 1420 | 1420 | None | 1.06 | 16.9 | ---- | ---- | ---- | Liquid |
| | 175 | 357 | 8.1 | 33.6 | 24.8 | 29.8 | 1443 | 1438 | 17.8 | 13.7 | 8.4 | 1420 | 1418 | 1416 | 1418 | 1418 | None | 1.06 | 16.7 | ---- | ---- | ---- | Liquid |
| | 175a | 355 | 8.1 | 31.8 | 23.1 | 28.1 | ---- | ---- | 15.9 | 12.0 | 6.9 | 1420 | ---- | ---- | ---- | ---- | None/Low/None | 1.03 | 16.7 | ---- | ---- | ---- | Incipient cavitation and flashing |
| | 176 | 297 | 5.6 | 32.7 | 26.4 | 30.1 | 1451 | 1442 | 21.5 | 12.0 | 15.0 | 1400 | 1363 | 1350 | 1350 | 1350 | None | 3.64 | 15.1 | 11.6 | 1.10 | 1.10 | Flashed |

| | | | | | | | | | | | | | | | | | | | | | | |
|----|------|-----|------|------|------|------|------|------|------|------|------|------|------|------|------|------|---------------|------|------|------|------|-----------------------------------|
| 17 | 177 | 481 | 14.7 | 47.2 | 31.0 | 40.5 | 1425 | 1420 | 31.5 | 24.2 | 14.0 | 1408 | 1405 | 1401 | 1409 | 1406 | None | 1.08 | 15.7 | ---- | ---- | Liquid |
| | 178 | 479 | 14.7 | 44.8 | 28.5 | 38.0 | 1430 | 1425 | 29.0 | 21.6 | 11.5 | 1411 | 1410 | 1409 | 1411 | 1410 | ↓ | 1.07 | 16.0 | ---- | ---- | ↓ |
| | 179 | 482 | 14.8 | 42.9 | 26.5 | 35.9 | 1430 | 1425 | 26.9 | 19.4 | 9.4 | 1411 | 1410 | 1409 | 1411 | 1410 | ↓ | 1.06 | 16.0 | ---- | ---- | ↓ |
| | 180 | 481 | 14.7 | 40.9 | 24.4 | 33.8 | 1428 | 1420 | 24.8 | 17.3 | 7.4 | 1410 | 1409 | 1405 | 1410 | 1409 | ↓ | 1.06 | 15.9 | ---- | ---- | ↓ |
| | 181 | 482 | 14.8 | 39.0 | 22.5 | 31.9 | 1429 | 1423 | 22.8 | 15.2 | 5.3 | 1410 | 1409 | 1406 | 1411 | 1409 | ↓ | 1.06 | 15.9 | ---- | ---- | ↓ |
| | 182 | 481 | 14.7 | 37.1 | 20.6 | 30.1 | 1430 | 1425 | 21.0 | 13.5 | 3.1 | 1410 | 1410 | 1409 | 1411 | 1410 | None High Low | 1.09 | 15.9 | ---- | ---- | Incipient cavitation and flashing |
| | 183 | 482 | 14.8 | 45.6 | 29.0 | 38.5 | 1430 | 1425 | 35.8 | 13.3 | 17.8 | 1400 | 1379 | 1369 | 1370 | 1369 | Low | 3.15 | 15.1 | 12.5 | 0.68 | Flashed |
| | 184 | 479 | 14.6 | 45.9 | 29.2 | 38.8 | 1435 | 1430 | 35.9 | 12.7 | 17.9 | 1400 | 1378 | 1360 | 1360 | 1360 | ↓ | 3.31 | 15.1 | 12.2 | .88 | ↓ |
| | 185 | 479 | 14.6 | 45.4 | 29.1 | 38.6 | ↓ | 1431 | 35.8 | 14.2 | 18.2 | 1402 | 1385 | 1379 | 1380 | 1379 | ↓ | 3.20 | 15.3 | 13.5 | .62 | ↓ |
| | 186 | 481 | 14.8 | 48.2 | 31.9 | 41.4 | 1430 | 36.2 | 16.1 | 18.5 | 1412 | 1403 | 1400 | 1402 | 1401 | ↓ | 2.94 | 16.1 | 15.2 | .24 | ↓ | |
| | 187 | 481 | ↓ | 50.6 | 34.2 | 43.7 | ↓ | 1429 | 36.4 | 17.8 | 18.7 | 1412 | 1410 | 1409 | 1411 | 1410 | Medium | 2.73 | 16.1 | 15.9 | ---- | ↓ |
| | 188 | 481 | ↓ | 51.6 | 35.1 | 44.6 | 1430 | 1425 | 36.2 | 19.3 | 18.4 | 1411 | 1410 | 1409 | 1411 | 1410 | Medium | 2.42 | 16.0 | 15.9 | ---- | ↓ |
| | 189 | 482 | ↓ | 52.5 | 36.1 | 45.5 | 1428 | 1422 | 36.0 | 20.8 | 18.2 | 1410 | 1409 | 1406 | 1410 | 1409 | Medium | 2.07 | 15.9 | 15.8 | ---- | ↓ |
| | 190 | 484 | 14.9 | 46.5 | 29.8 | 39.5 | 1431 | 1425 | 29.8 | 22.2 | 11.7 | 1411 | 1411 | 1410 | 1412 | 1411 | None | 1.08 | 16.0 | ---- | ---- | Liquid |
| | 191 | 481 | 14.7 | 48.8 | 32.2 | 41.6 | 1430 | 1422 | 32.1 | 24.6 | 15.0 | 1410 | 1410 | 1408 | 1410 | 1409 | None | 1.03 | 15.9 | ---- | ---- | Liquid |
| | 192 | 481 | 14.7 | 41.6 | 25.0 | 34.7 | 1425 | 1416 | 24.9 | 17.3 | 6.7 | 1405 | 1403 | 1402 | 1406 | 1404 | None | 1.09 | 15.5 | ---- | ---- | Liquid |
| | 193 | ↓ | ↓ | 39.2 | 22.7 | 32.2 | 1425 | 1416 | 22.5 | 14.9 | 4.6 | 1408 | 1405 | 1402 | 1408 | 1406 | None | 1.08 | 15.7 | ---- | ---- | Liquid |
| | 193a | ↓ | ↓ | 38.1 | 21.3 | 31.1 | ---- | ---- | 21.3 | 13.9 | 3.4 | 1408 | ---- | ---- | ---- | ---- | None High | 1.06 | 15.7 | ---- | ---- | Incipient cavitation and flashing |
| | 194 | ↓ | ↓ | 47.3 | 30.9 | 40.7 | 1425 | 1420 | 35.3 | 13.3 | 17.5 | 1398 | 1378 | 1369 | 1370 | 1369 | Low | 3.31 | 15.0 | 12.8 | 0.33 | Flashed |
| | 195 | ↓ | 14.8 | 46.9 | 30.3 | 39.7 | 1435 | 1430 | 36.7 | 17.5 | 18.8 | 1418 | 1413 | 1411 | 1418 | 1416 | Low | 2.69 | 16.6 | 16.3 | ---- | Flashed |
| | 196 | ↓ | 14.7 | 49.2 | 32.6 | 42.2 | 1430 | 1423 | 36.2 | 20.7 | 18.3 | 1410 | 1410 | 1405 | 1411 | 1410 | Medium | 2.23 | 15.9 | 15.9 | ---- | Flashed |
| | 197 | ↓ | 14.7 | 45.0 | 28.5 | 38.1 | 1427 | 1422 | 29.2 | 21.6 | 11.2 | 1410 | 1409 | 1405 | 1410 | 1409 | None | 1.09 | 15.9 | ---- | ---- | Liquid |
| | 198 | ↓ | 14.7 | 48.4 | 31.9 | 41.5 | 1425 | 1420 | 32.7 | 25.1 | 14.5 | 1408 | 1405 | 1402 | 1408 | 1407 | None | 1.10 | 15.7 | ---- | ---- | Liquid |
| | 199 | 481 | 14.7 | 61.0 | 44.8 | 54.0 | 1427 | 1422 | 32.6 | 25.1 | 15.2 | 1410 | 1409 | 1408 | 1411 | 1409 | None | 1.08 | 15.9 | ---- | ---- | Liquid |
| | 200 | 479 | ↓ | 55.9 | 39.7 | 49.1 | 1427 | 1421 | 27.3 | 19.8 | 9.5 | 1409 | 1409 | 1403 | 1410 | 1408 | ↓ | 1.10 | 15.8 | ---- | ---- | ↓ |
| | 201 | 479 | ↓ | 52.3 | 36.1 | 45.6 | 1427 | 1420 | 23.6 | 16.1 | 5.6 | 1409 | 1408 | 1403 | 1410 | 1410 | ↓ | 1.11 | 15.8 | ---- | ---- | ↓ |
| | 202 | 478 | ↓ | 50.5 | 34.4 | 43.8 | 1422 | 1417 | 21.7 | 14.3 | 3.8 | 1404 | 1402 | 1400 | 1405 | 1404 | ↓ | 1.11 | 15.4 | ---- | ---- | ↓ |
| | 202a | 478 | ↓ | 49.8 | 33.5 | 43.1 | ---- | ---- | 20.4 | 13.1 | 2.6 | 1404 | ---- | ---- | ---- | ---- | None High/Low | 1.09 | 15.4 | ---- | ---- | Incipient cavitation and flashing |
| | 203 | 485 | 14.5 | 49.0 | 32.6 | 42.1 | 1422 | 1416 | 35.3 | 12.7 | 17.1 | 1391 | 1370 | 1360 | 1360 | 1360 | Low | 3.30 | 14.5 | 12.2 | 0.68 | Flashed |
| | 204 | 481 | 15.0 | 47.9 | 31.5 | 41.0 | 1415 | 1410 | 28.5 | 21.0 | 10.7 | 1400 | 1399 | 1393 | 1400 | 1399 | None | 1.08 | 15.1 | ---- | ---- | Liquid |
| 18 | 205 | 427 | 11.6 | 38.7 | 25.8 | 33.2 | 1425 | 1420 | 26.5 | 20.6 | 12.7 | 1401 | 1401 | 1399 | 1402 | 1402 | None | 1.07 | 15.2 | ---- | ---- | Liquid |
| | 206 | 429 | 11.7 | 34.1 | 21.1 | 28.5 | 1425 | 1420 | 21.7 | 15.8 | 8.0 | 1405 | 1405 | 1401 | 1409 | 1406 | None | 1.06 | 15.5 | ---- | ---- | Liquid |
| | 207 | 424 | 11.5 | 31.5 | 18.7 | 26.0 | 1429 | 1421 | 19.3 | 13.5 | 5.6 | 1409 | 1407 | 1402 | 1409 | 1407 | None | 1.07 | 15.8 | ---- | ---- | Liquid |
| | 208 | 429 | 11.7 | 30.3 | 17.1 | 24.7 | 1424 | 1419 | 17.8 | 11.8 | 3.7 | 1403 | 1401 | 1400 | 1403 | 1402 | High | 1.07 | 15.3 | ---- | ---- | Incipient cavitation |
| | 209 | 424 | 11.5 | 27.9 | 15.1 | 22.4 | 1430 | 1422 | 15.7 | 9.8 | 2.1 | 1410 | 1409 | 1404 | 1410 | 1408 | High | 1.06 | 15.9 | ---- | ---- | Cavitated |
| | 210 | 421 | 11.3 | 25.5 | 12.9 | 20.1 | 1431 | 1435 | 13.5 | 7.6 | -.3 | ↓ | 1409 | 1405 | 1410 | 1409 | Low | 1.09 | 15.9 | ---- | ---- | Cavitated |
| | 210a | 425 | 11.5 | 25.0 | 12.2 | 19.5 | ---- | ---- | 12.8 | 7.3 | .1 | ↓ | ---- | ---- | ---- | ---- | ↓ | 1.00 | 15.9 | ---- | ---- | Cavitated |
| | 210b | 425 | 11.5 | 29.8 | 17.1 | 24.3 | ---- | ---- | 17.6 | 11.9 | 4.3 | ↓ | ---- | ---- | ---- | ---- | ↓ | 1.04 | 15.9 | ---- | ---- | Incipient flashing |
| | 211 | 424 | 11.4 | 36.8 | 24.0 | 31.3 | 1435 | 1430 | 30.2 | 11.9 | 16.3 | 1398 | 1369 | 1350 | 1350 | 1350 | ↓ | 3.33 | 15.0 | 11.6 | 1.05 | Flashed |
| | 212 | 424 | 11.5 | 40.0 | 27.4 | 34.7 | 1445 | 1440 | 30.8 | 12.4 | 17.0 | 1402 | 1375 | 1359 | 1359 | 1358 | ↓ | 3.43 | 15.3 | 12.1 | .97 | Flashed |
| | 213 | 421 | 11.3 | 42.2 | 29.6 | 37.0 | 1439 | 1430 | 30.7 | 13.4 | 17.0 | 1402 | 1380 | 1370 | 1370 | 1369 | ↓ | 3.30 | 15.3 | 12.8 | .73 | Flashed |
| | 214 | 424 | 11.5 | 39.0 | 26.2 | 33.8 | 1433 | 1427 | 27.3 | 21.3 | 12.6 | 1411 | 1411 | 1410 | 1412 | 1411 | None | 1.15 | 16.0 | ---- | ---- | Liquid |
| 19 | 215 | 427 | 11.6 | 42.5 | 29.4 | 37.0 | 1431 | 1425 | 30.6 | 24.5 | 16.1 | 1410 | 1410 | 1408 | 1411 | 1409 | None | 1.11 | 15.9 | ---- | ---- | Liquid |
| | 216 | 427 | 11.6 | 26.8 | 13.9 | 21.2 | 1435 | 1427 | 14.7 | 8.8 | 1.1 | ↓ | 1410 | 1409 | 1411 | 1410 | None/High | 1.05 | 15.9 | ---- | ---- | Incipient cavitation |
| | 217 | 425 | 11.5 | 25.2 | 12.3 | 19.7 | ---- | ---- | 12.9 | 7.0 | -.8 | ↓ | ---- | ---- | ---- | ---- | Low | 1.07 | 15.9 | ---- | ---- | Cavitated |
| | 218 | 425 | 11.5 | 29.7 | 16.8 | 24.3 | ---- | ---- | 17.6 | 11.7 | 3.5 | ↓ | ---- | ---- | ---- | ---- | Low | 1.09 | 15.9 | ---- | ---- | Incipient flashing |
| | 219 | 424 | 11.4 | 40.6 | 27.9 | 35.1 | 1432 | 1425 | 29.9 | 11.8 | 16.6 | 1392 | 1368 | 1350 | 1350 | 1349 | Low | 3.32 | 14.5 | 11.5 | 0.94 | Flashed |
| 20 | s | 124 | 0.9 | 43.0 | 42.0 | 42.6 | 965 | 962 | 41.7 | 41.3 | 40.7 | 949 | 949 | 942 | 946 | 945 | None | 1.00 | 0.7 | ---- | ---- | All-liquid flow calibration |
| | t | 248 | 3.6 | 45.4 | 41.5 | 43.7 | 924 | 922 | 43.4 | 41.6 | 39.3 | 905 | 903 | 900 | 903 | 900 | ↓ | 1.06 | .4 | ---- | ---- | ↓ |
| | u | 373 | 8.0 | 38.6 | 29.6 | 34.7 | 828 | 828 | 34.1 | 29.9 | 24.4 | 822 | 820 | 818 | 820 | 818 | ↓ | 1.08 | .2 | ---- | ---- | ↓ |
| | v | 495 | 14.0 | 45.4 | 29.6 | 38.6 | 851 | 851 | 37.6 | 30.4 | 20.9 | 842 | 845 | 842 | 845 | 841 | ↓ | 1.06 | .2 | ---- | ---- | ↓ |
| | w | 619 | 21.9 | 54.1 | 29.7 | 43.7 | 838 | 835 | 42.2 | 31.1 | 16.1 | 828 | 830 | 828 | 830 | 829 | ↓ | 1.07 | .2 | ---- | ---- | ↓ |
| | y | 660 | 25.0 | 57.4 | 29.6 | 45.6 | 853 | 850 | 43.9 | 31.3 | 14.2 | 842 | 845 | 843 | 846 | 845 | ↓ | 1.07 | .2 | ---- | ---- | ↓ |

^aShown only for flashed runs.

TABLE III. - Continued. DETAILED DATA FOR VENTURI WITH ARTIFICIAL THROAT CAVITY (SERIES II)

(b) SI units^a

| Set | Run | Flow rate, W, g/sec | Dynamic head, q, N/cm ² | Control venturi | | | | | | Test venturi | | | | | | | | | | Noise indication | Pressure-drop ratio, $\frac{P_4 - P_5}{P_1 - P_3}$ | Vapor pressure at T _{in} , P _{vin} , N/cm ² abs | Vapor pressure at T _{out} , P _{vout} , N/cm ² abs |
|-----|-----|---------------------|------------------------------------|---------------------------------|------------------------|------------------------|------------------------|-------------------------|-----------------------|---------------------------------|------------------------|------------------------|------------------------|------------------------|------------------------|--------------------------|------|------------|------|------------------|--|--|--|
| | | | | Pressure, N/cm ² abs | | | Temperature, K | | | Pressure, N/cm ² abs | | | Temperature, K | | | | | | | | | | |
| | | | | Inlet, P ₁ | Throat, P ₂ | Outlet, P ₃ | Inlet, T _{C1} | Outlet, T _{C2} | Inlet, P ₄ | Outlet, P ₅ | Throat, P _t | Inlet, T _{in} | Distance from inlet | | | Outlet, T _{out} | | | | | | | |
| | | | | | | | | | | | | | 2.3 cm, T ₂ | 3.3 cm, T ₃ | 4.3 cm, T ₄ | | | | | | | | |
| 11 | h | 68.7 | 13.0 | 35.9 | 21.6 | 29.9 | 1026 | 1023 | 29.0 | 22.7 | 14.1 | 1018 | 1018 | 1017 | 1020 | 1019 | None | 1.04 | 9.0 | --- | | | |
| | j | 75.6 | 15.7 | 38.7 | 21.5 | 31.6 | 1022 | 1019 | 30.6 | 22.9 | 12.1 | 1015 | 1015 | 1014 | 1016 | 1016 | | 1.08 | 8.8 | --- | | | |
| | k | 60.6 | 10.1 | 32.6 | 21.7 | 28.1 | 1026 | 1023 | 27.4 | 22.4 | 15.4 | 1017 | 1017 | 1016 | 1018 | 1017 | | 1.10 | 9.0 | --- | | | |
| | m | 52.8 | 7.7 | 30.1 | | 26.5 | 1015 | 1012 | 26.1 | 22.3 | 17.1 | 1005 | 1005 | 1005 | 1006 | 1006 | | 1.07 | 8.0 | --- | | | |
| | n | 45.4 | 5.7 | 27.9 | | 25.3 | 1013 | 1010 | 24.9 | 22.1 | 18.2 | 1003 | 1003 | 1002 | 1004 | 1004 | | 1.07 | 7.8 | --- | | | |
| | p | 37.4 | 3.9 | 25.9 | | 24.1 | 1024 | 1025 | 23.9 | 21.9 | 19.3 | 1011 | 1010 | 1010 | 1012 | 1011 | | 1.06 | 8.8 | --- | | | |
| | q | 30.2 | 2.5 | 24.3 | 21.6 | 23.1 | 1024 | 1021 | 23.0 | 21.7 | 20.1 | 1011 | 1010 | 1009 | 1010 | 1010 | | 1.03 | 8.3 | --- | | | |
| | r | 15.0 | .6 | 28.7 | 27.9 | 28.3 | 1043 | 1041 | 28.3 | 28.0 | 27.6 | 1026 | 1026 | 1024 | 1026 | 1025 | | .87 | 9.8 | --- | | | |
| 12 | 73 | 61.2 | 10.1 | 37.6 | 26.5 | 33.1 | 990 | 986 | 26.8 | 21.7 | 14.1 | 979 | 979 | 978 | 981 | 981 | None | 1.14 | 6.1 | --- | | | |
| | 74 | 61.6 | 10.3 | 35.4 | 24.1 | 30.8 | 993 | 990 | 24.3 | 19.2 | 12.1 | 983 | 983 | 980 | 983 | 983 | | 1.08 | 6.3 | --- | | | |
| | 75 | 61.4 | 10.2 | 31.1 | 19.8 | 26.3 | 993 | 990 | 19.9 | 14.8 | 8.0 | 983 | 983 | 980 | 983 | 983 | | 1.05 | 6.3 | --- | | | |
| | 76 | 61.0 | 10.1 | 28.8 | 17.6 | 24.0 | 991 | 989 | 17.6 | 12.5 | 5.6 | 981 | 981 | 979 | 983 | 982 | | 1.07 | 6.3 | --- | | | |
| | 77 | 61.2 | 10.1 | 27.8 | 16.3 | 22.8 | 989 | 986 | 16.4 | 11.3 | 4.4 | 979 | 979 | 977 | 979 | 979 | | None/High | 1.06 | 6.1 | --- | | |
| | 78 | 61.4 | 10.2 | 26.6 | 15.2 | 21.8 | 990 | 988 | 15.2 | 10.1 | 3.0 | 980 | 980 | 979 | 982 | 981 | | High | 1.07 | 6.2 | --- | | |
| | 79 | 61.4 | 10.2 | 25.5 | 14.1 | 20.7 | 990 | 988 | 14.1 | 9.0 | 2.1 | 981 | 981 | 979 | 982 | 981 | | High | 1.05 | 6.2 | --- | | |
| | 80 | 61.4 | 10.2 | 23.9 | 12.5 | 19.1 | 990 | 987 | 12.5 | 7.3 | .3 | 981 | 981 | 979 | 983 | 982 | | Medium | 1.06 | 6.3 | --- | | |
| | 81 | 60.9 | 10.1 | 31.1 | 20.1 | 26.5 | 1000 | 997 | 20.5 | 7.4 | 8.8 | 989 | 988 | 986 | 988 | 987 | | Low | 2.89 | 6.8 | 6.6 | | |
| | 82 | 61.0 | | 30.0 | 18.7 | 25.2 | 997 | 994 | 20.1 | 6.1 | 8.1 | 983 | 977 | 972 | 975 | 974 | | | 2.92 | 6.3 | 5.7 | | |
| | 83 | 61.0 | | 29.1 | 17.9 | 24.3 | 995 | 993 | 19.9 | 5.6 | 8.0 | 982 | 972 | 966 | 967 | 966 | | | 2.99 | 6.3 | 5.2 | | |
| | 84 | 61.0 | | 28.6 | 17.3 | 23.9 | 995 | 991 | 20.0 | 5.4 | 8.0 | 979 | 971 | 964 | 966 | 965 | | | 3.09 | 6.1 | 5.2 | | |
| | 85 | 61.6 | 10.3 | 28.8 | 17.4 | 24.1 | 995 | 991 | 20.2 | 5.7 | 8.1 | 980 | 972 | 967 | 971 | 971 | | | 3.04 | 6.2 | 5.6 | | |
| | 86 | 61.2 | 10.2 | 29.6 | 18.3 | 24.8 | 993 | 991 | 20.0 | 6.9 | 8.0 | 983 | 982 | 979 | 983 | 983 | | | 2.74 | 6.3 | 6.3 | | |
| | 87 | 60.9 | 10.1 | 29.5 | 18.1 | 24.6 | 990 | 988 | 19.9 | 7.7 | 7.9 | 982 | 980 | 978 | 983 | 981 | | Medium | 2.54 | 6.3 | 6.3 | | |
| | 88 | 61.2 | 10.1 | 25.6 | 14.3 | 20.9 | 978 | 975 | 14.6 | 9.4 | 2.3 | 971 | 970 | 967 | 971 | 971 | | High | 1.09 | 5.6 | --- | | |
| | 89 | 61.6 | 10.3 | 26.5 | 15.2 | 21.8 | 982 | 979 | 15.6 | 10.4 | 3.2 | 972 | 972 | 971 | 972 | 971 | | High | 1.08 | 5.7 | --- | | |
| | 90 | 61.5 | 10.2 | 27.9 | 16.5 | 23.1 | 983 | 980 | 16.8 | 11.7 | 4.6 | 972 | 972 | 971 | 973 | 972 | | High | 1.07 | 5.7 | --- | | |
| | 91 | 61.5 | 10.2 | 27.9 | 16.4 | 23.0 | 983 | 981 | 16.8 | 11.7 | 4.5 | 973 | 972 | 971 | 973 | 972 | | None | 1.08 | 5.7 | --- | | |
| | 92 | 61.2 | 10.1 | 29.2 | 17.7 | 24.3 | 980 | 979 | 18.1 | 13.0 | 5.9 | 971 | 971 | 969 | 972 | 971 | | None | 1.07 | 5.6 | --- | | |
| | 93 | 61.2 | 10.1 | 27.4 | 16.0 | 22.7 | 986 | 983 | 16.4 | 11.2 | 3.9 | 977 | 977 | 974 | 978 | 977 | | None | 1.09 | 6.0 | --- | | |
| | 94 | 61.2 | | 26.0 | 14.7 | 21.3 | 987 | 983 | 15.0 | 9.9 | 2.6 | 977 | 977 | 974 | 978 | 977 | | | 1.10 | 6.0 | --- | | |
| | 95 | 60.9 | | 25.2 | 13.9 | 20.4 | 991 | 989 | 14.3 | 9.1 | 2.1 | 981 | 981 | 978 | 983 | 982 | | | 1.08 | 6.2 | --- | | |
| | 96 | 60.9 | | 24.4 | 13.2 | 19.7 | 993 | 989 | 13.4 | 8.3 | 1.4 | 983 | 983 | 981 | 983 | 983 | | | 1.07 | 6.3 | --- | | |
| | 97 | 61.6 | 10.3 | 24.2 | 12.7 | 19.3 | 992 | 989 | 13.0 | 7.8 | .8 | | 983 | 980 | 983 | 983 | | | 1.06 | | --- | | |
| | 98 | 61.0 | 10.1 | 23.2 | 11.7 | 18.3 | 993 | 990 | 12.1 | 6.9 | -.1 | | 983 | 982 | 984 | 983 | | High | 1.07 | | --- | | |
| | 98a | 61.1 | | 23.0 | 11.5 | 18.1 | ---- | ---- | 11.7 | 6.6 | -.3 | ---- | ---- | ---- | ---- | ---- | | Medium/Low | 1.04 | | --- | | |
| | 99 | 60.9 | | 29.2 | 18.1 | 24.6 | 996 | 993 | 20.3 | 6.2 | 8.3 | | 978 | 977 | 978 | 978 | | Low | 3.06 | | 6.0 | | |
| | 100 | 61.0 | | 29.8 | 18.5 | 25.0 | 999 | 996 | 20.6 | 7.3 | 8.5 | 988 | 988 | 985 | 988 | 988 | | Medium | 2.80 | 6.7 | 6.6 | | |
| | 101 | 61.0 | | 29.9 | 18.5 | 25.1 | 1000 | 997 | 20.8 | 8.5 | 8.5 | 989 | 989 | 988 | 989 | 989 | | High | 2.57 | 6.8 | 6.8 | | |
| | 102 | 61.0 | | 24.7 | 13.2 | 19.9 | 997 | 994 | 15.4 | 10.1 | 2.8 | 988 | 986 | 984 | 988 | 988 | | High | 1.10 | 6.7 | --- | | |
| | 103 | 60.9 | | 25.6 | 14.3 | 20.9 | 993 | 990 | 16.4 | 11.2 | 3.9 | 983 | 982 | 980 | 984 | 984 | | None | 1.11 | 6.3 | --- | | |
| | 104 | 60.9 | | 27.7 | 16.3 | 22.8 | 990 | 988 | 18.5 | 13.2 | 6.2 | 980 | 980 | 979 | 981 | 981 | | None | 1.07 | 6.2 | --- | | |

| | | | | | | | | | | | | | | | | | | | | |
|----|------|------|------|------|------|------|------|------|------|------|------|------|------|------|------|------|-----------|------|-----|-----|
| 13 | 105 | 61.7 | 10.3 | 27.9 | 16.3 | 23.1 | 991 | 989 | 18.6 | 13.3 | 5.8 | 982 | 982 | 980 | 983 | 983 | None | 1.11 | 6.3 | --- |
| | 105a | 61.7 | 10.3 | 21.6 | 10.1 | 16.8 | ---- | ---- | 12.1 | 6.9 | -3 | 983 | ---- | ---- | ---- | ---- | High | 1.07 | 6.3 | --- |
| | 105b | 61.7 | 10.3 | 20.5 | 9.0 | 15.8 | ---- | ---- | 11.2 | 6.0 | -1.5 | 984 | ---- | ---- | ---- | ---- | High/Low | 1.10 | 6.3 | --- |
| | 106 | 46.4 | 5.9 | 21.4 | 14.8 | 18.5 | 1025 | 1022 | 16.0 | 6.1 | 8.7 | 1003 | 988 | 979 | 978 | 977 | Low | 3.45 | 7.7 | 5.9 |
| | 107 | 60.9 | 10.1 | 27.5 | 16.2 | 22.8 | 991 | 989 | 18.5 | 13.2 | 6.1 | 982 | 981 | 980 | 983 | 981 | None | 1.10 | 6.3 | --- |
| 14 | 108 | 45.5 | 5.6 | 30.5 | 24.2 | 27.8 | 972 | 969 | 15.6 | 12.8 | 9.2 | 960 | 960 | 959 | 962 | 961 | None | 1.02 | 5.0 | --- |
| | 109 | 45.6 | 5.6 | 27.9 | 21.7 | 25.3 | 972 | 970 | 13.0 | 10.1 | 6.1 | 961 | 960 | 959 | 962 | 960 | None | 1.12 | 5.1 | --- |
| | 109a | 45.1 | 5.4 | 25.7 | 19.4 | 22.9 | ---- | ---- | 10.8 | 8.0 | 4.7 | 961 | ---- | ---- | ---- | ---- | None/High | .97 | 5.1 | --- |
| | 110 | 45.1 | 5.4 | 25.4 | 19.4 | 22.8 | 972 | 970 | 10.7 | 8.0 | 4.4 | 961 | 960 | 959 | 962 | 960 | High | 1.03 | 5.0 | --- |
| | 111 | 44.7 | 5.4 | 24.0 | 18.1 | 21.4 | 971 | 969 | 9.4 | 6.6 | 3.0 | 960 | 958 | 957 | 959 | 958 | ↓ | 1.07 | 5.0 | --- |
| | 112 | 45.4 | 5.5 | 22.7 | 16.6 | 20.1 | 965 | 963 | 8.3 | 5.5 | 1.9 | 954 | 953 | 951 | 954 | 953 | ↓ | 1.06 | 4.7 | --- |
| | 113 | 44.7 | 5.4 | 21.4 | 15.5 | 18.8 | 964 | 961 | 7.3 | 4.6 | 1.1 | 952 | 951 | 950 | 953 | 952 | ↓ | 1.06 | 4.6 | --- |
| | 114 | 44.7 | 5.4 | 20.8 | 14.9 | 18.3 | 962 | 960 | 6.7 | 3.9 | .3 | 951 | 950 | 949 | 951 | 950 | Medium | 1.08 | 4.6 | --- |
| | 115 | 45.1 | 5.4 | 20.4 | 14.4 | 17.8 | 961 | 958 | 6.1 | 3.4 | -1 | 950 | 949 | 949 | 950 | 950 | Low | 1.04 | 4.5 | --- |
| | 116 | 44.5 | 5.3 | 19.9 | 14.1 | 17.4 | 961 | 958 | 6.0 | 3.3 | -2 | 949 | 949 | 947 | 950 | 949 | ↓ | 1.06 | 4.4 | --- |
| | 117 | 45.7 | 5.6 | 14.4 | 8.1 | 11.7 | 958 | 956 | 6.1 | 3.3 | -4 | 949 | 947 | 946 | 948 | 947 | ↓ | 1.04 | 4.4 | --- |
| | 118 | ↓ | ↓ | 18.5 | 12.5 | 15.9 | 956 | 953 | 6.0 | 3.2 | -6 | 944 | 943 | 942 | 944 | 943 | ↓ | 1.10 | 4.3 | --- |
| | 118a | ↓ | ↓ | 19.9 | 13.8 | 17.3 | ---- | ---- | 6.9 | 4.1 | .3 | 944 | ---- | ---- | ---- | ---- | ↓ | 1.05 | ↓ | --- |
| | 119 | ↓ | ↓ | 19.9 | 13.9 | 17.3 | 956 | 954 | 11.2 | 4.1 | 4.8 | 944 | 938 | 936 | 938 | 936 | ↓ | 2.75 | ↓ | 3.9 |
| | 120 | ↓ | ↓ | 21.5 | 15.5 | 19.0 | 956 | 954 | 11.3 | 5.4 | 5.4 | 945 | 943 | 943 | 945 | 944 | ↓ | 2.37 | ↓ | 4.2 |
| | 121 | 45.4 | 5.5 | 22.9 | 16.8 | 20.3 | 957 | 955 | 9.4 | 6.7 | 3.0 | 945 | 945 | 943 | 945 | 944 | High | 1.06 | ↓ | --- |
| | 122 | 45.4 | 5.5 | 24.3 | 18.3 | 21.7 | 958 | 956 | 10.9 | 8.1 | 4.6 | 946 | 947 | 945 | 948 | 948 | High | 1.04 | ↓ | --- |
| | 123 | 45.5 | 5.6 | 25.5 | 19.3 | 22.8 | 959 | 957 | 11.9 | 9.0 | 5.2 | 949 | 948 | 946 | 949 | 948 | None | 1.07 | 4.4 | --- |
| 15 | 124 | 45.5 | 5.7 | 25.4 | 19.3 | 22.9 | 997 | 994 | 11.9 | 9.0 | 5.2 | 984 | 984 | 983 | 985 | 983 | None | 1.08 | 6.4 | --- |
| | 125 | 45.4 | 5.6 | 24.1 | 17.9 | 21.4 | 999 | 995 | 10.3 | 7.6 | 3.9 | 986 | 986 | 984 | 988 | 987 | High | 1.04 | 6.6 | --- |
| | 125a | ↓ | ↓ | 23.0 | 16.9 | 20.7 | ---- | ---- | 9.2 | 6.6 | 2.4 | 986 | ---- | ---- | ---- | ---- | High/Low | 1.15 | 6.6 | --- |
| | 126 | ↓ | ↓ | 27.4 | 21.3 | 24.8 | 1000 | 997 | 13.8 | 6.3 | 7.4 | 986 | 978 | 977 | 979 | 978 | Low | 2.81 | 6.6 | 6.0 |
| | 127 | ↓ | ↓ | 27.6 | 21.4 | 25.0 | 1003 | 1000 | 14.0 | 5.5 | 7.6 | 984 | 972 | 966 | 967 | 966 | ↓ | 3.17 | 6.4 | 5.3 |
| | 128 | 45.5 | 5.7 | 21.0 | 14.9 | 18.3 | 1000 | 997 | 13.9 | 5.1 | 7.7 | 983 | 967 | 961 | 961 | 960 | ↓ | 3.38 | 6.3 | 5.0 |
| | 129 | 45.4 | 5.6 | 20.3 | 14.2 | 17.7 | 997 | 994 | 13.8 | 4.8 | 7.1 | 979 | 965 | 956 | 956 | 955 | ↓ | 3.32 | 6.1 | 4.8 |
| | 130 | 45.4 | ↓ | 20.3 | ↓ | 17.6 | 997 | 994 | 13.8 | 5.5 | 7.4 | 980 | 969 | 964 | 966 | 965 | ↓ | 3.08 | 6.1 | 5.2 |
| | 131 | 45.4 | ↓ | 20.3 | ↓ | 17.7 | 995 | 993 | 13.9 | 6.6 | 7.4 | 983 | 980 | 978 | 983 | 979 | ↓ | 2.05 | 6.3 | 6.1 |
| | 132 | 45.7 | ↓ | 20.4 | ↓ | 17.7 | 994 | 990 | 13.8 | 7.3 | 7.2 | 983 | 980 | 978 | 983 | 979 | ↓ | 2.39 | 6.3 | 6.1 |
| | 133 | 45.4 | ↓ | 19.0 | 12.9 | 16.3 | 993 | 989 | 11.7 | 8.8 | 5.2 | 980 | 980 | 978 | 982 | 981 | None | 1.05 | 6.2 | --- |
| | 134 | 44.7 | 5.4 | 19.9 | 13.8 | 17.2 | 994 | 991 | 12.6 | 9.9 | 6.2 | 983 | 983 | 980 | 983 | 982 | None | 1.06 | 6.3 | --- |
| | 135 | 45.4 | 5.6 | 18.9 | 12.7 | 16.2 | 995 | 991 | 11.4 | 8.6 | 5.0 | 983 | 983 | 980 | 983 | 982 | ↓ | 1.03 | 6.3 | --- |
| | 136 | ↓ | ↓ | 17.8 | 11.5 | 15.0 | 997 | 994 | 10.3 | 7.5 | 3.8 | 988 | 988 | 985 | 988 | 986 | ↓ | 1.05 | 6.7 | --- |
| | 136a | ↓ | ↓ | 16.9 | 10.6 | 14.3 | ---- | ---- | 9.3 | 6.6 | 2.7 | 988 | ---- | ---- | ---- | ---- | ↓ | 1.05 | 6.7 | --- |
| | 137 | ↓ | ↓ | 21.6 | 15.4 | 19.0 | 1000 | 997 | 14.2 | 6.7 | 7.7 | 988 | 981 | 978 | 979 | 978 | ↓ | 2.88 | 6.7 | 6.0 |
| | 138 | ↓ | ↓ | 21.5 | 15.3 | 18.9 | ↓ | 997 | 14.1 | 5.5 | 7.6 | 983 | 972 | 966 | 967 | 966 | ↓ | 3.24 | 6.3 | 5.3 |
| | 139 | ↓ | ↓ | 22.1 | 15.9 | 19.4 | ↓ | 998 | ↓ | 5.2 | 7.7 | 983 | 967 | 961 | 961 | 961 | ↓ | 3.44 | 6.3 | 5.0 |
| | 140 | ↓ | ↓ | 22.1 | 15.8 | 19.5 | ↓ | 997 | ↓ | 5.0 | 7.5 | 983 | 967 | 960 | 960 | 958 | ↓ | 3.49 | 6.3 | 4.9 |
| | 141 | 45.0 | 5.5 | 21.9 | 15.8 | 19.3 | 1001 | 1000 | ↓ | 6.6 | 7.7 | 988 | 983 | 978 | 980 | 979 | ↓ | 2.89 | 6.7 | 6.1 |
| | 142 | 45.1 | 5.6 | 22.1 | 15.9 | 19.4 | 999 | 995 | 14.2 | 7.0 | 7.7 | ↓ | 984 | 983 | 984 | 983 | Low | 2.71 | ↓ | 6.3 |
| | 143 | 45.1 | 5.6 | 22.0 | 15.8 | 19.4 | 999 | 996 | 14.1 | 8.1 | 7.6 | ↓ | 985 | 984 | 988 | 986 | Medium | 2.28 | ↓ | 6.6 |
| | 144 | 45.4 | 5.6 | 19.9 | 13.7 | 17.2 | 999 | 996 | 11.9 | 9.0 | 5.1 | ↓ | 986 | 984 | 988 | 987 | None | 1.11 | ↓ | --- |

^aFor quality values and remarks see table III(a).

^bShown only for flashed runs.

TABLE III. - Concluded. DETAILED DATA FOR VENTURI WITH ARTIFICIAL THROAT CAVITY (SERIES II)

(b) Concluded. SI units^a

| Set | Run | Flow rate, W, g/sec | Dynamic head, q, N/cm ² | Control venturi | | | | | | Test venturi | | | | | | | | | | Noise indica- tion | Pressure drop ratio, P ₄ - P ₅ P ₁ - P ₃ | Vapor pressure at T _{in} , P _{vin} ' N/cm ² abs | Vapor pressure at T _{out} , P _{vout} ' N/cm ² abs |
|-----|------|------------------------------|---|------------------------------------|---------------------------|---------------------------|---------------------------|----------------------------|--------------------------|------------------------------------|---------------------------|---------------------------|---------------------------|---------------------------|---------------------------|-----------------------------|---------------|------|------|--------------------------|--|--|--|
| | | | | Pressure, N/cm ² abs | | | Temperature, K | | | Pressure, N/cm ² abs | | | Temperature, K | | | | | | | | | | |
| | | | | Inlet, P ₁ | Throat, P ₂ | Outlet, P ₃ | Inlet, T _{C1} | Outlet, T _{C2} | Inlet, P ₄ | Outlet, P ₅ | Throat, P _t | Inlet, T _{in} | Distance from inlet | | | Outlet, T _{out} | | | | | | | |
| | | | | | | | | | | | | | 2.3 cm, T ₂ | 3.3 cm, T ₃ | 4.3 cm, T ₄ | | | | | | | | |
| 16 | 145 | 44.3 | 5.4 | 25.2 | 19.1 | 22.6 | 1058 | 1055 | 17.5 | 14.7 | 10.8 | 1044 | 1044 | 1042 | 1044 | 1044 | None | 1.10 | 11.5 | ---- | | | |
| | 146 | 44.3 | 5.4 | 23.9 | 17.9 | 21.4 | 1058 | 1055 | 16.2 | 13.4 | 9.5 | 1045 | 1044 | 1044 | 1045 | 1044 | None | 1.11 | 11.6 | ---- | | | |
| | 147 | 44.6 | 5.5 | 20.0 | 13.9 | 17.4 | 1059 | 1055 | 12.2 | 9.4 | 5.7 | 1045 | 1044 | 1044 | 1045 | 1044 | None | 1.06 | 11.7 | ---- | | | |
| | 147a | 45.0 | 5.6 | 19.0 | 12.9 | 16.5 | ---- | ---- | 11.0 | 8.3 | 4.3 | ↓ | ---- | ---- | ---- | ---- | Medium | 1.11 | 11.7 | ---- | | | |
| | 147b | ↓ | ↓ | 18.8 | 12.7 | 16.3 | ---- | ---- | 10.8 | 8.2 | 4.4 | ↓ | ---- | ---- | ---- | ---- | Low | 1.06 | 11.7 | ---- | | | |
| | 148 | ↓ | ↓ | 25.9 | 19.8 | 23.3 | 1064 | 1059 | 18.1 | 8.5 | 11.6 | 1038 | 1018 | 1007 | 1006 | 1006 | ↓ | 3.65 | 10.8 | 8.1 | | | |
| | 149 | ↓ | ↓ | 25.9 | 19.7 | 23.2 | 1064 | 1061 | 18.1 | 8.2 | 11.6 | 1038 | 1018 | 1006 | 1005 | 1004 | ↓ | 3.81 | 10.9 | 7.9 | | | |
| | 150 | 44.6 | 5.5 | 25.7 | 19.7 | 23.2 | 1064 | 1060 | 18.0 | 8.5 | 11.6 | 1038 | 1020 | 1010 | 1008 | 1007 | ↓ | 3.71 | 10.9 | 8.1 | | | |
| | 151 | 44.4 | 5.4 | 26.0 | 19.9 | 23.5 | 1066 | 1061 | 18.2 | 9.0 | 11.8 | 1039 | 1023 | 1015 | 1014 | 1014 | ↓ | 3.67 | 11.0 | 8.6 | | | |
| | 152 | 44.6 | 5.5 | 26.0 | 19.9 | 23.4 | 1064 | 1058 | 18.2 | 9.6 | 11.7 | 1039 | 1024 | 1020 | 1021 | 1021 | ↓ | 3.35 | 11.0 | 9.3 | | | |
| | 153 | 44.6 | 5.5 | 26.0 | 19.9 | 23.4 | 1061 | 1058 | 18.3 | 10.3 | 11.8 | 1041 | 1028 | 1027 | 1027 | 1027 | ↓ | 3.14 | 11.2 | 9.9 | | | |
| | 154 | 44.4 | 5.4 | 26.1 | 20.1 | 23.6 | 1060 | 1055 | 18.5 | 11.0 | 12.1 | 1044 | 1034 | 1033 | 1033 | 1033 | ↓ | 2.98 | 11.5 | 10.4 | | | |
| | 155 | 44.6 | 5.5 | 26.9 | 20.8 | 24.3 | 1058 | 1055 | 19.2 | 12.0 | 12.7 | 1044 | 1041 | 1040 | 1041 | 1040 | ↓ | 2.77 | 11.5 | 11.1 | | | |
| | 156 | 44.4 | 5.4 | 26.8 | 20.8 | 24.2 | 1063 | 1059 | 19.7 | 12.6 | 13.2 | 1049 | 1045 | 1044 | 1045 | 1044 | ↓ | 2.76 | 12.1 | 11.5 | | | |
| | 157 | 44.7 | 5.6 | 26.9 | 20.8 | 24.3 | 1062 | 1059 | 19.7 | 13.3 | 13.2 | 1050 | 1048 | 1045 | 1050 | 1049 | Medium | 2.45 | 12.1 | 11.9 | | | |
| | 158 | 44.7 | 5.6 | 31.2 | 25.0 | 28.6 | 1061 | 1058 | 17.3 | 14.5 | 10.5 | 1048 | 1045 | 1045 | 1048 | 1046 | None | 1.11 | 11.9 | ---- | | | |
| | 159 | 45.4 | 5.7 | 24.9 | 18.5 | 22.4 | 1060 | 1056 | 17.0 | 14.3 | 10.1 | 1046 | 1045 | 1044 | 1046 | 1045 | None | 1.08 | 8.3 | ---- | | | |
| | 160 | 45.1 | ↓ | 22.7 | 16.5 | 20.0 | 1059 | 1056 | 15.2 | 12.3 | 8.7 | 1045 | 1043 | 1043 | 1046 | 1044 | None | 1.06 | 11.7 | ---- | | | |
| | 161 | ↓ | ↓ | 20.7 | 14.6 | 18.0 | 1061 | 1058 | 13.2 | 10.3 | 6.8 | 1047 | 1047 | 1046 | 1046 | 1047 | None | 1.04 | 11.8 | ---- | | | |
| | 161a | ↓ | ↓ | 19.4 | 13.3 | 16.8 | ---- | ---- | 11.8 | 9.1 | 5.6 | 1047 | ---- | ---- | ---- | ---- | None/Medium | 1.03 | 11.8 | ---- | | | |
| | 161b | ↓ | ↓ | 19.0 | 13.0 | 16.5 | ---- | ---- | 11.4 | 8.8 | 5.2 | 1047 | ---- | ---- | ---- | ---- | Medium/Low | 1.03 | 11.8 | ---- | | | |
| | 162 | 45.0 | 5.6 | 25.9 | 19.7 | 23.2 | 1067 | 1064 | 18.3 | 8.9 | 11.8 | 1041 | 1023 | 1014 | 1013 | 1013 | Low | 3.54 | 11.2 | 8.6 | | | |
| | 163 | 45.4 | 5.7 | 26.5 | 20.4 | 24.0 | 1072 | 1069 | 19.1 | 10.1 | 12.5 | 1049 | 1032 | 1025 | 1025 | 1025 | Low | 3.50 | 11.9 | 9.7 | | | |
| | 164 | 45.1 | 5.7 | 23.0 | 16.9 | 20.3 | 1065 | 1061 | 15.6 | 12.8 | 9.1 | 1051 | 1050 | 1049 | 1051 | 1050 | None | 1.06 | 12.2 | ---- | | | |
| | 165 | ↓ | ↓ | 21.9 | 15.7 | 19.2 | 1071 | 1067 | 14.3 | 11.4 | 7.8 | 1056 | 1055 | 1054 | 1056 | 1055 | ↓ | 1.06 | 12.8 | ---- | | | |
| | 166 | ↓ | ↓ | 20.3 | 14.1 | 17.7 | 1072 | 1069 | 12.8 | 9.9 | 6.2 | 1058 | 1057 | 1055 | 1056 | 1056 | ↓ | 1.06 | 13.0 | ---- | | | |
| | 166a | ↓ | ↓ | 19.4 | 13.4 | 16.8 | ---- | ---- | 11.8 | 9.1 | 5.8 | 1058 | ---- | ---- | ---- | ---- | ↓ | 1.00 | 13.0 | ---- | | | |
| | 167 | 44.6 | 5.5 | 25.9 | 19.9 | 23.4 | 1072 | 1068 | 18.6 | 9.2 | 12.3 | 1044 | 1025 | 1016 | 1016 | 1016 | ↓ | 3.81 | 11.5 | 9.3 | | | |
| | 168 | 45.0 | 5.7 | 30.8 | 24.7 | 28.1 | 1071 | 1069 | 20.2 | 13.2 | 13.8 | 1056 | 1051 | 1050 | 1051 | 1051 | ↓ | 2.69 | 12.8 | 12.2 | | | |
| | 169 | 45.4 | 5.7 | 30.8 | 24.5 | 28.1 | 1071 | 1067 | 20.0 | 17.2 | 13.4 | 1056 | 1056 | 1055 | 1059 | 1056 | ↓ | 1.06 | 12.8 | ---- | | | |
| | 170 | 45.0 | 5.7 | 27.1 | 21.0 | 24.4 | 1069 | 1066 | 16.3 | 13.6 | 10.1 | 1056 | 1055 | 1054 | 1056 | 1055 | None | 1.02 | 12.7 | ---- | | | |
| | 171 | 44.4 | 5.5 | 24.9 | 18.9 | 22.3 | 1065 | 1065 | 14.2 | 11.4 | 7.9 | 1053 | 1051 | 1051 | 1053 | 1052 | ↓ | 1.06 | 12.4 | ---- | | | |
| | 172 | 45.0 | 5.6 | 23.6 | 17.6 | 21.0 | 1060 | 1058 | 12.8 | 10.0 | 6.5 | 1048 | 1047 | 1046 | 1048 | 1048 | ↓ | 1.03 | 11.9 | ---- | | | |
| | 173 | 45.4 | 5.7 | 22.5 | 16.3 | 19.8 | 1061 | 1057 | 11.5 | 8.7 | 5.2 | 1047 | 1046 | 1045 | 1048 | 1046 | ↓ | 1.03 | 11.8 | ---- | | | |
| | 173a | 45.0 | 5.6 | 21.2 | 15.3 | 18.8 | ---- | ---- | 10.4 | 7.7 | 3.7 | 1047 | ---- | ---- | ---- | ---- | None/High/Low | 1.11 | 11.8 | ---- | | | |
| | 174 | 44.7 | 5.6 | 24.5 | 18.5 | 21.9 | 1059 | 1055 | 13.8 | 11.0 | 7.4 | 1045 | 1044 | 1043 | 1044 | 1044 | None | 1.06 | 11.7 | ---- | | | |
| | 175 | 45.0 | 5.6 | 23.2 | 17.1 | 20.5 | 1057 | 1054 | 12.3 | 9.4 | 5.8 | 1044 | 1043 | 1042 | 1043 | 1043 | None | 1.06 | 11.5 | ---- | | | |
| | 175a | 44.7 | 5.6 | 21.9 | 15.9 | 19.4 | ---- | ---- | 11.0 | 8.3 | 4.8 | 1044 | ---- | ---- | ---- | ---- | None/Low/None | 1.03 | 11.5 | ---- | | | |
| | 176 | 37.4 | 3.9 | 22.5 | 18.2 | 20.8 | 1061 | 1056 | 14.8 | 8.3 | 10.3 | 1033 | 1013 | 1005 | 1005 | 1005 | None | 3.64 | 10.4 | 8.0 | | | |

| | | | | | | | | | | | | | | | | | | | | |
|----|------|------|------|------|------|------|------|------|------|------|------|------|------|------|------|------|---------------|------|------|------|
| 17 | 177 | 60.6 | 10.1 | 37.5 | 21.4 | 27.9 | 1047 | 1044 | 21.7 | 16.7 | 9.7 | 1038 | 1036 | 1034 | 1038 | 1036 | None | 1.08 | 10.8 | ---- |
| | 178 | 60.4 | 10.1 | 30.9 | 19.7 | 26.2 | 1050 | 1047 | 20.0 | 14.9 | 7.9 | 1039 | 1039 | 1038 | 1039 | 1039 | ↓ | 1.07 | 11.0 | ---- |
| | 179 | 60.7 | 10.2 | 29.6 | 18.3 | 24.8 | 1050 | 1047 | 18.5 | 13.4 | 6.5 | 1039 | 1038 | 1038 | 1039 | 1039 | ↓ | 1.06 | 10.6 | ---- |
| | 180 | 60.6 | 10.1 | 28.2 | 16.8 | 23.3 | 1049 | 1044 | 17.1 | 11.9 | 5.1 | 1038 | 1036 | 1038 | 1038 | 1038 | ↓ | 1.06 | 10.6 | ---- |
| | 181 | 60.7 | 10.2 | 26.9 | 15.5 | 22.0 | 1049 | 1046 | 15.7 | 10.5 | 3.7 | 1038 | 1036 | 1038 | 1038 | 1038 | ↓ | 1.06 | 10.6 | ---- |
| | 182 | 60.6 | 10.1 | 25.6 | 14.2 | 20.8 | 1050 | 1047 | 14.5 | 9.3 | 2.1 | 1039 | 1038 | 1038 | 1039 | 1039 | Low/High/Low | 1.09 | 10.9 | ---- |
| | 183 | 60.7 | 10.2 | 31.4 | 20.0 | 26.5 | 1050 | 1047 | 24.7 | 9.2 | 12.3 | 1033 | 1021 | 1016 | 1016 | 1016 | Low | 3.15 | 10.4 | 8.8 |
| | 184 | 60.4 | 10.1 | 31.6 | 20.1 | 26.8 | 1053 | 1050 | 24.8 | 8.8 | 12.3 | 1033 | 1021 | 1011 | 1011 | 1011 | ↓ | 3.31 | 10.4 | 8.4 |
| | 185 | 60.4 | 10.1 | 31.3 | 20.1 | 26.6 | 1050 | 1047 | 24.7 | 9.8 | 12.5 | 1034 | 1025 | 1021 | 1022 | 1021 | ↓ | 3.20 | 10.5 | 9.3 |
| | 186 | 60.6 | 10.2 | 33.2 | 22.0 | 28.5 | 1050 | 1050 | 25.0 | 11.1 | 12.8 | 1040 | 1035 | 1033 | 1034 | 1034 | ↓ | 2.94 | 11.1 | 10.5 |
| | 187 | 60.6 | 10.1 | 34.9 | 23.6 | 30.1 | 1049 | 1049 | 25.1 | 12.3 | 12.9 | 1040 | 1039 | 1038 | 1039 | 1039 | Medium | 2.73 | 11.1 | 11.0 |
| | 188 | 60.6 | 10.1 | 35.6 | 24.2 | 30.8 | 1050 | 1047 | 25.0 | 13.3 | 12.7 | 1039 | 1039 | 1038 | 1039 | 1039 | Medium | 2.42 | 11.0 | 11.0 |
| | 189 | 60.7 | 10.1 | 36.2 | 24.9 | 31.4 | 1049 | 1045 | 24.8 | 14.3 | 12.5 | 1038 | 1036 | 1039 | 1039 | 1038 | Medium | 2.07 | 10.9 | 10.9 |
| | 190 | 61.0 | 10.3 | 32.1 | 20.5 | 27.2 | 1050 | 1047 | 20.5 | 15.3 | 8.1 | 1039 | 1039 | 1040 | 1039 | 1039 | None | 1.08 | 10.8 | ---- |
| | 191 | 60.6 | 10.1 | 33.6 | 22.2 | 28.7 | 1050 | 1045 | 22.1 | 17.0 | 10.3 | 1039 | 1038 | 1039 | 1038 | 1038 | None | 1.03 | 10.3 | ---- |
| | 192 | 60.6 | 10.1 | 28.7 | 17.2 | 23.9 | 1047 | 1042 | 17.2 | 11.9 | 4.6 | 1036 | 1035 | 1034 | 1036 | 1035 | None | 1.09 | 10.7 | ---- |
| | 193 | 60.4 | 10.1 | 27.0 | 15.7 | 22.2 | 1047 | 1042 | 15.5 | 10.3 | 3.2 | 1038 | 1036 | 1034 | 1038 | 1036 | None | 1.08 | 10.8 | ---- |
| | 193a | 60.4 | 10.1 | 26.3 | 14.7 | 21.4 | 1047 | 1042 | 14.7 | 9.6 | 2.3 | 1038 | 1036 | 1034 | 1038 | 1036 | None/High | 1.06 | 10.6 | ---- |
| | 194 | 60.4 | 10.1 | 32.6 | 21.3 | 28.1 | 1047 | 1044 | 24.3 | 9.2 | 12.1 | 1032 | 1021 | 1016 | 1016 | 1016 | Low | 3.31 | 10.3 | 8.8 |
| | 195 | 60.4 | 10.2 | 32.3 | 20.9 | 27.4 | 1053 | 1050 | 25.3 | 12.1 | 13.0 | 1043 | 1040 | 1039 | 1043 | 1042 | Low | 2.69 | 11.4 | 11.2 |
| | 196 | 60.4 | 10.1 | 33.9 | 22.5 | 29.1 | 1050 | 1046 | 25.0 | 14.3 | 12.6 | 1039 | 1039 | 1036 | 1039 | 1039 | Medium | 2.23 | 11.0 | 11.0 |
| | 197 | 60.4 | 10.1 | 31.0 | 19.7 | 26.3 | 1048 | 1045 | 20.1 | 14.9 | 7.7 | 1039 | 1038 | 1036 | 1039 | 1038 | None | 1.09 | 11.0 | ---- |
| | 198 | 60.4 | 10.1 | 33.4 | 22.0 | 28.6 | 1047 | 1044 | 22.5 | 17.3 | 10.0 | 1038 | 1036 | 1034 | 1038 | 1037 | None | 1.10 | 10.8 | ---- |
| | 199 | 60.6 | 10.1 | 42.1 | 30.9 | 37.2 | 1048 | 1045 | 22.5 | 17.3 | 10.5 | 1039 | 1038 | 1038 | 1039 | 1038 | None | 1.08 | 11.0 | ---- |
| | 200 | 60.4 | 10.1 | 38.5 | 27.4 | 33.9 | 1048 | 1045 | 18.8 | 13.7 | 6.6 | 1038 | 1038 | 1035 | 1039 | 1038 | ↓ | 1.10 | 10.9 | ---- |
| | 201 | 60.4 | 10.1 | 36.1 | 24.9 | 31.4 | 1048 | 1044 | 16.3 | 11.1 | 3.9 | 1038 | 1038 | 1035 | 1039 | 1039 | ↓ | 1.11 | 10.9 | ---- |
| | 202 | 60.2 | 10.1 | 34.8 | 23.7 | 30.2 | 1045 | 1043 | 15.0 | 9.9 | 2.6 | 1035 | 1034 | 1033 | 1036 | 1035 | ↓ | 1.11 | 10.6 | ---- |
| | 202a | 60.2 | 10.1 | 34.3 | 23.1 | 29.7 | 1045 | 1043 | 14.1 | 9.0 | 1.8 | 1035 | 1034 | 1033 | 1036 | 1035 | None/High/Low | 1.09 | 10.6 | ---- |
| | 203 | 61.1 | 10.0 | 33.8 | 22.5 | 29.0 | 1045 | 1042 | 24.3 | 8.8 | 11.8 | 1028 | 1017 | 1011 | 1011 | 1011 | Low | 3.30 | 10.0 | 8.4 |
| | 204 | 60.6 | 10.3 | 33.0 | 21.7 | 28.3 | 1041 | 1039 | 19.7 | 14.5 | 7.4 | 1033 | 1033 | 1029 | 1033 | 1033 | None | 1.08 | 10.4 | ---- |
| 18 | 205 | 53.8 | 8.0 | 26.7 | 17.8 | 22.9 | 1047 | 1044 | 18.3 | 14.2 | 8.8 | 1034 | 1034 | 1033 | 1034 | 1034 | None | 1.07 | 10.5 | ---- |
| | 206 | 54.1 | 8.1 | 23.5 | 14.5 | 19.5 | 1047 | 1044 | 15.0 | 10.9 | 5.5 | 1036 | 1036 | 1034 | 1038 | 1036 | None | 1.06 | 10.7 | ---- |
| | 207 | 53.4 | 7.9 | 21.7 | 12.9 | 17.9 | 1049 | 1045 | 13.3 | 9.3 | 3.9 | 1038 | 1037 | 1034 | 1038 | 1037 | None | 1.07 | 10.9 | ---- |
| | 208 | 54.1 | 8.1 | 20.9 | 11.8 | 17.0 | 1046 | 1044 | 12.3 | 8.1 | 2.5 | 1035 | 1034 | 1033 | 1035 | 1034 | High | 1.07 | 10.5 | ---- |
| | 209 | 53.4 | 7.9 | 19.2 | 10.4 | 15.4 | 1050 | 1045 | 10.8 | 6.8 | 1.4 | 1039 | 1038 | 1035 | 1039 | 1038 | High | 1.06 | 11.0 | ---- |
| | 210 | 53.0 | 7.8 | 17.6 | 8.9 | 13.9 | 1050 | 1053 | 9.3 | 5.2 | -2 | 1038 | 1036 | 1039 | 1038 | 1038 | Low | 1.09 | 10.9 | ---- |
| | 210a | 53.6 | 7.9 | 17.2 | 8.4 | 13.4 | 1050 | 1053 | 8.8 | 5.0 | 1 | 1038 | 1036 | 1039 | 1038 | 1038 | ↓ | 1.00 | 10.0 | ---- |
| | 210b | 53.6 | 7.9 | 20.5 | 11.8 | 16.8 | 1050 | 1053 | 12.1 | 8.2 | 3.0 | 1032 | 1016 | 1005 | 1005 | 1005 | ↓ | 1.04 | 10.4 | ---- |
| | 211 | 53.4 | 7.9 | 25.4 | 16.5 | 21.6 | 1053 | 1050 | 20.8 | 8.2 | 11.2 | 1032 | 1016 | 1005 | 1005 | 1005 | ↓ | 3.33 | 10.3 | 8.0 |
| | 212 | 53.4 | 7.9 | 27.6 | 18.9 | 23.9 | 1058 | 1055 | 21.2 | 8.5 | 11.7 | 1034 | 1019 | 1010 | 1010 | 1010 | ↓ | 3.43 | 10.5 | 8.3 |
| | 213 | 53.0 | 7.8 | 29.1 | 20.4 | 25.5 | 1055 | 1050 | 21.2 | 9.2 | 11.7 | 1034 | 1022 | 1017 | 1017 | 1016 | ↓ | 3.30 | 10.5 | 8.8 |
| | 214 | 53.4 | 7.9 | 26.9 | 18.1 | 23.3 | 1051 | 1048 | 18.8 | 14.7 | 8.7 | 1039 | 1039 | 1039 | 1040 | 1039 | None | 1.15 | 11.0 | ---- |
| 19 | 215 | 53.8 | 8.0 | 29.3 | 20.3 | 25.5 | 1050 | 1047 | 21.1 | 16.9 | 11.1 | 1039 | 1039 | 1038 | 1039 | 1038 | None | 1.11 | 11.0 | ---- |
| | 216 | 53.8 | 8.0 | 18.5 | 9.6 | 14.6 | 1053 | 1048 | 10.1 | 6.1 | 8 | 1039 | 1038 | 1039 | 1039 | 1039 | None/High | 1.05 | 10.5 | ---- |
| | 217 | 53.6 | 7.9 | 17.4 | 8.5 | 13.6 | 1053 | 1048 | 8.9 | 4.8 | 6 | 1039 | 1038 | 1039 | 1039 | 1039 | Low | 1.07 | 10.7 | ---- |
| | 218 | 53.6 | 7.9 | 20.5 | 11.6 | 16.8 | 1053 | 1048 | 12.1 | 8.1 | 2.4 | 1039 | 1038 | 1039 | 1039 | 1039 | Low | 1.09 | 10.9 | ---- |
| | 219 | 53.4 | 7.9 | 28.0 | 19.2 | 24.2 | 1051 | 1047 | 20.6 | 8.1 | 11.4 | 1029 | 1015 | 1005 | 1005 | 1005 | Low | 3.32 | 10.0 | 7.9 |
| 20 | s | 15.6 | 0.6 | 29.6 | 29.0 | 29.4 | 791 | 790 | 28.8 | 28.5 | 28.1 | 783 | 783 | 779 | 781 | 780 | None | 1.00 | 0.5 | ---- |
| | t | 31.2 | 2.5 | 31.3 | 28.6 | 30.1 | 769 | 768 | 29.9 | 28.7 | 27.1 | 758 | 757 | 755 | 757 | 755 | ↓ | 1.06 | 1.3 | ---- |
| | u | 47.0 | 5.5 | 26.6 | 20.4 | 23.9 | 715 | 715 | 23.5 | 20.6 | 16.8 | 712 | 711 | 710 | 711 | 710 | ↓ | 1.08 | 1.1 | ---- |
| | v | 62.4 | 9.7 | 31.3 | 20.4 | 26.6 | 728 | 728 | 25.9 | 21.0 | 14.4 | 723 | 725 | 723 | 725 | 723 | ↓ | 1.06 | 1.1 | ---- |
| | w | 78.0 | 15.1 | 37.3 | 20.5 | 30.1 | 721 | 719 | 29.1 | 21.4 | 11.1 | 715 | 716 | 715 | 716 | 716 | ↓ | 1.07 | 1.1 | ---- |
| | y | 83.2 | 17.2 | 39.6 | 20.4 | 31.4 | 729 | 728 | 30.3 | 21.6 | 9.8 | 723 | 725 | 724 | 725 | 725 | ↓ | 1.07 | 1.1 | ---- |

^aFor quality values and remarks see table III(a).

^bShown only for flashed runs.

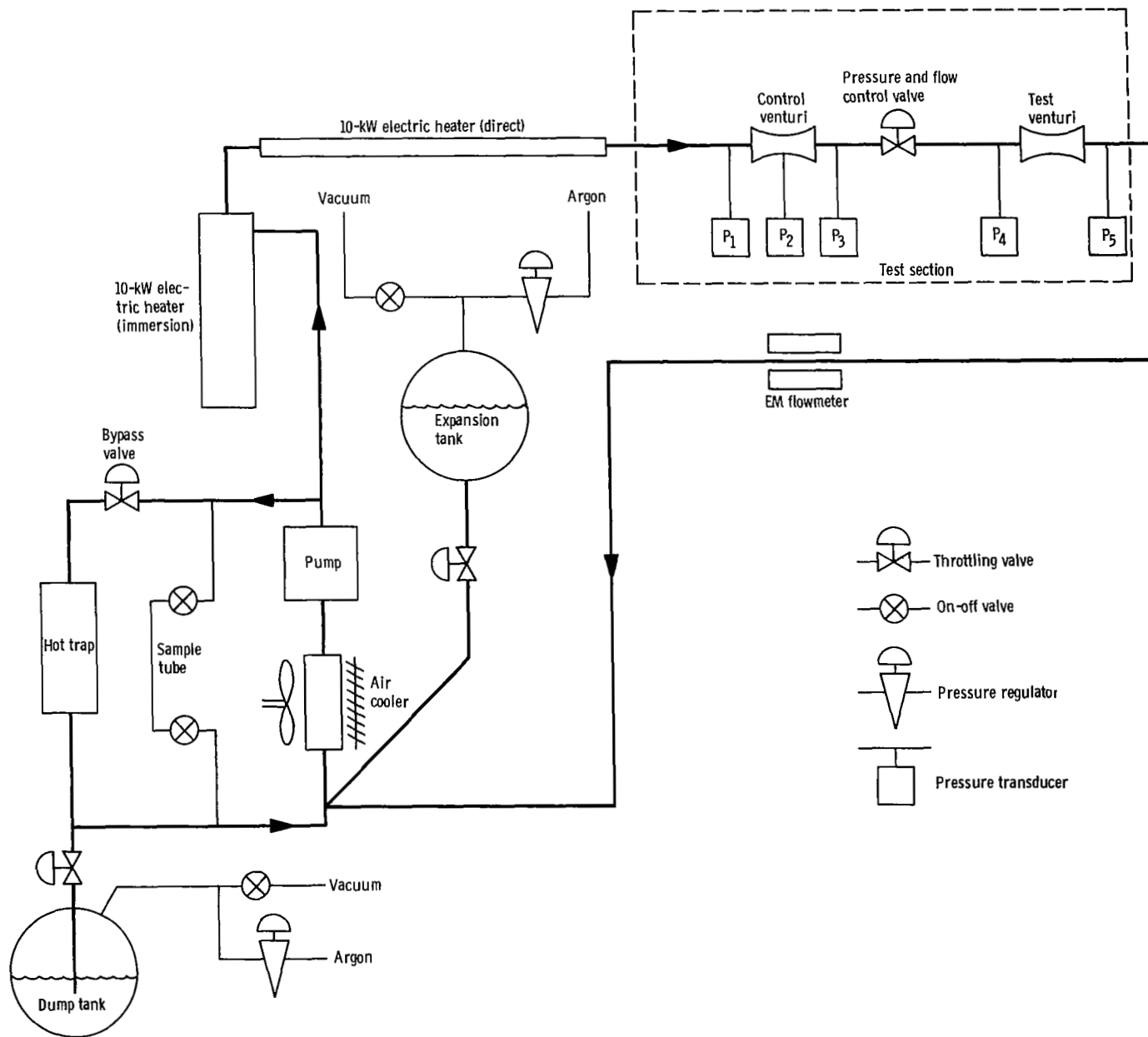


Figure 1. - Schematic diagram of test equipment.

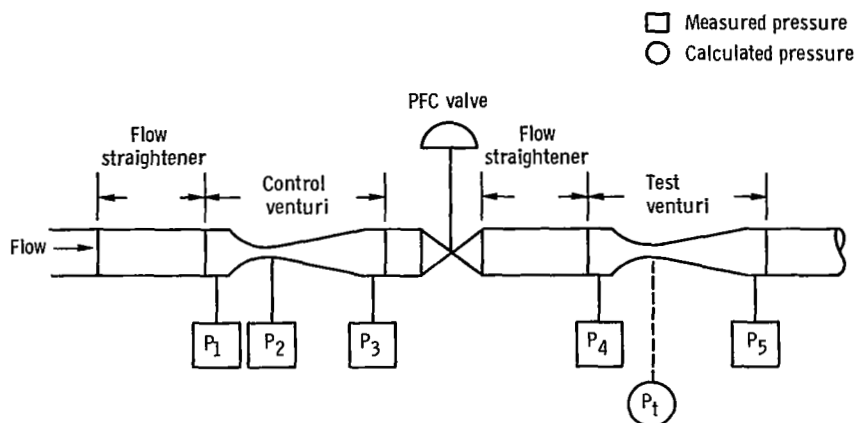


Figure 2. - Diagram of test section showing how test-venturi throat pressure is calculated from control-venturi-measured throat pressure, $P_t = P_4 - (P_1 - P_2)[(P_4 - P_5)/(P_1 - P_3)]$.

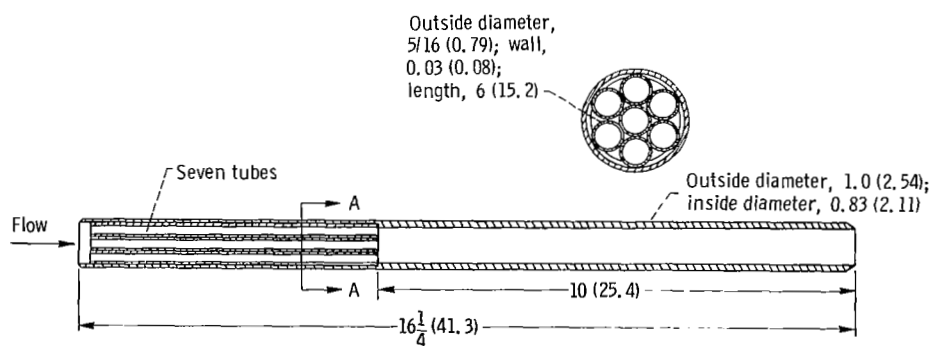
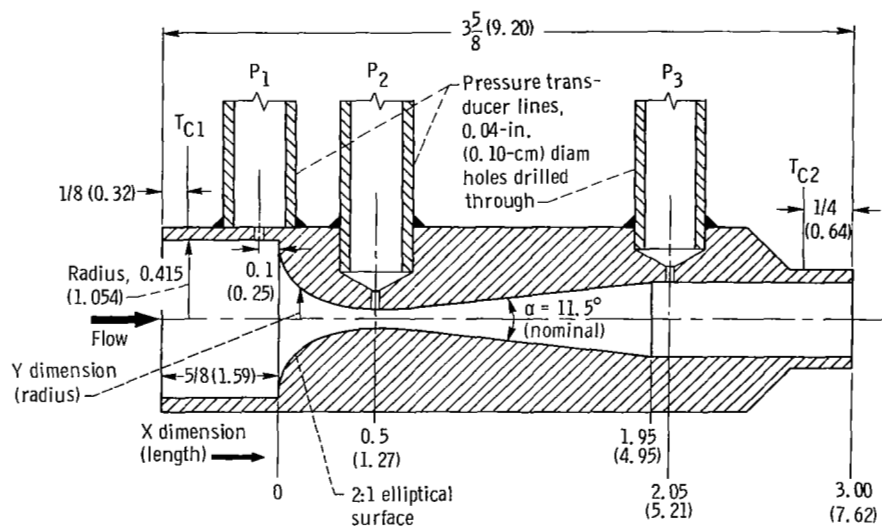
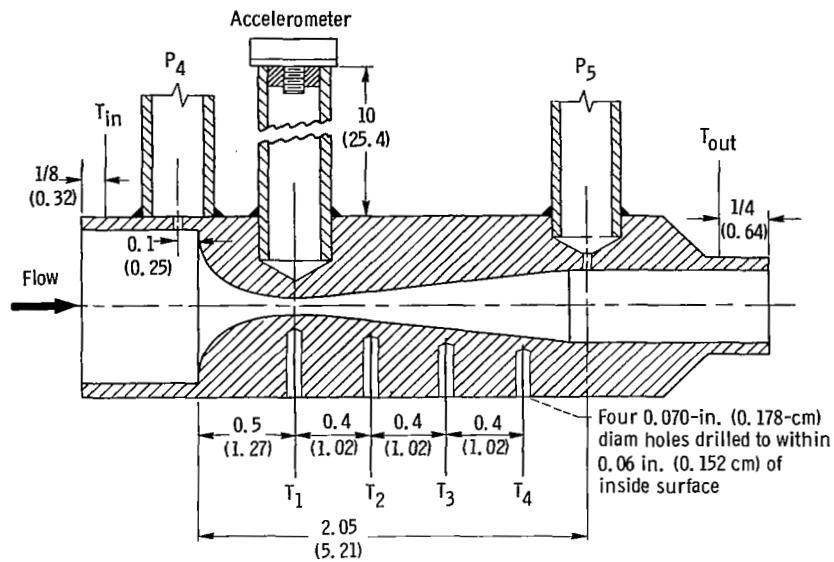


Figure 3. - Flow straighteners used directly upstream of both venturimeters. Material, type-316 stainless steel; dimensions are in inches (cm).

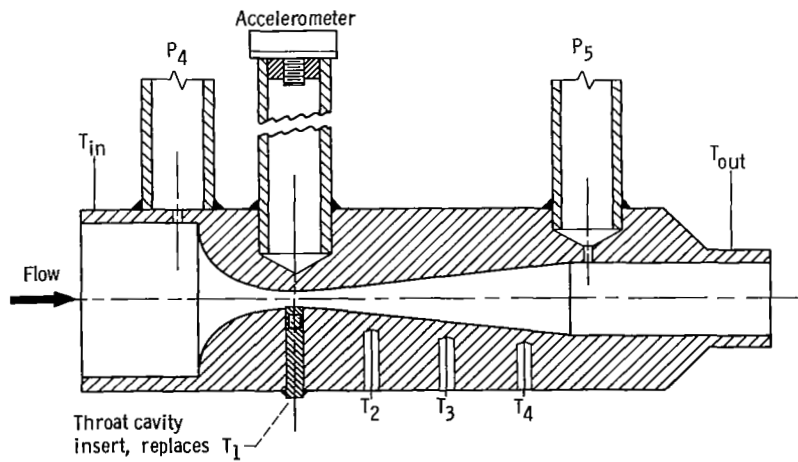


| Venturi dimensions | | | | | | | | | | | |
|--------------------|-------|----------|-------|----------------|--------|-------------|-------|----------|-------|----------------|--------|
| X dimension | | Y radius | | Tolerance in Y | | X dimension | | Y radius | | Tolerance in Y | |
| in. | cm | in. | cm | in. | cm | in. | cm | in. | cm | in. | cm |
| 0 | 0 | 0.300 | 0.762 | +0.010 | +0.025 | 0.750 | 1.905 | 0.070 | 0.178 | +0.002 | +0.005 |
| .050 | .127 | .189 | .480 | + .005 | + .013 | .800 | 2.032 | .079 | .191 | | |
| .100 | .254 | .150 | .381 | + .005 | + .013 | .850 | 2.159 | .080 | .203 | | |
| .150 | .381 | .121 | .307 | + .004 | + .010 | .900 | 2.286 | .085 | .216 | | |
| .200 | .508 | .100 | .254 | + .004 | + .010 | .950 | 2.413 | .090 | .229 | | |
| | | | | | | 1.000 | 2.540 | .095 | .241 | + .004 | + .010 |
| .250 | .635 | .084 | .213 | + .002 | + .005 | | | | | | |
| .300 | .762 | .071 | .180 | + .002 | + .005 | 1.100 | 2.794 | .105 | .257 | + .004 | + .010 |
| .350 | .889 | .062 | .157 | + .002 | + .005 | 1.200 | 3.048 | .115 | .292 | + .005 | + .013 |
| .400 | 1.016 | .055 | .140 | + .001 | + .003 | 1.300 | 3.307 | .125 | .318 | | |
| .450 | 1.143 | .051 | .130 | | | 1.400 | 3.556 | .135 | .343 | | |
| | | | | | | 1.500 | 3.810 | .145 | .369 | | |
| .500 | 1.270 | .050 | .127 | | | 1.600 | 4.064 | .155 | .394 | | |
| .550 | 1.397 | .051 | .130 | | | | | | | | |
| .600 | 1.524 | .055 | .140 | + .002 | + .005 | 1.700 | 4.318 | .165 | .419 | | |
| .650 | 1.651 | .060 | .152 | + .002 | + .005 | 1.800 | 4.572 | .175 | .445 | | |
| .700 | 1.778 | .065 | .165 | + .002 | + .005 | 1.900 | 4.826 | .185 | .470 | | |
| | | | | | | 1.950 | 4.953 | .190 | .483 | | |
| | | | | | | 2.050 | 5.207 | .190 | .483 | | |

Figure 4. - Control venturi. Dimensions are in inches (cm); all tolerances, -0.000.



(a) Test venturi without artificial throat cavity.



(b) Test venturi with artificial throat cavity.

Figure 5. - Test venturi. Dimensions are in inches (cm).

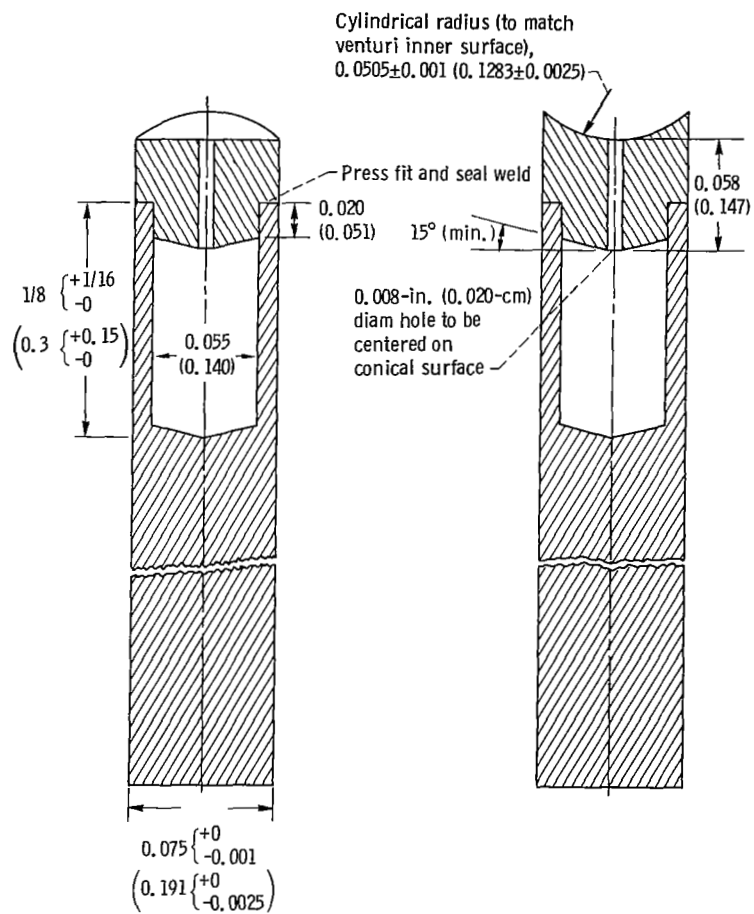
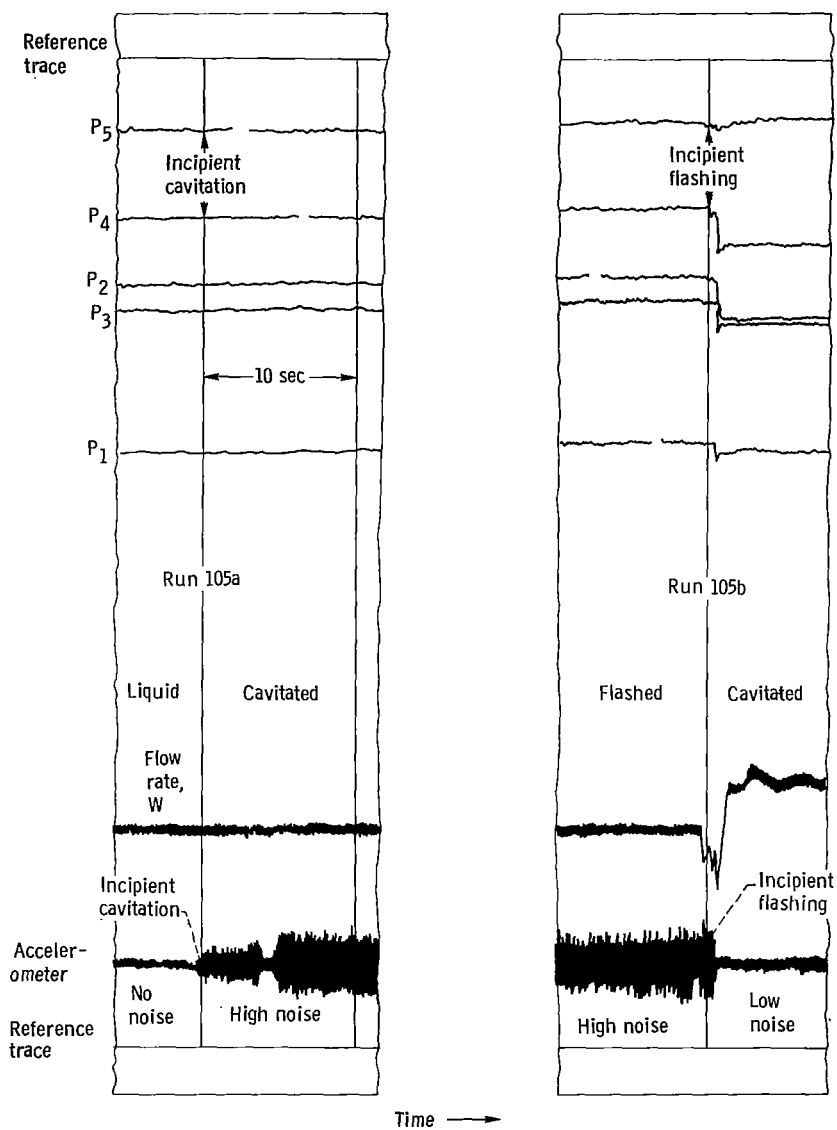


Figure 6. - Throat cavity insert. Material, type-316 stainless steel; dimensions are in inches (cm).



(a) Change from liquid to cavitating flow.

(b) Change from cavitating to flashed flow.

Figure 7. - Pressure decrease ramp between runs 105 and 106, set 13. Sections of oscillogram showing points of incipient cavitation and incipient flashing.

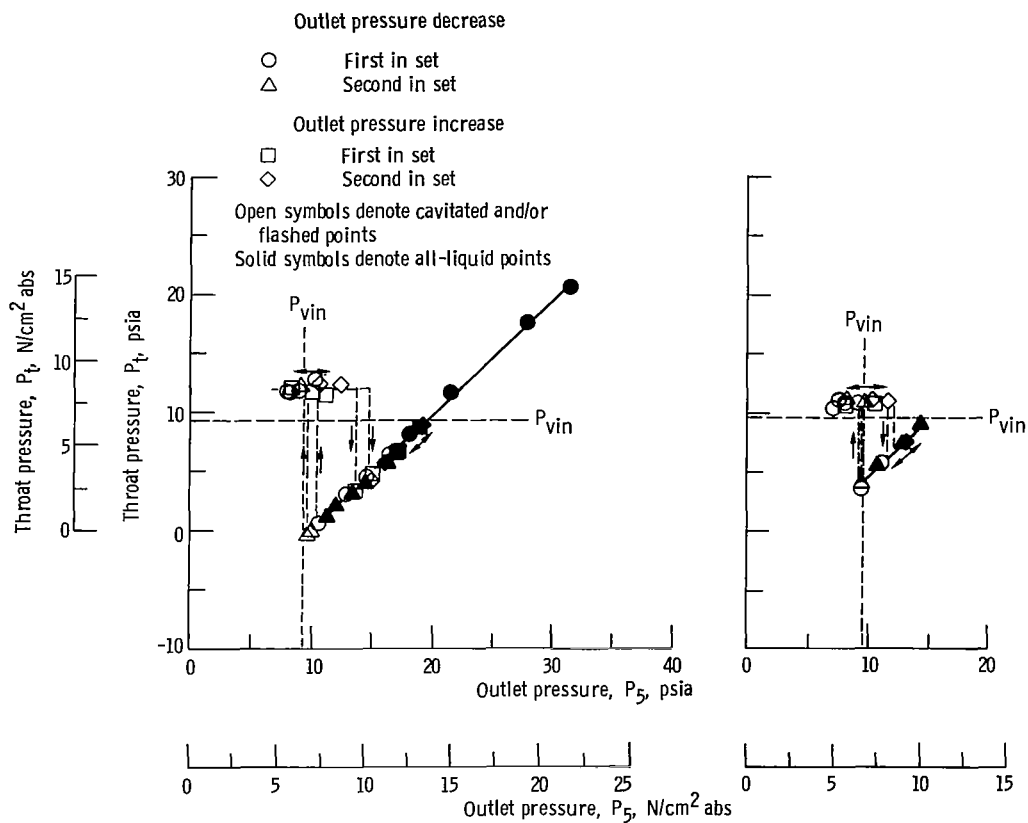


Figure 9. - Test venturi with artificial throat cavity: throat pressure as function of outlet pressure.

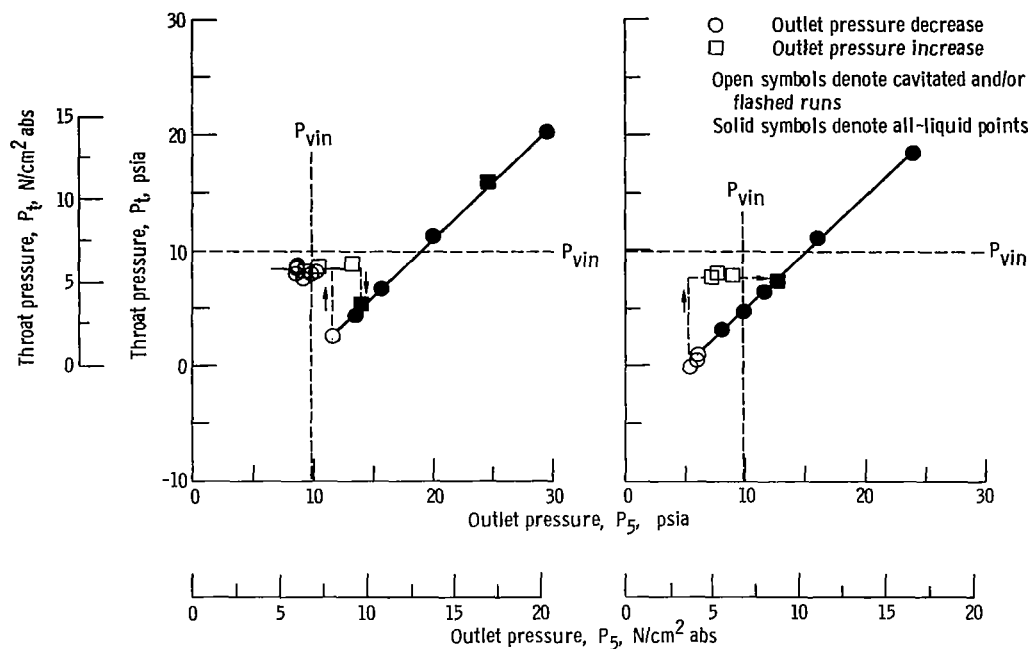


Figure 8. - Test venturi without artificial throat cavity: throat pressure as function of outlet pressure.

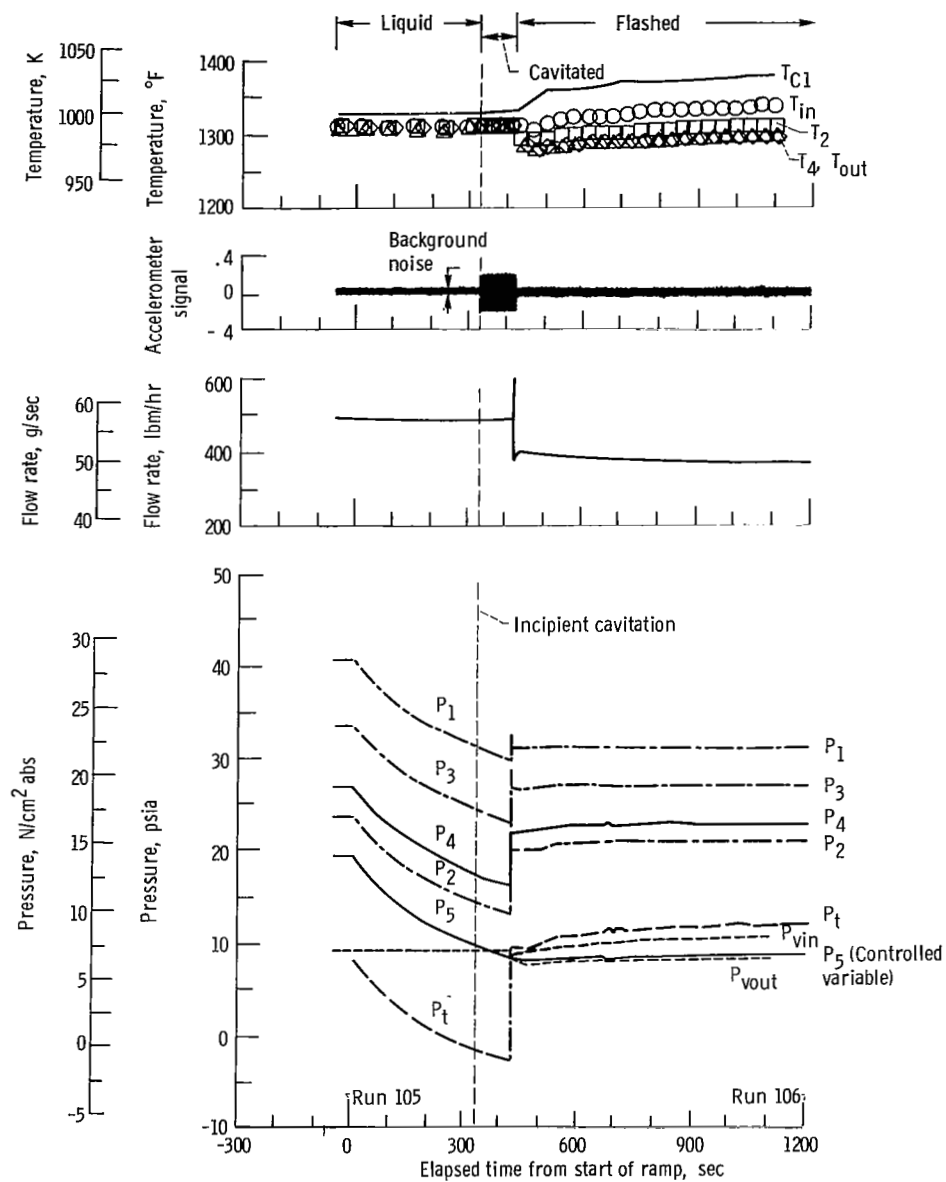


Figure 10. - Behavior of test venturi during pressure ramp between runs 105 and 106. Exit quality at 1200 seconds, approximately 1 percent; controlled variable, P_5 .

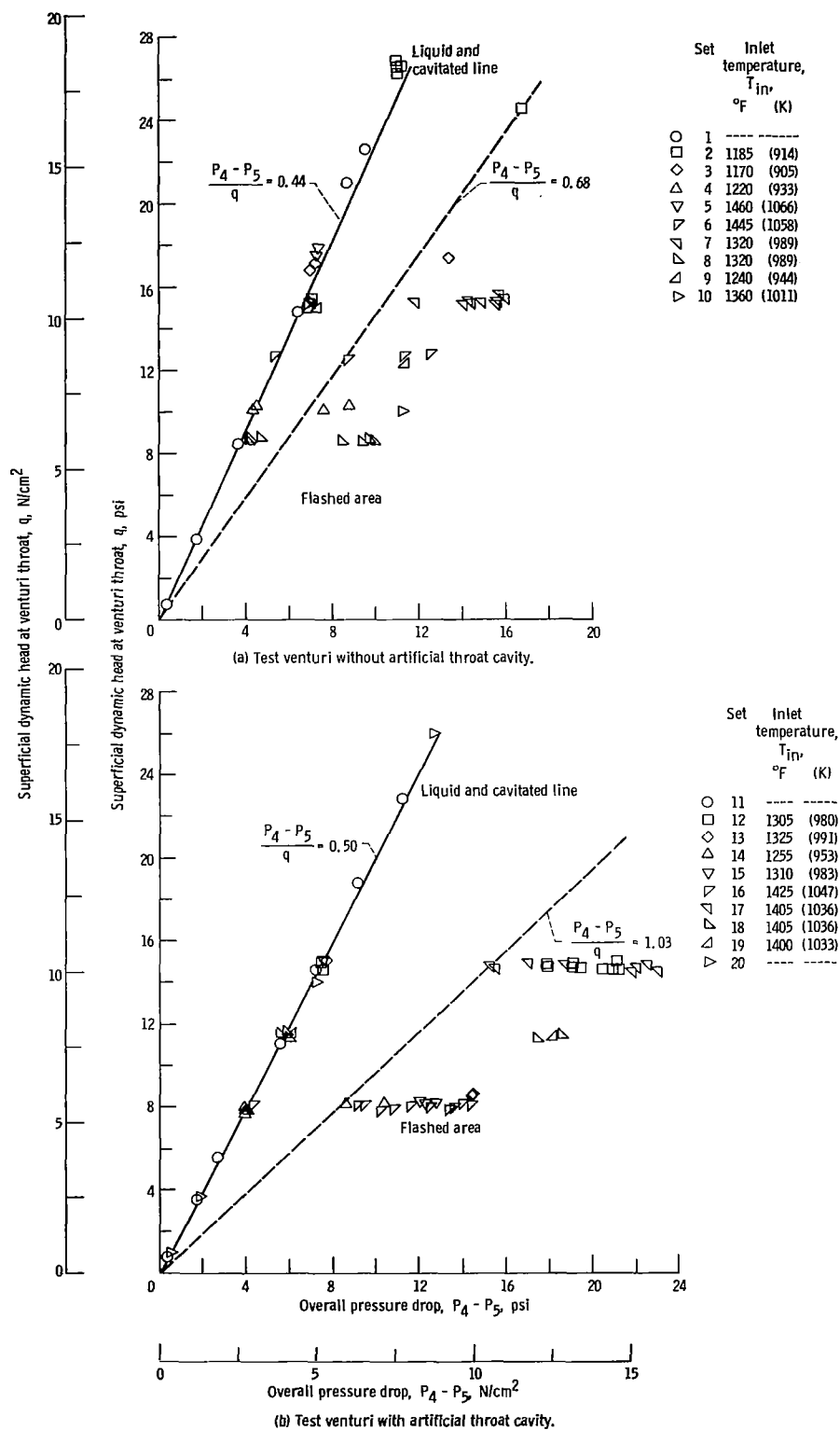


Figure 11. - Overall pressure drop as function of superficial dynamic head for all runs.

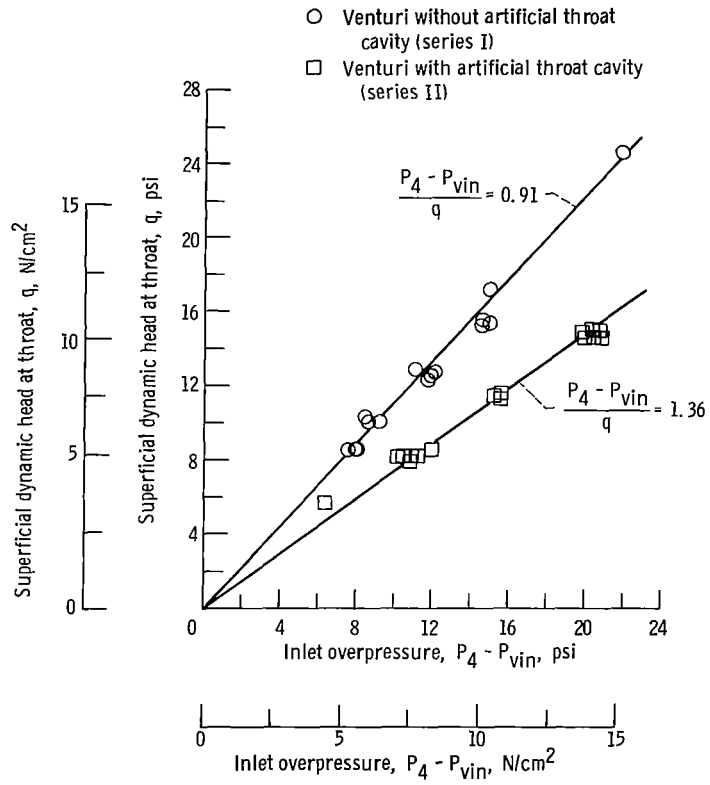
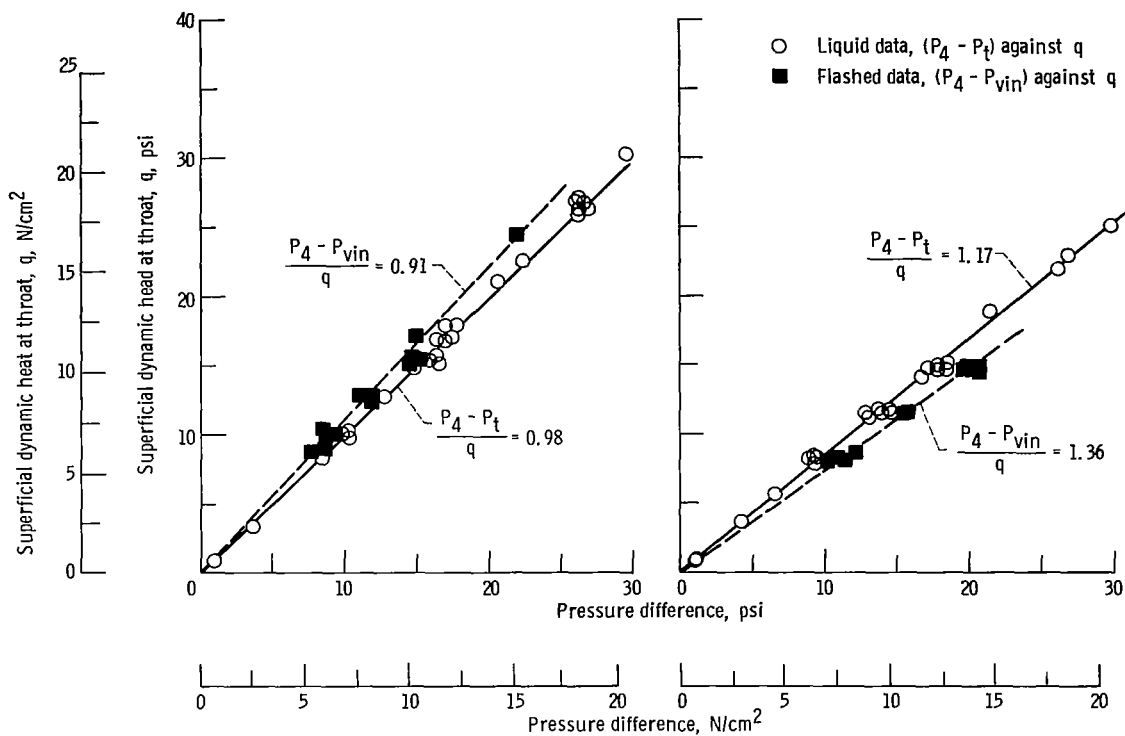
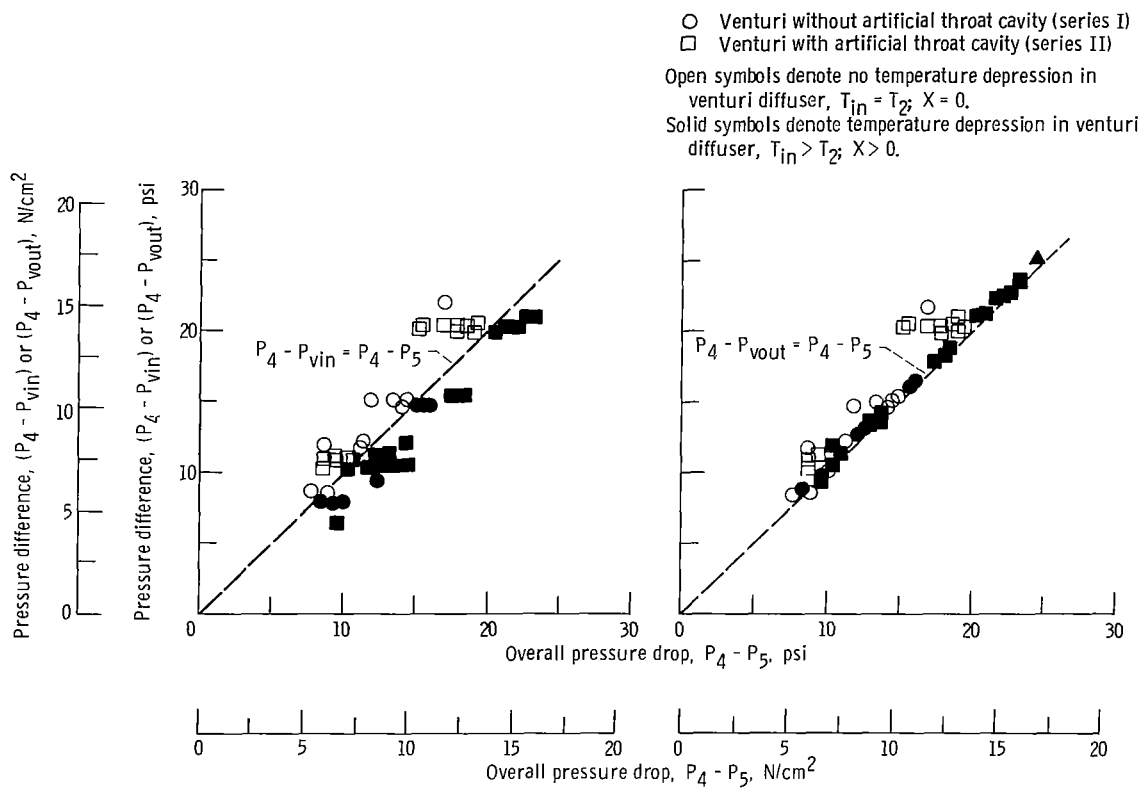


Figure 12. - Flashed venturi performance. Difference between venturi inlet pressure and potassium vapor pressure corresponding to inlet temperature $P_4 - P_{vin}$ (inlet overpressure) as function of superficial dynamic head at throat.



(a) Venturi without artificial throat cavity (series I). (b) Venturi with artificial throat cavity (series II).

Figure 13. - Flashed venturi performance, nozzle section. Comparison of inlet overpressure for flashed runs $P_4 - P_{vin}$ with all-liquid nozzle pressure drop to the throat $P_4 - P_t$ as function of superficial dynamic head at throat.



(a) Pressure difference between inlet pressure and vapor pressure at inlet temperature, $P_4 - P_{vin}$.

(b) Pressure difference between inlet pressure and vapor pressure at outlet temperature, $P_4 - P_{vout}$.

Figure 14. - Flashed venturi performance, diffuser section. Effect of venturi backpressure on diffuser temperature and pressure drop.

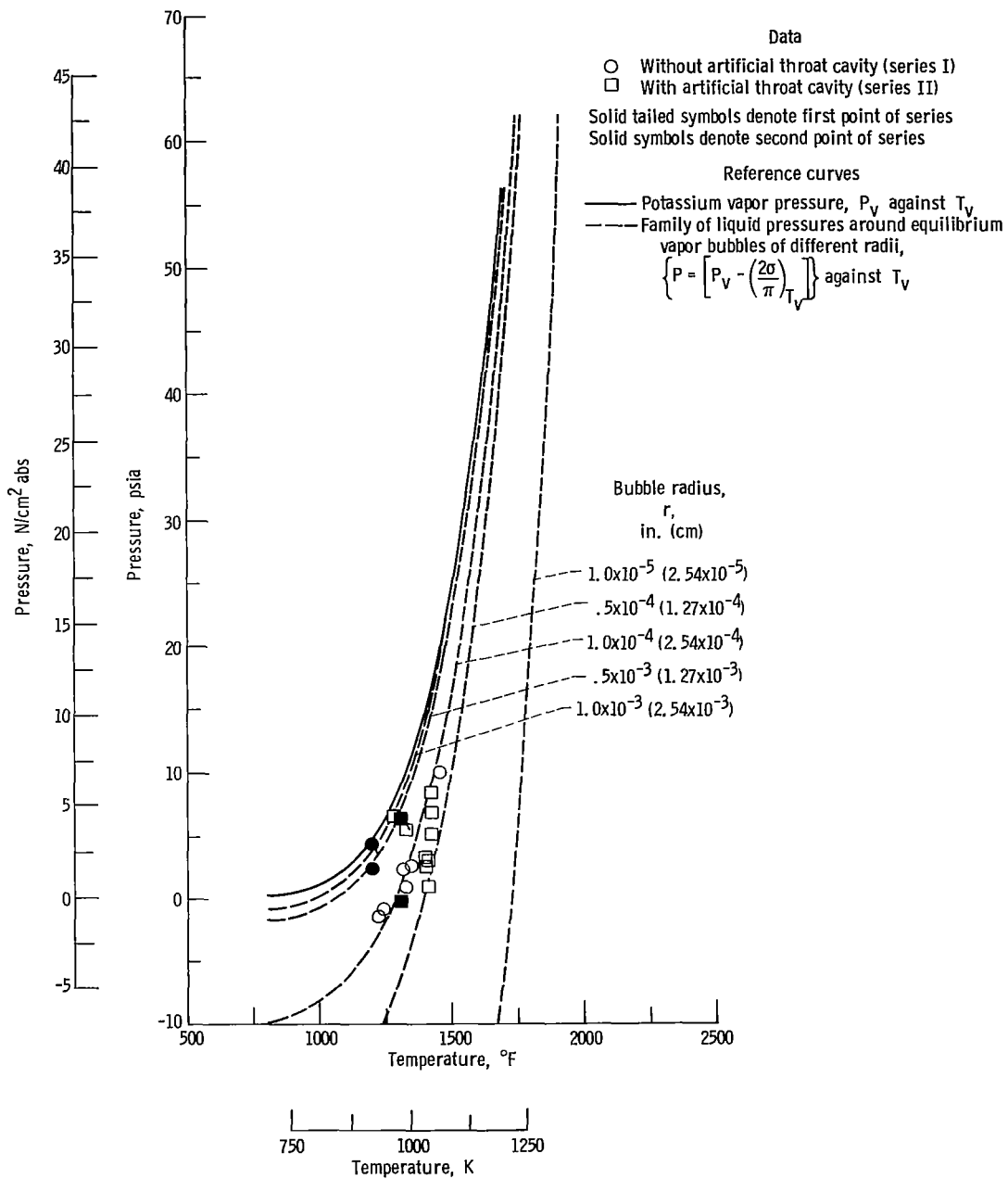


Figure 15. - Cavitation incipency. Throat pressure as function of inlet temperature for incipient cavitation.

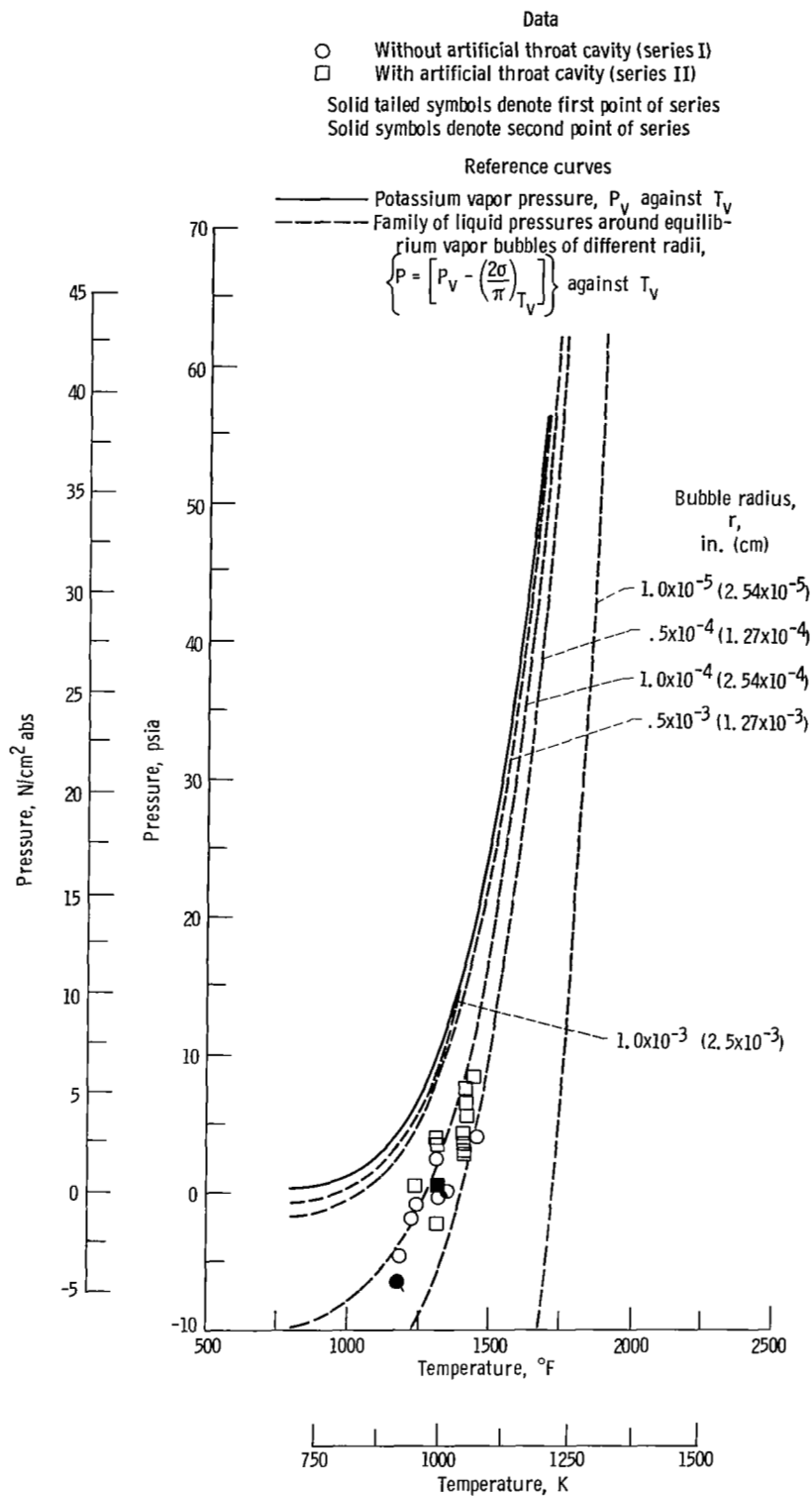


Figure 16. - Flashing incipency. Throat pressure as function of inlet temperature for incipient flashing.

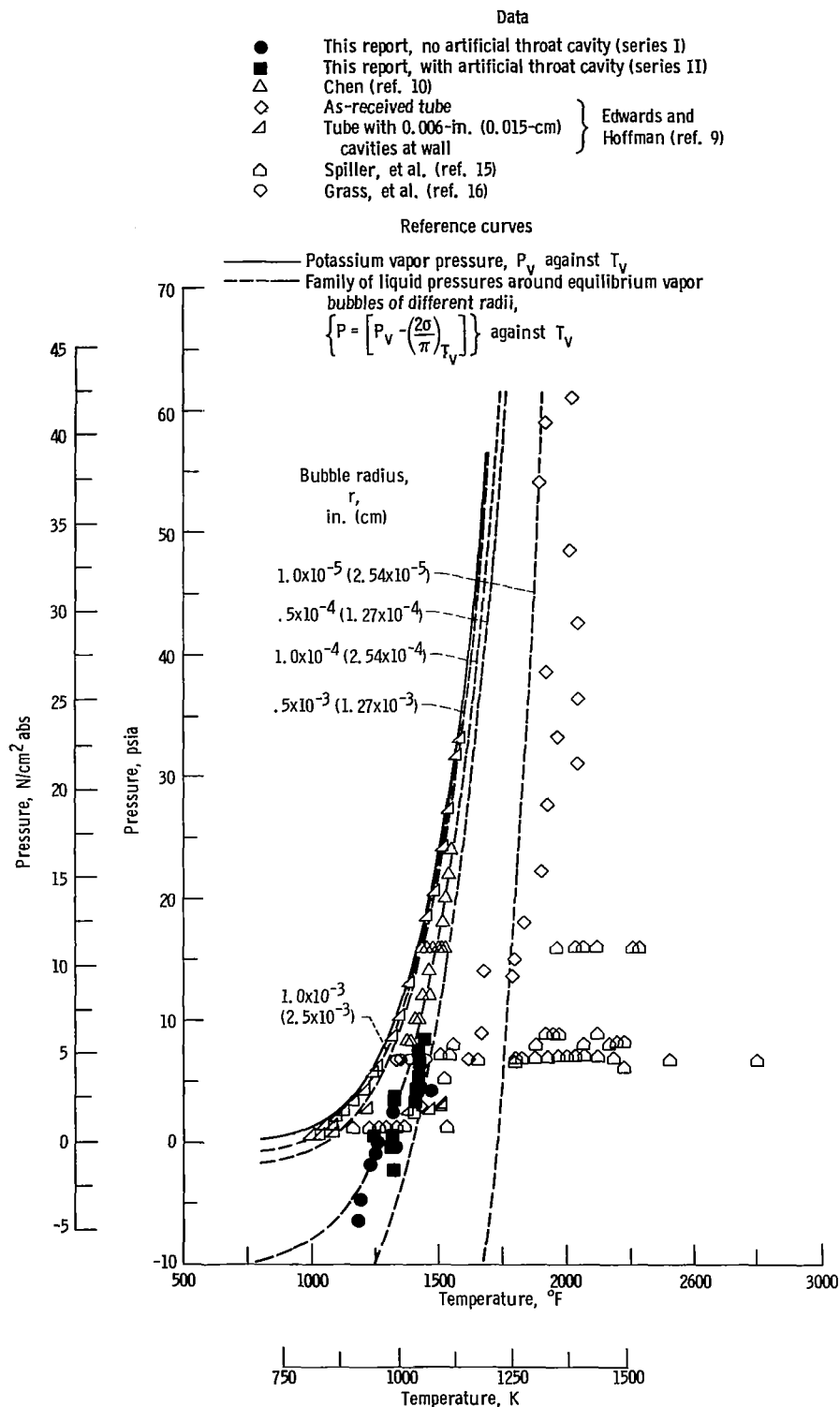
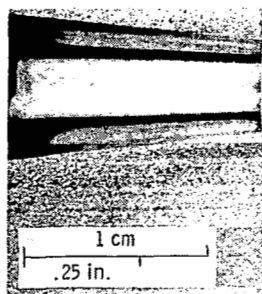
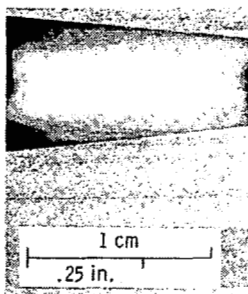


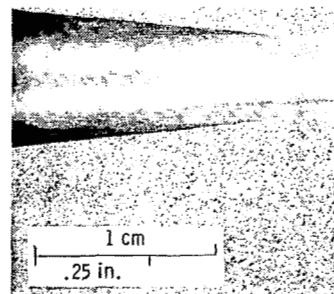
Figure 17. - Comparison of incipient flashing data with potassium data from other investigators; liquid minimum pressure as function of liquid temperature. See table in corresponding section of tests for comparison of test conditions.



(a-1) As-received venturi.

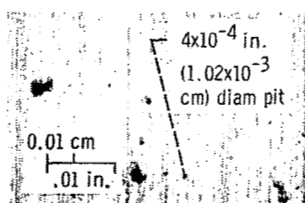


(a-2) Test venturi.



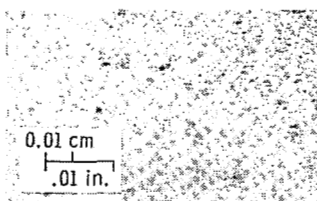
(a-3) Control venturi.

(a) Longitudinal sections of portion of diffusers. As-received venturi was not used. Sections from test and control venturis exposed to potassium flow for approximately 250 hours; note change in surface shine.



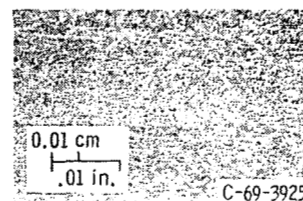
Intended flow direction

(b-1) As-received venturi.



Flow direction

(b-2) Test venturi.

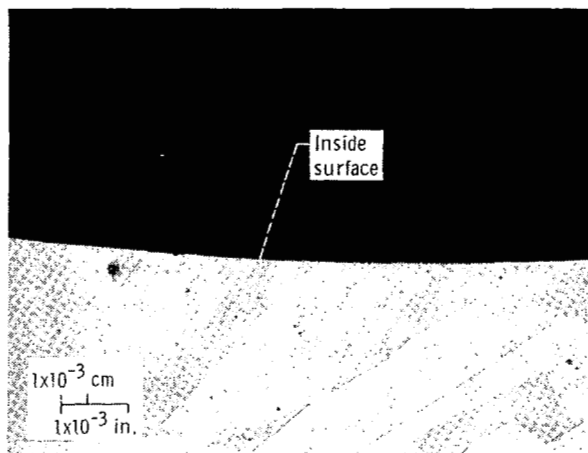


Flow direction

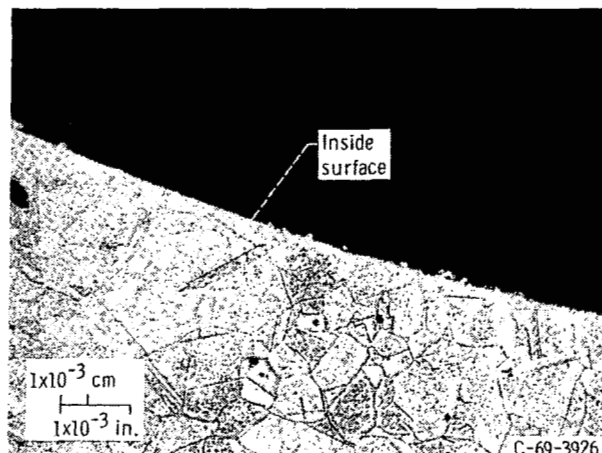
(b-3) Control venturi.

(b) Photomicrographs of venturi diffusers inside surfaces. Note polishing scratches and large-size pits in as-received venturi, and disappearance of these features in test and control venturis.

Figure 18. - Photographs of venturi taken normal to inside surface at diffuser.



(a) As-received venturi. Very smooth inside surface; no disturbances in surface can be appreciated. Notice large grains and absence of carbide precipitation in metal.



(b) Test venturi. Rougher surface; small cavities in range of 10^{-4} to 10^{-5} inch (2.54×10^{-4} to 2.54×10^{-5} cm) can be seen on surface. Notice change in structure within metal and presence of intergranular and matrix carbide precipitation.

Figure 19. - Photomicrographs of venturi cross section showing edge of inside surface, taken at beginning of diffuser near throat. Material, type-316 stainless steel.

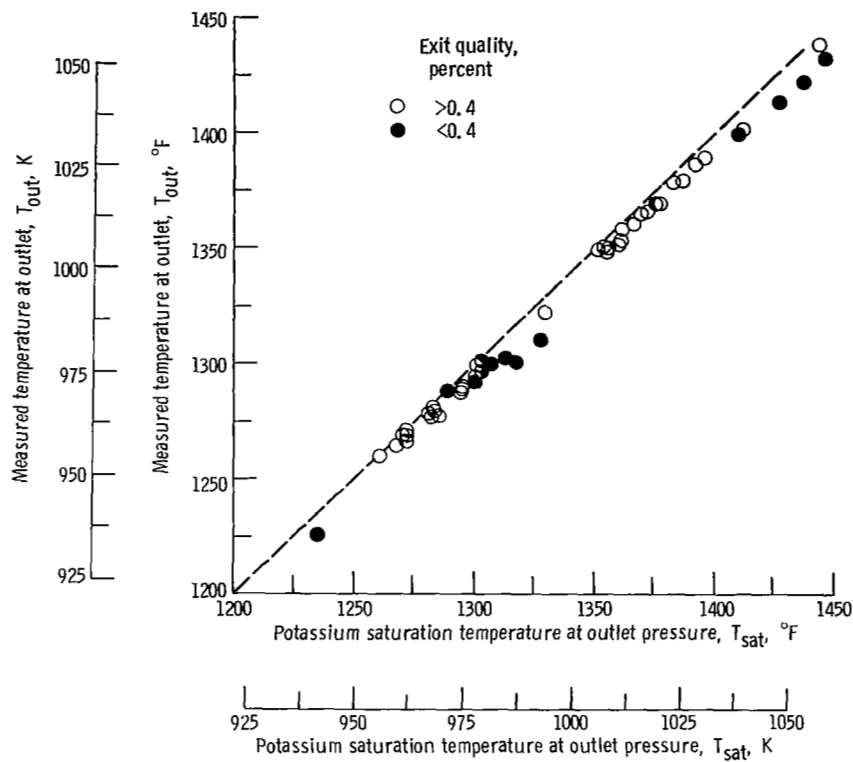


Figure 20. - Comparison of test venturi measured outlet temperature with corresponding potassium saturation temperature at outlet pressure. Flashed runs.

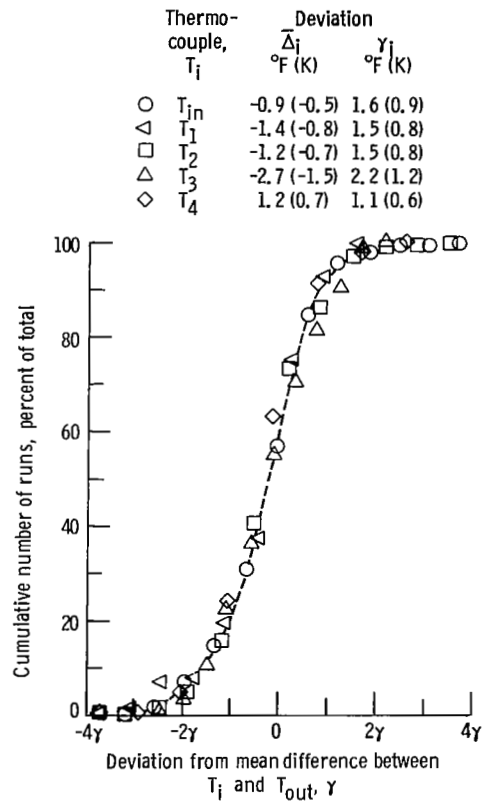


Figure 21. - Distribution of thermocouple reading deviations for thermocouples T_{in} , T_1 , T_2 , T_3 , and T_4 when compared to thermocouple T_{out} . All-liquid runs.
 $\gamma_i = [\sum (\Delta_i - \bar{\Delta}_i)^2 / N_i]^{1/2}$; $\bar{\Delta}_i = \sum \Delta_i / N_i$;
 $\Delta_i = (T_i - T_{out})$ where N_i = number of readings (56 for T_1 , 158 for all others).

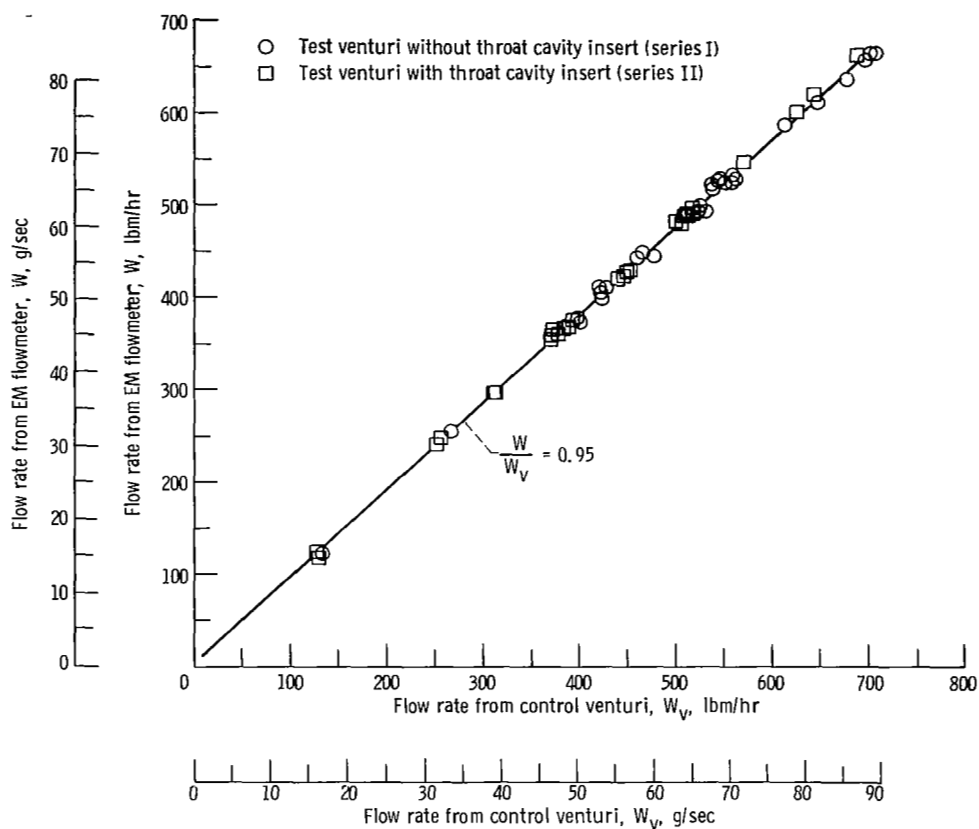


Figure 22. - Comparison of potassium flow rate data from electromagnetic flowmeter with those obtained from control venturi using results of water calibration of as-received venturi.

NATIONAL AERONAUTICS AND SPACE ADMINISTRATION

WASHINGTON, D. C. 20546

OFFICIAL BUSINESS

FIRST CLASS MAIL



POSTAGE AND FEES PAID
NATIONAL AERONAUTICS
SPACE ADMINISTRATION

120 001 58 51 305 70075 00903
AIR FORCE WEAPONS LABORATORY /WLOL/
KIRTLAND AFB, NEW MEXICO 87117

ATTN: E. LUDWIG, CHIEF, TECH. LIBRARY

POSTMASTER: If Undeliverable (Section
Postal Manual) Do Not Return

"The aeronautical and space activities of the United States shall be conducted so as to contribute . . . to the expansion of human knowledge of phenomena in the atmosphere and space. The Administration shall provide for the widest practicable and appropriate dissemination of information concerning its activities and the results thereof."

— NATIONAL AERONAUTICS AND SPACE ACT OF 1958

NASA SCIENTIFIC AND TECHNICAL PUBLICATIONS

TECHNICAL REPORTS: Scientific and technical information considered important, complete, and a lasting contribution to existing knowledge.

TECHNICAL NOTES: Information less broad in scope but nevertheless of importance as a contribution to existing knowledge.

TECHNICAL MEMORANDUMS: Information receiving limited distribution because of preliminary data, security classification, or other reasons.

CONTRACTOR REPORTS: Scientific and technical information generated under a NASA contract or grant and considered an important contribution to existing knowledge.

TECHNICAL TRANSLATIONS: Information published in a foreign language considered to merit NASA distribution in English.

SPECIAL PUBLICATIONS: Information derived from or of value to NASA activities. Publications include conference proceedings, monographs, data compilations, handbooks, sourcebooks, and special bibliographies.

TECHNOLOGY UTILIZATION PUBLICATIONS: Information on technology used by NASA that may be of particular interest in commercial and other non-aerospace applications. Publications include Tech Briefs, Technology Utilization Reports and Notes, and Technology Surveys.

Details on the availability of these publications may be obtained from:

SCIENTIFIC AND TECHNICAL INFORMATION DIVISION
NATIONAL AERONAUTICS AND SPACE ADMINISTRATION
Washington, D.C. 20546